Pot1 phosphorylation regulates telomere function

Yuan Zhao

University College London

and

Cancer Research UK London Research Institute

PhD Supervisor: Julia Promisel Cooper

A thesis submitted for the degree of

Doctor of Philosophy

University College London

September 2012

Declaration

I, Yuan Zhao, confirm that the work presented in this thesis is my own. Where information has been derived from other sources, I confirm that this has been indicated in the thesis.

Abstract

The telomere is a conserved nucleoprotein structure at the ends of eukaryotic chromosomes. It is essential for maintenance of genomic stability: on the one hand, it suppresses DNA damage response and protects the natural chromosome ends from repair activities; on the other hand, it recruits telomerase, the specialized reverse transcriptase, to counteract the end-replication problem. The telomeric G-strand ssDNA-binding protein Pot1 plays a crucial role in both of these functions. In fission yeast *S. pombe*, inhibition of Pot1 induces rampant 5' resection and loss of telomere signal in a single cell cycle.

It was recently shown that *sp*Pot1 interacts with, and is phosphorylated by, the master cell cycle regulator DDK. Alleles of a V5-tagged version of *pot1*$^{+}$ were constructed with mutations at the putative phosphorylation sites, which reside in the N-terminal OB-fold DNA binding domain of Pot1 (Kuznetsov, 2008). The goal of this study was to determine the molecular mechanism by which phosphorylation of Pot1 regulates telomere function. We found that the phospho-deficient mutants of Pot1 induce telomere elongation, checkpoint activation, and deregulation of ssDNA generation, suggesting reduced association with the ssDNA. Our data point to a model in which cell cycle-regulated Pot1 phosphorylation coordinates telomere replication and telomerase activity in different cell cycle phases. Furthermore, we showed that the C-terminal V5-tagging of Pot1 also affects its functions, suggesting an additional layer of complexity governing Pot1 function.

Acknowledgement

First and foremost, I would like to express my sincere gratitude to my PhD supervisor Julie for giving me the opportunity to be part of this amazing group, and for her immense enthusiasm, patience, inspiration and support through this journey.

My deepest appreciation goes to all the present and past members of the lab, who has made the lab such a fantastic and stimulating place to work in. A most sincere thank you to Cecile for always being there for me; to Sophie for making the lab such a fun place to be; to Pierre-Marie and Kuza for all the help before and after you leave the lab; to Vitaliy for the inheritance of the project and for all the guidance at the start of my PhD. Thank you to Chris, Jessica, Ofer, Thomas, Devanshi, Alex, Martina, Alf, and Hani for the insightful discussion, whether its science-related or not. A special thank you to Nadeem, who helped with the experiments in the last months.

I would also like to thank my thesis committee Dr. Simon Boulton and Dr. Jacky Hayles for their continued support and valuable input during my study, and all the yeast groups – the Toda lab, the Uhlmann lab and the Nurse lab – for their help and discussion.

A big thank you to my family for the constant love and encouragement, I wouldn't have been able to come this far without you. To my friends in UK, China and other parts of the world for your your friendship and support, and special thanks to Eliza for putting up with my phone calls in the middle of the night. And to the nickname master, whose love has helped me through all my doubts and obstacles. Thank you.

Table of Contents

Table of figures

List of tables

Abbreviations

Δ	gene deletion
2DGE	2-dimensional gel electrophoresis
5-FOA	5-fluoroorotic acid
ALT	alternative lengthening of telomeres
aur	Aureobasidin A
ATM	Ataxia Telangiectasia mutated
ATR	ATM and Rad3 related
BSA	bovine serum albumin
ChIP	Chromatin immunoprecipitation
CST	Cdc13-Stn1-Ten1 or CTC1-STN1-TEN1
DAPI	4'-6-diamidino-2-phenylindole
DDK	Dbf4 dependent kinase
DDR	DNA damage response
DMSO	dimmmethyl sulfocide
DNA	deoxyribonucleic acid
DSB	double strand break
dsDNA	double-stranded DNA
EDTA	ethylenediaminetetraacetic acid
EMSA	electrophoresis mobility shift assay

dNTP	deoxymnucleotide 5’-triphosphate
HR	homologous recombination
HU	hydroxyurea
hph	Hygromycin B
IF	indirect immunofluorescence
IP	immunoprecipitation
kan	geneticin418
λPPase	lambda phosphatase
ME	bacto-malt extract
MMS	methylmethane sulfonate
nat	nourseothricin
NHEJ	non-homologous end joining
OB-fold	oligonucleotide/oligosaccharide binding-fold
ORF	open reading frame
PFGE	pulse field gel electrophoresis
pI	isoelectric point
PMSF	phenilmethylsulphonyl fluoride
RPA	replication protein A
SSA	single strand annealing
ssDNA	single-stranded DNA
STE	subtelomeric sequences

TCA	trichloroacetic acid
TIFs	telomere dysfunction-induced foci
ts	temperature sensitive
T-SCE	telomeric sister chromatid exchange
wt	*wild-type*
YES	yeast extract supplements media

Chapter 1. Introduction

1.1 Telomeres

1.1.1 Structure of the telomeres

The word ‘telomere’ is derived from the Greek words *telos*, which means ‘ends’, and *meros*, which means ‘parts’. It describes the nucleoprotein structure at the natural ends of linear chromosomes that distinguishes the ends from double strand breaks (DSBs). The existence of such a structure was predicted by the work of McClintock and Muller, when they independently noted that X-ray induced breaks resulted in fusions everywhere in the genome but at natural ends of chromosomes, and disrupting the natural ends resulted in fusion and chromosomal breakage and rearrangements (McClintock, 1939, Muller, 1938). The nature of this structure was first determined in 1978 in the unicellular eukaryote *Tetrahymena* (Blackburn and Gall, 1978), and has since been studied and characterized in numerous other organisms from yeast to human.

In most eukaryotes, telomeric DNA is composed of tandem repeats of GC-rich sequences. The bulk of the telomere is comprised of double stranded DNA (dsDNA), and ends with a 3’ G-rich single-stranded overhang (ssDNA). The length of telomeres varies greatly among different species, from around 300bp in fission and budding yeast to 10-15kb in human (Shampay et al., 1984, de Lange et al., 1990). Long tracts of loosely repetitive sequences called sub-telomeric elements (STE) are found immediately centromere-proximal to the telomere sequences, also contributing to telomere functions.

Specialized telomeric proteins are recruited both to the dsDNA and ssDNA regions of the telomeres due to sequence specificity (Figure 1.1). Together with the telomeric DNA, they form the ‘cap’ that protects the end of chromosomes. In budding yeast *S. cerevisiae*, the Myb-domain protein Rap1 binds the telomeric dsDNA region and recruits other telomeric components, including Rif1/2 and SIRs (Lustig et al., 1990, Wotton and Shore, 1997). The overhang region is coated by the CST (Cdc13-Stn1-Ten1) complex, which binds ssDNA via the

oligonucleotide/oligosaccharide-binding motifs (OB-fold) and structurally resembles the RPA (replication protein A) complex (Nugent et al., 1996, Gao et al., 2007).

Many other eukaryotes seemed to have evolved a slightly different chromosomal end structure. In human cells, the dsDNA region is coated by the Myb-domain proteins TRF1 and TRF2 (Chong et al., 1995, Broccoli et al., 1997), while the ssDNA region is bound by the OB-fold containing proteins POT1 and TPP1, which form a heterodimer (Baumann and Cech, 2001, Ye et al., 2004); these two regions are linked via Rap1 and TIN2 to form the telomere binding complex. Collectively, these six telomere proteins are known as shelterin (Palm and de Lange, 2008). A CST (CTC1-STN1-TEN1) complex homologous to the budding yeast Stn1-Ten1 complex was also found at the telomeric ssDNA with a specificity for the G-strand *in vitro*, albeit also being found at numerous other locations and showing no sequence specificity *in vitro* (Martín et al., 2007, Miyake et al., 2009, Chen et al., 2012).

A shelterin-like protein component list similar to that in human is found at fission yeast telomeres. The TRF1/2 homolog Taz1 coats the telomeric dsDNA, and recruits Rap1 and Rif1 proteins (Cooper et al., 1997, Kanoh and Ishikawa, 2001). The Taz1-Rap1 complex is bridged to the ssDNA binding complex Pot1-Tpz1-Ccq1 via a bridge comprising Rap1 and an additional protein, Poz1 (Baumann and Cech, 2001, Miyoshi et al., 2008). Like in human, a Stn1-Ten1 complex also binds the ssDNA and is required for telomere protection (Martín et al., 2007). See section 1.6 for more details of the ssDNA-binding complexes.

Importantly, the telomere is a heterochromatic region, which is characterized by histone H3K9 methylation and $HP1^{Swi6}$ enrichment (Kanoh et al., 2003, Garcia-Cao et al., 2004). The telomeric heterochromatin imposes transcriptional silencing effect on the adjacent regions, a phenotype known as the telomere position effect (Cooper et al., 1997, Baur et al., 2001). In spite of telomere silencing, the telomeric and subtelomeric sequences are transcribed into long non-coding telomeric repeat-containing RNA, which has been shown to function in telomere length regulation via control of exonuclease resection (Pfeiffer and Lingner, 2012); an inhibitory effect of such RNAs on telomerase activity is also suggested by *in vitro* experiments (Redon et al., 2010). Additionally, the nucleosome organisation at

telomere regions is distinct from bulk chromatin, showing in humans a diffuse micrococcal nuclease cleavage pattern at short (2-7kb) telomeres, and a more canonical but compact structure with short spacing at long telomeres (Tommerup et al., 1994).

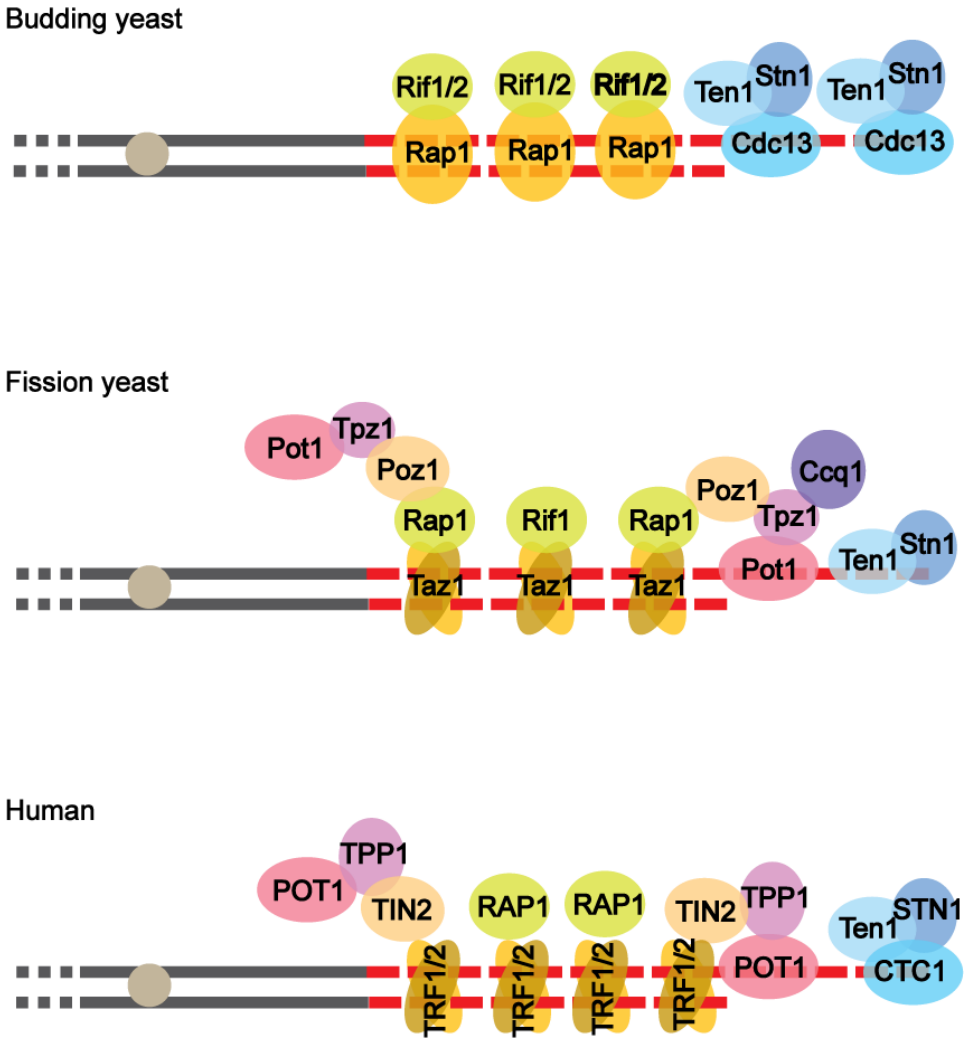

Figure 1.1 Schematic presentation of telomere structures in different organisms

A schematic diagram showing core components of the telomeric complex in model organisms budding yeast, fission yeast, and human. The grey line represents genomic DNA, while the red dashed line represents the telomeric repeats, which ends in a 3' overhang. Proteins are colour-coded to indicate functional homology between different organisms.

1.1.2 Main functions of the telomeres

Being a conserved structure in essentially all eukaryotes, telomeres are crucial for the maintenance of genomic stability for at least two reasons. One of the main functions of the telomeres is to solve the end-replication problem, which refers to the inability of the conventional replication mechanism to completely duplicate linear DNA molecules to the very end (Watson, 1972). As the semi-conservative replication can only synthesize DNA in the 5' to 3' direction and requires a pre-existing 3' hydroxyl group for addition of new nucleotides, once the final RNA primer is removed from the terminus of the strand produced by lagging strand synthesis, the 5' end of the DNA cannot be replenished, thus resulting in shortening after every round of replication. In addition, end processing by exonucleases leads to further erosion of the product (see section 1.2). A common way of solving this problem is by employing telomerase, the specialized traverse transcriptase. It synthesizes telomeric repeats using its RNA subunit as a template, thus counteracting the loss of telomeric DNA after replication (reviewed in (Lingner and Cech, 1998)). The fact that telomere length is species-specific indicates that the process of telomerase action is tightly regulated to maintain homeostasis (see below).

The other major function of the telomeres is to protect the chromosomal ends from DNA damage response (DDR). DDR is the complicated signalling cascade that leads to detection and repairing of DNA damage, thus ensuring faithful transmission of genetic information. However, improper attempts to 'repair' natural chromosomal ends can lead to chromosomal fusion and mitotic catastrophe of breakage-fusion-bridge cycles. Therefore, it is essential that a functional telomere be not recognized as a DNA lesion, even though it structurally resembles one. Suppression of DDR signalling at telomeres is achieved collaboratively by the specialized protein complexes that are recruited to both the double-stranded and single stranded telomeric repeats; disruption of the protective telomeric structures elicits a DNA damage response (see section 1.3). At least in fission yeast, telomeres are further distinguished from bulk DNA by the unique epigenetic modification pattern, i.e. lack of the ubiquitous H4K20me2 histone marker, which is

required for stable association of the DDR transducer Crb2^{53BP1} (Carneiro et al., 2010).

1.2 Maintenance mechanisms at functional telomeres

An obvious prerequisite for telomeres to function in genomic stability is that they can be maintained during genome duplication. While the rest of the genome simply duplicates via bi-directional semi-conservative replication, the telomeres need to go through multiple steps to duplicate completely. The three main steps are conventional replication, end processing, and telomerase action (Figure 1.2).

1.2.1 Semi-conservative replication

Although much of the work in the telomere maintenance field seemed to focus on telomerase and the alternative pathways that elongate the telomeres, the bulk of the telomeric DNA is actually synthesized by the conventional machinery of semi-conservative replication. Replication at telomeres has two unique features. First, unlike the rest of the genome, where replication can be initiated from replication origins on both sides, telomere replication is unidirectional from the centromere-proximal side. Therefore, the RNA primer of the final Okazaki fragment cannot be replenished by fill-in synthesis, causing at least part of the end-replication problem. Second, telomeric DNA is consisting of GC-rich repetitive sequences that are prone to form secondary structures, which poses challenge to the conventional replication machinery. The telomeric noncoding RNAs may also interact with telomeric DNA and create an obstacle to replication fork progression.

It has been shown that telomeric dsDNA-binding proteins, Taz1 in fission yeast or TRF1 in human, is required to facilitate fork passage through the telomere sequences (Miller et al., 2006, Sfeir et al., 2009). In fission yeast, replication forks stall at telomeres in the absence of Taz1 protein, causing telomere breakage and rapid deletion when telomerase is not available to replenish telomeres. It was proposed that in *taz1*Δ cells, stalled replication forks provide powerful telomerase substrate, leading to elevated telomerase recruitment, excessive 3’ overhang and telomere elongation (Dehe et al., 2012).

As the fork progresses to the end of the telomere, a replication product that is shorter than the parental DNA is generated due to the positioning and removal of the RNA primer for the final Okazaki fragment on the lagging strand (Watson, 1972, Chow et al., 2012). The leading strand supposedly duplicates fully to generate a blunt end; however, the 3' overhang needs to be re-established by end processing, as it is essential for end protection and telomerase recruitment (Lingner et al., 1995).

1.2.2 End processing

The products of semi-conservative replication are further processed to generate 3' telomeric overhangs on both the leading and lagging strands (Makarov et al., 1997, Wellinger et al., 1996). Many proteins of DSB processing pathway are shown to be involved in this process. In the best studied model organism, the budding yeast *S. cerevisiae*, the Mre11-Rad50-Xrs2 (MRX) complex was shown to be important for overhang generation at leading-strand telomeres (Larrivee et al., 2004, Bonetti et al., 2009, Faure et al., 2010). Sae2, the ssDNA specific endonuclease, cooperates with MRX in the processing of the overhang; in the absence of Sae2, the RecQ helicase Sgs1 and the exonuclease Exo1 become crucial for overhang generation (Bonetti et al., 2009).

End processing is tightly controlled, as excessive resection leads to telomere shortening and DDR activation. In budding yeast, the length of the 3' overhang is 12-14 nt in most of the cell cycle, but transiently increases to 50-100nt in late S/G_2 phase when it can be detected by in-gel hybridization analysis (Larrivee et al., 2004, Wellinger et al., 1993b, Wellinger et al., 1993a). This is in part achieved via the cyclin-dependent kinase Cdk1, which is required for Sae2^{CtIP} phosphorylation to promote resection (Vodenicharov and Wellinger, 2006, Huertas et al., 2008). Cdk1 has low activity in G_1 phase, thereby limiting such resection to S/G_2 phase of the cell cycle in a *wt* background (Frank et al., 2006). Similarly, the cell cycle-regulated ssDNA overhang signal is also found in human and fission yeast (Dai et al., 2010, Kibe et al., 2003).

Telomeric proteins are also involved in regulation of resection at chromosomal ends. It was first shown in budding yeast that mutations in the telomeric ssDNA

binding protein Cdc13 lead to accumulation of telomeric ssDNA generated in a telomere-to-centromere direction, and Rad9-dependent cell cycle arrest (Garvik et al., 1995, Booth et al., 2001). These results are consistent with a role of Cdc13 in inhibition of telomeric resection. Later it was found that Pot1, the counterpart of Cdc13 that binds telomeric ssDNA in mammals and fission yeast, is also required for proper regulation of resection. In mice liver and kidney cells, disruption of Pot1b leads to a 7- to 11-fold increase of overhang signal independently of telomerase (Hockemeyer et al., 2006). In fission yeast, inactivating Pot1 using a temperature-sensitive allele also result in rampant resection in S/G_2 phase and loss of telomere signal within one cell cycle (Pitt and Cooper, 2010).

1.2.3 Elongation by telomerase and fill-in synthesis

The overhang generated either by lagging strand replication or by end resection can be used as the substrate for telomerase action. The telomeric repeats are added to the G-rich strand by reverse transcription, which contributes to the increased overhang in S phase, and fill-in synthesis involving DNA polymerase α (Polα) is thought to extend the C-strand. Although reconstitution of telomerase action *in vitro* requires only the template RNA and the catalytic subunit of telomerase (Cohn and Blackburn, 1995, Weinrich et al., 1997), telomerase action *in vivo* is controlled both spatially and temporally by numerous factors, thereby maintaining the species-specific length homeostasis.

The recruitment of telomerase involves highly regulated interactions between the telomerase RNP and the telomeric chromatin. In budding yeast, the ssDNA binding protein Cdc13 was shown to interact directly with Est1, the regulatory subunit of telomerase (Nugent et al., 1996, Wu and Zakian, 2011). Cdk1 regulates the cell cycle control of this interaction by Cdc13 phosphorylation, which is required for efficient recruitment of telomerase (Li et al., 2009). A spatial regulation also exists to ensure telomere length homeostasis by preferential elongation of the shortest telomeres. Telomere length signal is transduced by a counting mechanism in which the number of Rif1 and Rif2 molecules located at the telomeric dsDNA region regulates recruitment of $Tel1^{ATM}$ kinase (Levy and Blackburn, 2004, Hirano and Sugimoto, 2007). Tel1 therefore accumulates only at short telomeres, and in turn phosphorylates Cdc13 proteins (Teixeira et al., 2004, Bianchi and Shore, 2007,

Hector et al., 2007). In addition, short telomeres induce transient DDR response, leading to an MRX-dependent checkpoint response during the prolonged elongation (Viscardi et al., 2007).

Although the same telomere homeostasis is seen in other organisms, the regulatory mechanism of telomerase action is less well defined. In fission yeast, Ccq1, which binds the telomeric ssDNA via the Pot1-Tpz1 complex, is required for telomerase recruitment (Tomita and Cooper, 2008). Phosphorylation on Thr93 by $Tel1^{ATM}$ and $Rad3^{ATR}$ is essential for its interaction with Est1 (Moser et al., 2011, Yamazaki et al., 2012). In human cells, where a *ccq1* homolog has not been identified, recruitment of telomerase is dependent on the TEL patch on the surface of TPP1 (Zhong et al., 2012, Sexton et al., 2012, Nandakumar et al., 2012). An additional mechanism of regulation was also suggested, based on the regulation of repeat addition processivity of telomerase *in vitro* by POT1-TPP1 (Xin et al., 2007, Wang et al., 2007). It was proposed that a direct interaction between POT1-TPP1 complex and telomerase inhibits primer dissociation, which in turn increases telomerase processivity (Latrick and Cech, 2010).

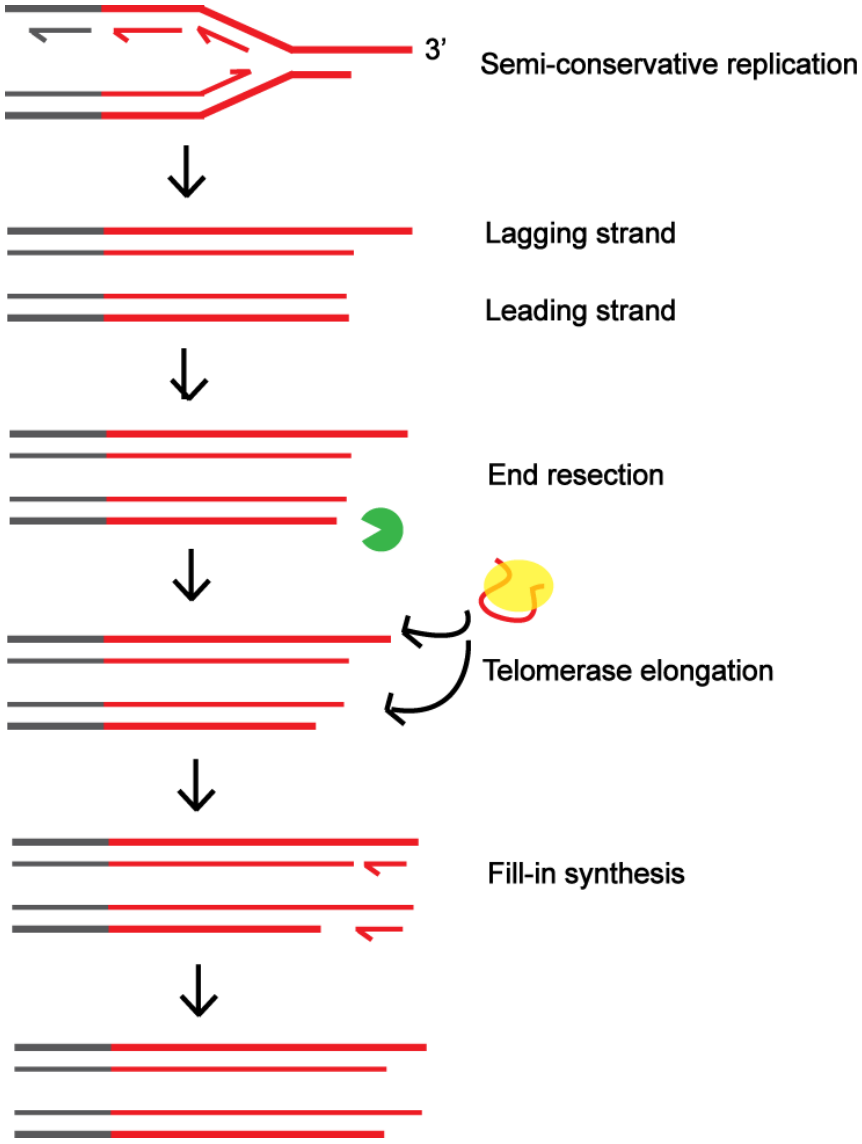

Figure 1.2 Mechanisms of telomere synthesis

DNA synthesis at functional telomere occurs in multiple steps. Semi-conservative replication duplicate the bulk of telomeric DNA (red lines), leaving a leading strand shorter than the parent molecule, and a lagging strand with a recessed 5' end due to end-replication problem. The leading strand is further processed by nucleolytic resection (green) to generate a 3' overhang. Telomerase is recruited to the 3' overhangs, which act as templates for telomerase to elongate the 3' strand, and the 5' ends are replenished by fill-in synthesis.

1.3 Telomeres are protected from DNA damage response

1.3.1 DNA damage response

DNA lesions can occur either as intermediates of normal cellular metabolism such as DNA replication and meiotic recombination, or by exposure to exogenous DNA-damaging agents such as UV and IR or endogenous damaging agents such as free radicals. In order to maintain genomic stability, cells have developed a conserved network known as the DNA damage response (DDR), which recognizes the DNA lesion, stalls the cell cycle to allow repair to happen, and recruits DNA repair machinery to remove the lesion. Double strand breaks (DSBs) are a highly toxic form of DNA lesion, which, if not properly repaired, can lead to loss of genetic information and large-scale genomic instability. Therefore, the DDR pathways for DSB repair are highly efficient; a single unrepaired DSB can trigger checkpoint-mediated cell cycle arrest (Sandell and Zakian, 1993).

The repair of a DSB involves a highly regulated network that detects, signals, and repairs the lesion. The DSB is first detected by the sensor kinase ATM, a member of the phosphatidylinositol 3' kinase-like kinase (PIKK) family, via its binding partner MRN/X (Mre11-Rad50-Nbs1/Xrs2) complex. At this point, the DSB can be repaired by two classic repair pathways: non-homologous end joining (NHEJ), and homologous recombination (HR). The choice between the two pathways is largely determined by both the cell cycle stage and the nature of the DSB ends (reviewed in (Jeggo et al., 2011, Symington and Gautier, 2011)). In mammals, NHEJ is active throughout the cell cycle and represent the major repair pathway, while HR is mainly restricted to S and G2 phase, and appears especially important for replication-associated DSBs (Rothkamm et al., 2003). In fission yeast, NHEJ is critical for DSB repair in G1 phase (induced by nitrogen starvation), while HR is the predominant repair pathway in other cell cycle phases when a sister chromatid is available to conduct error-free repair (Ferreira and Cooper, 2004).

The mechanism of cell cycle-regulation is best illustrated in budding yeast. In the G_1 phase of the cell cycle, recruitment of the Ku heterodimer to the dsDNA end protects the ends from degradation, and favours the Lig4-dependent NHEJ repair pathway (Wu et al., 2008). In S/G_2 phase, Ku is inhibited from the binding the ends,

and the MRN/X complex can either act alone or recruit additional nucleases to resect the 5' ends of the DNA to produce an invasive 3' ssDNA end, thus favouring the HR-mediated repair pathways (Mimitou and Symington, 2009). The resected tail is then bound by the ssDNA-binding RPA complex, which is displaced by the RecA-like recombination protein Rad51 to form a nucleoprotein filament that initiates homologous pairing and strand invasion (reviewed in (Bianco et al., 1998)).

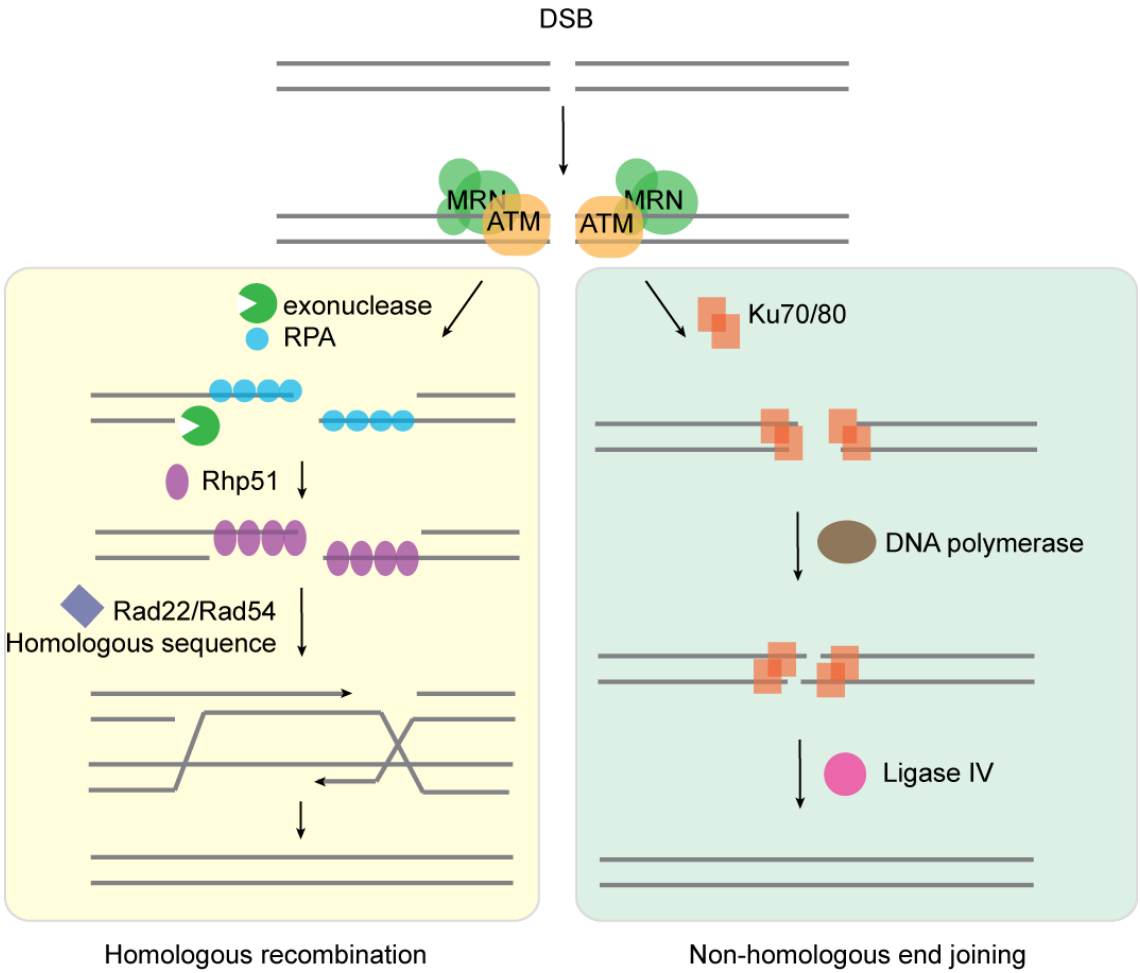

Figure 1.3 DSB repair by HR and NHEJ

Schematic model of the two major double strand repair pathways. The DSB is first sensed by PIKK kinase ATM/Tel1. Depending on the cell cycle stage, Ku or exonucleases is activated or recruited to the break, which determines the choice of the two pathways. Left: homologous recombination involves exonucleases resection, recruitment of RPA, formation of Rad51 filament, strand invasion and strand resolve. Right: non-homologous end joining depends on Ku70/80 heterodimer that binds and tethers the two ends, along with DNA polymerase that resynthesize damaged or mismatched nucleotides, and ligase 4 that fills the gap between the break.

A checkpoint is also activated in response to the DSB to allow enough time for repair before the cell cycle progresses, and many DNA repair proteins are also involved in this process. ATM, which is recruited to the DSB, activates the end processing that generates 3'-ended ssDNA and in doing so, stimulates both repair and checkpoint activation. RPA-coated ssDNA activates a second PIKK family kinase, ATR, and its binding partner ATRIP. Along with mediator proteins including 53BP1, they activate of the checkpoint proteins Chk1 and Chk2, which inhibit the mitosis induction phosphatase Cdc25 and prevent entry into mitosis until DNA repair is completed (Khanna et al., 2001). Meanwhile, activated Chk1 regulates the HR repair pathway via phosphorylation of Rad51 (Sorensen et al., 2005).

1.3.2 Telomeres avoid checkpoint signalling via specialized chromatin

Telomeres structurally resemble DSBs in that they both mark the ends of chromosomes. While telomeres do engage a range of DDR components, including MRN, ATM and ATR (Verdun et al. 2005, Moser et al. 2009, and see below), a full DNA damage response is repressed at functional telomeres. Disruption of shelterin complex often evokes a fully activated checkpoint and DDR; therefore, telomeres are distinguished from DSBs by the specialized protein complexes that are recruited by the telomeric repeats (reviewed in (Longhese, 2008)). In human cells, the telomeric dsDNA binding protein TRF2 has been shown to repress ATM, while the ssDNA binding protein Pot1 was suggested to repress ATR signalling (Karlseder et al., 2004, Lazzerini Denchi and de Lange, 2007). The involvement of telomere proteins in ATM and ATR suppression is also indicated from research in budding yeast. The ssDNA binding protein Cdc13 attenuates $Mec1^{ATR}$ association at telomeres, while the $Tel1^{ATM}$ localization is inhibited by the Rap1-Rif1/2 complex at the telomeric dsDNA (Hirano and Sugimoto, 2007, Hirano et al., 2009). Additionally, it has been shown in fission yeast that telomeres lack H4K20me2, a ubiquitous histone H4 marker in most of the genome that is a prerequisite to stable association of the checkpoint mediator Crb2 (Du et al., 2006), thereby forming a chromatin-privileged region exempt from checkpoint signal (Carneiro et al., 2010).

1.3.3 DDR proteins are involved in telomere maintenance

Even though functional telomeres do not evoke a full DNA damage response, they recruit proteins involved in DDR during a normal cell cycle, in particular in S/G_2 phase during telomere replication (reviewed in (Rog and Cooper, 2008, Subramanian and Nakamura, 2010)). This recruitment is not a passive process where the telomeres are caught with insufficient protection; rather, several DDR proteins have been shown to be actively required for stable telomere maintenance in a range of model organisms. Take fission yeast for example: $Tel1^{ATM}$ and $Rad3^{ATR}$ are redundantly required for telomere maintenance; their simultaneous inactivation leads to a severe telomere maintenance defect and loss of telomere signal (Naito et al., 1998, Moser et al., 2009b). In addition, generation of the G-rich overhang requires the MRN complex and the DNA helicase-nuclease Dna2 at least in a *taz1Δ* background (Tomita et al., 2003, Tomita et al., 2004), while the Ku70-Ku80 heterodimer is proposed to inhibit recombination and nucleolytic activity at telomeres (Baumann and Cech, 2000).

The roles of DNA damage response proteins at dysfunctional telomeres are slightly more confusing. Telomerase removal and/or certain disruptions of shelterin lead to DDR responses and attempts to repair telomeres as DSBs. At this point, maintenance of chromosomal linearity via elevated HR and/or telomerase activity is presumably beneficial, as NHEJ between telomeres results in mitotic catastrophe and genomic instability (Karlseder et al., 1999). DDR proteins have been shown to be involved in both of these processes. In budding yeast, the HR repair proteins Rad52, Rad50 and Rad51 contribute to the protection of telomeres in the absence of telomerase even before they hit the critically short stage (Le et al., 1999). In *S. pombe*, Rad51 (previously Rhp51), but not Rad50, was shown to be required for telomere maintenance in the absence of the Ku70-Ku80 heterodimer (Kibe et al., 2003), while $Rad22^{Rad52}$ is required for robust inhibition of NHEJ at *taz1Δ* telomeres (Ferreira and Cooper, 2001). In *ccq1Δ* cells, HR proteins do not appear to contribute to telomere protection during the initial resulting telomere attrition; however, at a later stage when they maintain extremely short but stable telomeres based on HR, recombination proteins Rad51 and Rad54, as well as checkpoint

proteins Rad3^{ATR}, Rad17, Crb2^{53BP1} and Chk1, are required for maintenance of linear chromosomes (Tomita and Cooper, 2008).

1.4 Telomere dysfunction

Telomere dysfunction can occur as a result of a deficiency in shelterin, disruption of certain DDR factors, or telomere erosion in the absence of telomerase. With the complexity of telomere function and the numerous pathways that participate in it, telomere dysfunction comes in different flavours. A few phenotypes commonly observed at dysfunctional telomeres are described here.

1.4.1 Telomere dysfunction-induced focus

While functional telomeres are protected from unnecessary DNA repair machinery, dysfunctional, uncapped telomeres are often recognized as DNA lesions and targeted by DNA repair apparatus, inducing foci of DDR factors at telomeres. In mammalian cells, TRF2 deletion induces a robust DNA damage signal at telomeres that is dependent on ATM, with DDR factors such as 53BP1 and MRE11 accumulating at TRF2-deficient telomeres. Similarly, ATR-dependent DDR is observed at POT1a-deficient telomeres. The cytological characteristic, i.e. formation for repair foci that are otherwise suppressed at functional telomeres, is termed the telomere dysfunction-induced focus (TIF) (Takai et al., 2003, Lazzerini Denchi and de Lange, 2007). DNA damage foci induced by telomere dysfunction are also observed in fission yeast at Taz1-deficient telomeres (Carneiro et al., 2010). TIFs are used as a cytological marker for telomere dysfunction and are often accompanied by other maintenance defects (see below).

1.4.2 Excessive overhang

The telomeric overhang is crucial for telomere function both as a substrate for telomerase action, and as a platform for recruiting specific ssDNA binding proteins that are essential for telomere protection. Overhang generation involves multiple steps of telomere maintenance including end resection and elongation by telomerase. Perturbation of either of these processes can lead to abnormal

telomeric overhang, which can be detected using biochemical means such as in-gel hybridization and duplex-specific nuclease digestion (Dionne and Wellinger, 1996, Zhao et al., 2008).

Telomerase action affects the amount of overhang transiently during the late S/G_2 phase of the cell cycle, which is then compensated by C-strand fill-in synthesis. Therefore, elevated telomerase action alone does not necessarily lead to increased telomeric overhang (Cristofari and Lingner, 2006), but uncoupling between G- and C-strand synthesis does. In fission yeast, *taz1*Δ cells show elevated telomeric ssDNA signal partially dependent on telomerase (Tomita et al., 2003), which is consistent with elevated G-strand synthesis by telomerase due to fork stalling, while the C-strand fill-in is likely to be impaired due to Taz1 deficiency.

Regulation of end resection can be achieved by coordinated action between telomeric proteins and nucleases. The ssDNA binding proteins, including Pot1 in fission yeast and mammals and Cdc13 in budding yeast, play crucial roles, by hiding the ends of the telomeres and inhibiting DDR and resection (see section 1.2). Since generation of ssDNA is the determinant step of homologous recombination, and resection potentially reduces the amount of dsDNA and HR-inhibiting telomeric factors, excessive overhang is often associated with hyper-recombination at telomeres (see below).

1.4.3 Hyper-recombination

Unprotected telomeres are often recognized as DSBs, which in eukaryotes can be repaired by two major processes, recombination-based mechanism (including homologous recombination and break-induced replication), and non-homologous end joining (NHEJ). While NHEJ joins two broken ends with no homology, making it an error-prone pathway, the recombination-based mechanism requires homologous sequence and is initiated by resection of the 3' strand. The choice between the two mechanisms is regulated by the cell cycle, with homologous recombination being the preferred mechanism in S and G_2 phase when an intact sister chromatid is available to provide error free repair (Ferreira and Cooper, 2004) (reviewed in (Aylon and Kupiec, 2004)).

Although the outcome of recombination-based mechanisms at telomeric and sub-telomeric region is potentially silent due to reciprocal exchanges of the sequence, it can be examined experimentally by CO-FISH (telomeric chromosome-orientation fluorescence *in situ* hybridization) in mammalian cells, or by tracking the STE pattern on Southern blots (Lundblad and Blackburn, 1993, Cornforth and Eberle, 2001). In mouse, loss of either RAP1 or POT1a/b, or TRF2 Ku70 double deficiency, induces elevated level of telomere sister chromatid exchanges as visualized by CO-FISH (Celli et al., 2006, Palm et al., 2009, Sfeir et al., 2010). In fission yeast, lack of Ku or Taz1 also leads to hyper-recombination, as evidenced by erratic STE pattern (Baumann and Cech, 2000, Miller et al., 2006). Hyper-recombination at telomeric regions is also observed in telomerase-deficient cells that maintain telomeres via recombination-based mechanisms, such as linear telomerase-minus survivors in yeasts, and ALT cells in human.

1.4.4 Chromosome fusion

A more deleterious result of telomere dysfunction is chromosomal fusion, which during mitosis can lead to breakage-fusion-bridge cycles and severe genome instability. Chromosome end fusion can be mediated by different mechanisms, the choice of which is dependent on the cell cycle state and the cause of telomere dysfunction. The product of fusion can be visualized by cytological analysis, or by biochemical analysis of the DNA using PCR or pulse-field gel electrophoresis (PFGE).

As fission yeast lacks a discernible G_1 phase, HR-based mechanisms prevail at DSB sites and at dysfunctional telomeres. Fusion following telomere attrition induced by either inhibition of telomerase or disruption of Pot1 is mediated by single-strand annealing (SSA), a recombinational mechanism that occurs between repetitive elements (Wang and Baumann, 2008). The SSA-mediated fusion is dependent on the recombination protein $Rad22^{Rad52}$, and the endonuclease Rad16 and Swi10, but not the NHEJ proteins Ku and Lig4. In contrast, Ku- and Lig4-dependent NHEJ confer telomere fusion in G_1 arrested cells with deprotected telomeres, for example in *taz1*Δ strains after nitrogen starvation (Ferreira and Cooper, 2001).

In mammalian cells, removal of TRF2 from telomeres results in Ku- and DNA ligase IV-dependent canonical NHEJ throughout the cell cycle (Celli and de Lange, 2005, Smogorzewska et al., 2002). TRF1/2 double knockout further revealed an alternative NHEJ mechanism that is independent on Ku70/80 and Lig4, but is instead promoted by Lig3 and PARP1 (Sfeir and de Lange, 2012). Inhibition of the ssDNA binding proteins POT1a/b in mouse also lead to a 10-fold increase in chromosome end fusion compared to *wt* cells, although the phenotype is minor compared to TRF2-deficient cells (Hockemeyer et al., 2006).

1.5 Mode of survival without telomerase

In human, telomerase is expressed in germ cells, and not in most somatic cells. The lack of telomerase expression is proposed to be a mechanism to limit the lifespan and prevent accumulation of genetic error introduced by DNA replication and DNA damaging agents. For example, human fibroblasts can undergo 40-50 cell divisions before the telomeres become critically short and induce cellular senescence and apoptosis (Hayflick and Moorhead, 1961, Harley et al., 1990). However, in rare cases cells regain the ability to maintain telomeres, thereby bypassing this molecular 'clock' of cell division. These cells become immortalized, and *in vivo* they have the ability to proliferate indefinitely, a prerequisite for cancer.

Around 90% of cancers bypass telomere-mediated control of cell division by re-activating telomerase expression. Nonetheless, these cells often lose telomeres spontaneously, presumably due to oncogene-mediated replication stress and DDR deficiency, exacerbating genomic instability (Fouladi et al., 2000). The other 10-15% utilize the telomerase-independent, alternative lengthening of telomere (ALT) mechanisms to maintain the telomeres (Bryan et al., 1997). Additional mechanisms are found in other organisms, and may contribute to genomic instability in human cells as well.

1.5.1 Recombination-based telomere maintenance

The ALT pathway utilizes a recombination-based mechanism. Although the exact mechanism is yet to be determined, it has been proposed that the ALT pathway

uses a range of telomere sequence-containing structures as template, and a DNA replication mechanism similar to that of break-induced replication (BIR) to extend the telomeres (reviewed in (Cesare and Reddel, 2010)). The template can be the telomere of another chromosome or the sister chromatid; alternatively, BIR can occur intra-molecularly by t-loop formation (Henson et al., 2002, Muntoni et al., 2009). One feature of ALT cells is the abundance of extrachromosomal telomeric DNA such as t-circles and C-circles (double-stranded and single-stranded telomeric sequence containing circle), which can occur as a result of telomere loop (t-loop) excision, and were proposed to serve as the template for rolling-circle replication of the telomeres (Wang et al., 2004, Nabetani and Ishikawa, 2009). The MRN complex, the RecQ-like helicases BLM and WRN, and the recombination proteins RAD51 and RAD52, are involved in ALT activity (Yeager et al., 1999, Wu et al., 2000).

Recombination-based telomere maintenance is also found in other organisms, such as the budding yeast Type I and II survivors that arise in the absence of telomerase, where the mechanism has been studied in great detail. In budding yeast, recombination-based survival can occur via two different pathways, Rad50-dependent (Type I) or Rad51-dependent (Type II), both of which require the recombination protein Rad52 (reviewed in (McEachern and Haber, 2006)). While Type I survivors maintain chromosomal linearity by amplification of the Y' subtelomeric elements, Type II survivors require the MRX complex and Sgs1 helicase and display long tracts of telomeric repeat, resembling the ALT pathway in mammalian cells (Teng et al., 2000, Chen et al., 2001, Huang et al., 2001).

In fission yeast cells, linear survivors that utilize recombination-based telomere maintenance also form after telomerase removal (Nakamura et al., 1998). Like *wt* cells, linear survivors grow well in rich media, and are not sensitive to the DNA damaging agent MMS (Jain et al., 2010). However, their telomeres are unstable and are often subject to attrition, presumably due to the HR-inhibitory effect of Taz1 (Subramanian et al., 2008).

1.5.2 Circular survivors in fission yeast

A unique survival mode without telomerase exists in the fission yeast *S. pombe*. As these cells contain only three chromosomes, in theory it is relatively easy for all three chromosomes to undergo intra-chromosomal fusion in cells lacking inter-chromosomal fusions. Thus, fission yeast lacking telomerase can maintain circular chromosomes, thus avoiding the mitotic catastrophe associated with dicentric chromosomes (Nakamura et al., 1998). These survivors lack telomere sequences, but can retain sub-telomeric sequences at the fusion sites. Unlike *wt* and linear survivors, circular survivors are hyper-sensitive to MMS, and grow very slowly (Jain et al., 2010).

1.5.3 HAATI survivors

A third survival mode, HAATI (heterochromatin amplification-mediated and telomerase independent), was recently discovered in fission yeast (Jain et al., 2010). These survivors maintain chromosomal linearity by amplifying non-telomeric heterochromatin sequences such as the STE and rDNA repeats. Telomere-specific proteins Pot1 and Ccq1, as well as the recombination machinery, are crucial for HAATI formation. The HAATI mechanism to maintain chromosomal linearity is reminiscent of the one used by the fruit fly *Drosophila melanogaster*, which maintains linear chromosomes with heterochromatic retrotransposon elements (Biessmann et al., 1990).

Of the three telomerase-independent survival modes reported in fission yeast, formation of circular survivors appears to be the most frequent. This is evidenced by the early appearance of fusion bands after $trt1^{+}$ deletion. In addition, tetrad dissection analysis of $pot1^{+/\Delta}$ heterozygous diploid always yields small but viable colonies for the *pot1*Δ genotype, which suggests that chromosomal circularization after Pot1 removal is highly efficient. However, after prolonged propagation of a *trt1*Δ mutant, circular survivors are often outgrown by the faster growing, albeit less frequent, HAATI and linear survivors (Jain et al., 2010).

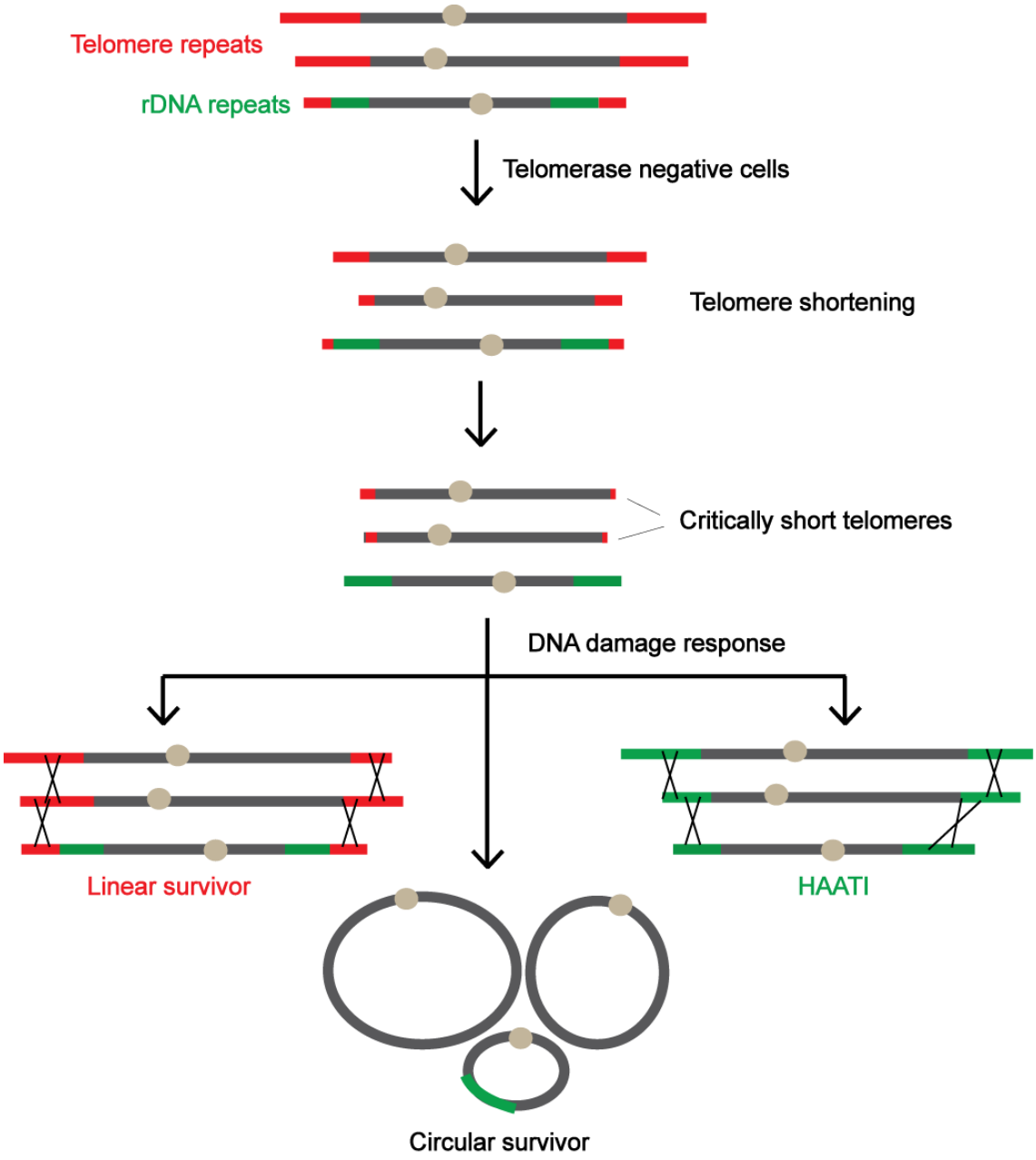

Figure 1.4 Modes of survival in the absence of telomerase in fission yeast

Telomeres gradually shorten with each cell division in the absence of telomerase, until they become critically short and lose the ability to inhibit DNA damage response. Attempts to repair exposed ends can result in three telomerase-independent survival modes. Left: linear survivors elongate telomeres by homologous recombination. Middle: circular survivors are formed by SSA-mediated intra-chromosomal fusion. Right: HAATI survivors maintain chromosomal linearity by amplifying generic heterochromatin (most frequently rDNA) to all chromosomal ends, which in turn recruits telomere proteins including Ccq1 and Pot1 for protection.

1.5.4 Telomere crisis and telomerase-independent maintenance

Telomerase-independent maintenance of chromosomal linearity is considered a last resort for cells lacking telomerase-mediated maintenance. Switching from telomerase-dependent to telomerase-independent survival is associated with a global change of gene expression profile, which takes place as the cells go through crisis upon complete loss of telomere protection (Mandell et al., 2005). As opposed to checkpoint activation and cell cycle arrest, which can occur at dysfunctional telomeres, telomere crisis is often accompanied by chromosomal aberrations and cell death (Shay and Wright, 1989). Only approximately 1 in 10^7 human cells emerge immortalized following crisis, which echoes the low frequency of linear and HAATI survivors in fission yeast, suggesting that successful switching during crisis is a rare event.

Loss of telomerase by itself does not induce the switch to telomerase-independent maintenance; rather, it is the loss of telomere repeats that induces the switch. In human, although telomerase is not expressed in somatic cells, chromosomal end protection is not normally impaired. Similarly, in *trt1*Δ yeast cells, although telomeres gradually shorten due to the end-replication problem, the capping function of telomere remains until it reaches a critically short length, at which point the telomeres become too short to accommodate enough telomere proteins to inhibit DNA repair.

Telomerase-independent maintenance is also distinct from telomeric hyper-recombination, which often occurs as a result of telomere dysfunction but still depends on telomerase to maintain telomeres. One example is the *taz1*Δ in fission yeast, which maintains long and heterogeneous telomeres typical of hyper-rec mutants. Nonetheless it requires deregulated telomerase action; removal of telomerase does not result in immediate recombinational telomere maintenance, but rather rapid telomere loss (Miller et al., 2006). So far, crisis and cell death appears to be a common step in the formation of telomerase-independent survival.

1.6 Telomeric ssDNA binding complexes

Oligonucleotide/oligosaccharide-binding (OB)-fold proteins are a family of ssDNA binding proteins that exist in both prokaryotes and eukaryotes. They have been shown to function in different aspects of DNA metabolism, including replication and DNA damage response pathways. While the sequence homology is low among members of this family, their OB-folds share conserved structural features that mediate protein-ssDNA interaction (Murzin, 1993).

In Eukaryotes, the telomeric overhang is a conserved feature in almost all organisms investigated; a few exceptions such as the fruit fly *Drosophila* and angiosperm plants are not known to display this feature, and instead may use alternative mechanisms to maintain chromosomal linearity (Biessmann et al., 1990, Kazda et al., 2012). The presence of ssDNA is justified by its function as the telomerase substrate. However, its reactive nature demands highly efficient and specialized protection to ensure genome stability, and eukaryotes employ two conserved complexes, the CST and Pot1-Tpz1, to fulfil these functions.

1.6.1 CST complex

The CST complex has been dubbed the telomere-specific RPA (t-RPA) due to its structural similarity to the replication protein A complex (Gao et al., 2007). In budding yeast where it was first discovered, the three subunits, Cdc13, Stn1 and Ten1, resemble the RPA subunits Rpa1, Rpa2 and Rpa3, respectively. Cdc13 contains two OB-folds, which bind telomeric ssDNA specifically and recruits Stn1 and Ten1. Together, they protect the telomeres from nucleolytic activities, and function in telomere replication by recruiting telomerase and DNA polymerase α (Garvik et al., 1995, Qi and Zakian, 2000). Disruption of CST leads to defects in both telomere end protection and in telomerase recruitment, which can be bypassed by tethering Stn1 and Est1 to the telomeres (Pennock et al., 2001).

Components of the CST complex in higher organisms were later discovered by sequence and/or structure homology to the budding yeast CST. In mammals, the CST complex is composed of CTC1, STN1 and TEN1. Similar to its orthologs in budding yeast, CTC1 contains multiple OB-folds, while STN1 and TEN1 each have

one. While the complex localizes to telomeric overhangs, it displays no sequence specificity for telomeric DNA, and was shown to have both telomeric and non-telomeric functions in replication (Miyake et al., 2009, Stewart et al., 2012). In fission yeast, although a Cdc13 ortholog is yet to be identified, a RPA2-Rpa3-like complex of Stn1-Ten1 has been shown to localize to the telomere and function in telomere maintenance (Martín et al., 2007, Sun et al., 2009). Stn1 and Ten1 each have a putative OB-fold that mediates their binding to the ssDNA. Deletion of either *stn1*$^{+}$ or *ten1*$^{+}$ leads to loss of telomere signal as seen with Pot1 deficiency (see below).

1.6.2 POT1-TPP1 complex

POT1-TPP1 (Pot1-Tpz1) is the telomeric overhang-binding sub-complex of shelterin and has been found in a wide range of eukaryotic organisms, including mammals, chicken, worm, *Arabidopsis* and fission yeast. While the C-terminal sequences of both proteins represent intrinsically disordered regions, the structures of the OB-fold domains are highly conserved (Wang et al., 2007). Pot1 contains two tandem OB-folds, of which the N-terminal one exhibits strong G-strand ssDNA binding ability *in vitro* (Lei et al., 2003, Lei et al., 2004). Tpp1 has one putative OB-fold, which does not bind ssDNA on its own but forms a heterodimer with Pot1 and increases its binding affinity to telomeric DNA.

In mammalian cells, the POT1-TPP1 complex suppresses ATR-mediated DNA damage response by controlling the amount of telomeric ssDNA and local exclusion of RPA (Hockemeyer et al., 2006, Gong and de Lange, 2010). This balance between RPA and POT1 at telomere ssDNA *in vitro* is orchestrated by hnRNPA1 and TERRA, whose levels are also regulated through the cell cycle *in vivo* (Flynn et al., 2011). The POT1-TPP1 complex also functions in telomere length regulation. Interestingly, this regulation acts both in a positive and a negative way. On one hand, overexpression of POT1 leads to telomerase-dependent over-elongation of the telomeres, suggesting its role as a positive regulator (Colgin et al., 2003). On the other hand, POT1 acts as a transducer of TRF1-mediated telomere length signal, providing negative feedback to ensure telomere length homeostasis

(Loayza and De Lange, 2003). The molecular mechanisms could involve its ability to inhibit formation of complex secondary structures at telomeric ssDNA, and increasing the activity and processivity of telomerase, possibly via interaction between TPP1 and telomerase (Wang et al., 2007, Zaug et al., 2010). However, how the balance between the positive and negative effects is controlled is currently unclear.

In fission yeast, the Pot1-Tpz1 complex appears to play a more crucial role in telomere maintenance. Disruption of this complex by deleting either of the components leads to rapid loss of telomere signal, with survival only by chromosome circularization (Baumann and Cech, 2001, Miyoshi et al., 2008). Pot1 is also involved in end protection by inhibition of resection at telomeres (Pitt and Cooper, 2010). In addition, the complex is crucial for the recruitment of telomerase via the interacting partner Ccq1 (Tomita and Cooper, 2008). However, the absolute requirement for the Pot1-Tpz1 complex in resection inhibition makes it difficult to dissect its additional function(s). Therefore, development of separation-of-function mutants could help achieve better understanding of the function and regulation of the proteins.

1.7 Fission yeast Pot1

1.7.1 Pot1 structure and ssDNA interaction

Fission yeast Pot1 was identified due to its sequence homology with the telomere protein TEBPα of the ciliate *Sterkiella nova* (formerly known as *Oxytricha nova*) (Baumann and Cech, 2001). The two OB-folds in the N-terminus interact with the telomeric ssDNA, whereas the C-terminal region was shown to mediate protein-protein interaction with it binding partner Tpz1 (Miyoshi et al., 2008). A truncation analysis showed that the isolated N-terminal region of Pot1 is not detected at the telomeres by immunofluorescence, while the isolated C-terminal region forms foci that co-localize with Taz1, suggesting that Pot1 indeed can be recruited via protein-protein interaction, presumably to the dsDNA region of the telomeres (Bunch et al., 2005). It is proposed that recruitment via protein-protein interaction to telomeric

dsDNA contributes to local enrichment of Pot1 and facilitates competition with other high affinity ssDNA binding proteins such as RPA. End protection by Pot1 requires both the N-terminal and the C-terminal regions, as mutants lacking either the OB-folds or a few amino acids at the C-terminus fail to complement for the loss of Pot1 (Bunch et al., 2005).

While a structure for full-length Pot1 is not available, the N-terminal OB-fold (residues 5-174), which shares strong sequence similarity with its ciliate ortholog TEBPα, has been solved in complex with telomeric ssDNA (Lei et al., 2003). Although Pot1-ssDNA interaction *in vivo* requires a second Pot1 OB-fold and Tpz1, the N-terminal OB-fold is capable of ssDNA binding *in vitro*. The X-ray crystallographic structure revealed a basic concave groove of β barrel and two protruding loops that form a clamp. Twelve residues, R56, S58, T62, D64, H86, F88, K90, T111, Y115, Q120, L122, K124 and D125, were shown to interact with ssDNA via hydrogen bond or van deer Waals interactions (see Figure 1.5A for relative position of these sites).

Another study attempted to identify residues within the N-terminal OB-fold that are important for telomeric ssDNA recognition *in vitro* by mutational analysis combined with electrophoretic mobility shift assays (Torigoe and Furukawa, 2007). Mutations of T62, D64, F88, L122, and K124 result in complete loss of ssDNA binding affinity, suggesting that interactions mediated by these residues play significant roles in ssDNA recognition.

1.7.2 *pot1-V5* phosphorylation mutants

A recent study in the Cooper Laboratory revealed that fission yeast Pot1 interacts with, and is phosphorylated *in vivo* by, the master cell cycle regulator DDK, or Dfp1-dependent kinase (Kuznetsov, 2008). As a Pot1 antibody was not available, Pot1 was visualized using a C-terminally V5-tagged allele by 2-dimensional protein gel electrophoresis (2DGE), which separates the protein based on its isoelectric point (pI) as well as its molecular mass; phosphatase treatment of the sample prior to electrophoresis was used to detect the existence of phosphorylation (see Figure 5.1 for an example). The phosphorylation pattern changes when amino acid

residues in different regions are mutated, allowing mapping of regions that are important for the phosphorylation *in vivo*. Mutations within the N-terminal OB-fold, which contains five possible phospho-residues, T68, T75, T78, S79 and S80, lead to complete abolition of the phosphorylated form on 2DGE, with two residues, T68 and T75, having the strongest phenotype (Figure 1.5B). Therefore, the five amino acid residues were considered phosphorylation sites of Pot1, with T68 and T75 being the major sites.

While none of the residues were shown to directly interact with ssDNA in the X-ray crystallographic structure (Lei et al., 2003), T68 sits in the ssDNA-binding groove of the OB-fold, and its modification could potentially affect the ability of the OB-fold to interact with ssDNA. On the other hand, T75, T78, S79 and S80 are located in a loop structure that protrudes away from the protein-ssDNA interface and close to the α-helix at the junction between the first and second OB-folds (Figure 1.5C). Hence, these residues are less likely to be involved in ssDNA recognition, although they may contribute to proper folding of the protein or its assembly onto ssDNA *in vivo*.

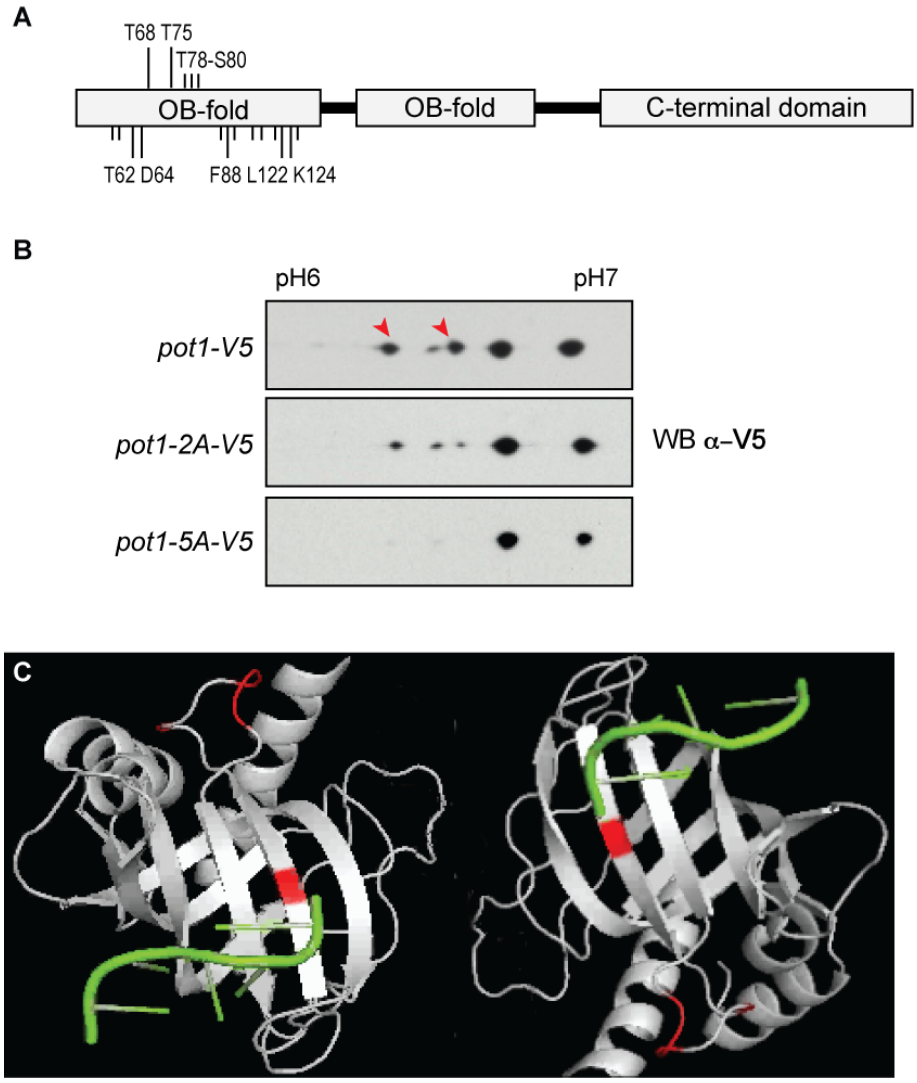

Figure 1.5 Structure of fission yeast Pot1

A. Schematic diagram of the functional domains of fission yeast Pot1. The N-terminal OB-fold mediates ssDNA interaction, while the C-terminal domain mediates protein interaction. Positions of the putative phosphorylation sites are marked above; long lines mark the major sites T68 and T75, short lines mark the minor sites T78, S79 and S80. Positions of the ssDNA-interacting residues (Lei et al., 2003) are marked beneath the box; the ones with *in vitro* phenotypes (Torigoe and Furukawa, 2007) marked by long lines. **B**. 2DGE showing loss of phosphorylation spots in *pot1-A-V5* mutants, mutants of Pot1-V5 are detected by α-V5 Western blot. Red arrowheads indicates phosphorylated spots in *wt* that are reduced or lost in the mutant strains. Adapted from (Kuznetsov, 2008). **C**. PyMol image of the N-terminal OB-fold crystal structure from different angles. The protein is coloured in grey and ssDNA in green. The red patch in the β-sheet marks T68, and the red lines in the loop mark T75, T78, S79 and S80.

Given the central role of DDK kinase in cell cycle regulation, in particular in licensing DNA replication and recovery from stalled replication forks, Pot1 phosphorylation by DDK would provide a useful mechanism to link S-phase events with those involved in telomere maintenance. Hence, the physiological function of the predicted phosphorylation was investigated *in vivo* (Kuznetsov, 2008). Phosphorylation-deficient mutants of *pot1-V5* (*pot1-A-V5*) were constructed by mutating either all five residues (*pot1-5A-V5*) or the two major phospho-sites (*pot1-2A-V5*) to Ala, which cannot be used as a phosphorylation substrate. The corresponding mutations to Asp, which carries a negative charge similar to a phosphate group, were considered as potential phospho-mimics (*pot1-2D-V5*). The *pot1-5D-V5* mutant was lethal to the cell, acting like a *pot1*$^{+}$ null. For simplicity, unless otherwise specified, the phospho-deficient mutants (*pot1-2A-V5* and *pot1-5A*-V5) are referred to as *pot1-A*-V5, and the phospho-mimic mutant (*pot1-2D-V5*) is referred to as *pot1-D-V5* in the text.

Phenotypic analysis of these mutants, either alone or in combination with other genetic alternations, showed that while the phospho-deficient mutants exhibit multiple defects in telomere maintenance, the phospho-mimic *pot1-D-V5* mutant behaves similarly to a *wt* allele in the V5-tagged background (Kuznetsov, 2008). The latter almost fully recapitulates the wild-type *pot1-V5* phenotype in terms of checkpoint suppression, telomere length, and telomerase dependence. Interestingly, however, it requires the DNA repair protein Rad51 for telomere maintenance. A model was proposed in which both the phosphorylated and unphosphorylated forms of Pot1 are required to maintain the telomere through the cell cycle: the phosphorylated form would function in telomere maintenance and protection against DDR, while the unphosphorylated form would act redundantly with Rad51 to protect the telomeres. Indeed, a model invoking sequential functions, coordinated by the arrival of DDK with the replication fork, could be envisioned. In such a model, unphosphorylated Pot1 would regulate telomeres prior to their replication, and upon arrival of DDK with the replication fork, Pot1 phosphorylation would alter its activities, thus contributing to the coupling between fork arrival and telomeric events.

1.8 Aim of this study

Pot1 is named in recognition of its role in telomere maintenance and protection. It has been shown to function in multiple aspects of suppression of DNA damage response and telomerase regulation. In fission yeast, inactivation of Pot1 leads to rampant end resection and loss of telomeres. This dramatic phenotype, however, complicates investigation of its function in other aspects. Development of new mutant alleles that do not shut off its function completely could therefore be interesting and beneficial.

Another point of interest is the regulation of telomere function in different cell cycle stages. Telomeres are responsible for two different, and almost opposite, functions: they need to allow the replication machinery and telomerase to access and duplicate the DNA during late S/G_2 phase, while protecting the chromosomal ends against attack from the DNA damage repair machinery in other phases of the cell cycle. These functions must be carefully coordinated and balanced at telomeres to maintain genomic stability. However, how the telomeres achieve the balance is not understood yet.

The discovery of Pot1 phosphorylation *in vivo* provides us an exciting opportunity to develop new alleles and explore potential modulation of Pot1 function through the cell cycle. Using mutants that are either deficient in or mimicking phosphorylation, we can investigate: 1, the functions of Pot1 in different aspects of telomere protection, which might be coordinated by phosphorylation *in vivo*; and 2, how this might be regulated in accordance with the cell cycle stages by regulation of the activity of DDK kinase. The model proposed by the previous work (Kuznetsov, 2008) was examined in detail in this study. A few caveats were identified due to experimental procedures, and a modified model is proposed to respond to the new data.

Chapter 2. Materials & Methods

2.1 Strains and growth

2.1.1 Fission yeast strain list

JCF	Relevant genotype	Source
20	*wt*	Lab stock
28	*taz1::ura4*	Lab stock
1131	*pot1-1:kan*	Lab stock
1675	*ura4::internal-telo:LEU2*	Lab stock
1677	*taz1::kan ura4::internal-telo:LEU2*	Lab stock
6369	*pot1-V5:kan*	Lab stock
6545	*aur1R::pot1-V5/aur1+ pot1::kan/pot1+*	Lab stock
6561	*aur1R::pot1-2A-V5/aur1+ pot1::kan/pot1+*	Lab stock
6609	*aur1R::pot1-2D-V5/aur1+ pot1::kan/pot1+*	Lab stock
6627	*aur1R::pot1-5A-V5/aur1+ pot1::kan/pot1+*	Lab stock
6699	*aur1R::pot1-V5/aur1+ pot1::kan/pot1+ chk1::hph/chk1+*	Lab stock
7001	*aur1R::pot1-2A-V5/aur1+ pot1::kan/pot1+ chk1::hph/chk1+*	Lab stock
7003	*aur1R::pot1-2D-V5/aur1+ pot1::kan/pot1+ chk1::hph/chk1+*	Lab stock
7005	*aur1R::pot1-5A-V5/aur1+ pot1::kan/pot1+ chk1::hph/chk1+*	Lab stock
7024	*aur1R::pot1-V5/aur1+ pot1::kan/pot1+ trt1::hph/trt1+*	Lab stock

JCF	Relevant genotype	Source
7026	*aur1R::pot1-2A-V5/aur1+ pot1::kan/pot1+ trt1::hph/trt1+*	Lab stock
7028	*aur1R::pot1-2D-V5/aur1+ pot1::kan/pot1+ trt1::hph/trt1+*	Lab stock
7030	*aur1R::pot1-V5/aur1+ pot1::kan/pot1+ rad51::hph/rad51+*	Lab stock
7032	*aur1R::pot1-2A-V5/aur1+ pot1::kan/pot1+ rad51::hph/rad51+*	Lab stock
7034	*aur1R::pot1-2D-V5/aur1+ pot1::kan/pot1+ rad51::hph/rad51+*	Lab stock
7036	*aur1R::pot1-5A-V5/aur1+ pot1::kan/pot1+ rad51::hph/rad51+*	Lab stock
7038	*aur1R::pot1-5A-V5/aur1+ pot1::kan/pot1+ trt1::hph/trt1+*	Lab stock
9005	*trt1-myc:hph pot1-V5:kan*	This study
9006	*trt1-myc:hph aur1R:pot1-V5 pot1:kan*	This study
9007	*trt1-myc:hph aur1R:pot1-2A-V5 pot1:kan*	This study
9008	*trt1-myc:hph aur1R:pot1-2D-V5 pot1:kan*	This study
9009	*trt1-myc:hph aur1R:pot1-5A-V5 pot1:kan*	This study
9019	*pot1-V5:kan/pot1+ taz1:hph/taz1+*	This study
9020	*aur1R:pot1-V5/aur1+ pot1::kan/pot1+ taz1::hph/taz1+*	This study
9021	*aur1R:pot1-2A-V5/aur1+ pot1::kan/pot1+ taz1::hph/taz1+*	This study
9022	*aur1R:pot1-2D-V5/aur1+ pot1::kan/pot1+ taz1::hph/taz1+*	This study
9023	*aur1R:pot1-5A-V5/aur1+ pot1::kan/pot1+ taz1::hph/taz1+*	This study

JCF	Relevant genotype	Source
9031	*pot1::kan/pot1+ aur1R:pot1-2A/aur1+*	This study
9032	*pot1::kan/pot1+ aur1R:pot1-2D/aur1+*	This study
9033	*pot1::kan/pot1+ aur1R:pot1-5A/aur1+*	This study
9034	*pot1::kan/pot1+ aur1R:pot1-5D/aur1+*	This study
9035	*pot1::kan/pot1+ aur1R:pot1/aur1+*	This study
9044	*pot1::kan/pot1+ aur1R:pot1/aur1+ rad22::nat/rad22+*	This study
9045	*pot1::kan/pot1+ aur1R:pot1-2A/aur1+ rad22::nat/rad22+*	This study
9046	*pot1::kan/pot1+ aur1R:pot1-2D/aur1+ rad22::nat/rad22+*	This study
9047	*pot1::kan/pot1+ aur1R:pot1-5A/aur1+ rad22::nat/rad22+*	This study
9048	*pot1::kan/pot1+ aur1R:pot1/aur1+ rad51::hph/rad51+*	This study
9049	*pot1::kan/pot1+ aur1R:pot1-2A/aur1+ rad51::hph/rad51+*	This study
9050	*pot1::kan/pot1+ aur1R:pot1-2D/aur1+ rad51::hph/rad51+*	This study
9051	*pot1::kan/pot1+ aur1R:pot1-5A/aur1+ rad51::hph/rad51+*	This study
9052	*pot1::kan/pot1+ aur1R:pot1/aur1+ trt1::hph/trt1+*	This study
9053	*pot1::kan/pot1+ aur1R:pot1-2A/aur1+ trt1::hph/trt1+*	This study
9054	*pot1::kan/pot1+ aur1R:pot1-2D/aur1+ trt1::hph/trt1+*	This study
9055	*pot1::kan/pot1+ aur1R:pot1-5A/aur1+ trt1::hph/trt1+*	This study

JCF	Relevant genotype	Source
9062	*pot1::kan/pot1+ aur1R:pot1/aur1+ rad3::hph/rad3+*	This study
9063	*pot1::kan/pot1+ aur1R:pot1-2A/aur1+ rad3::hph/rad3+*	This study
9064	*pot1::kan/pot1+ aur1R:pot1-2D/aur1+ rad3::hph/rad3+*	This study
9065	*pot1::kan/pot1+ aur1R:pot1-5A/aur1+ rad3::hph/rad3+*	This study
9070	*Pnmt81:kan:HA-pot1*	This study
9077	*pot1::kan ura4::internal-telo:LEU2*	This study
9078	*pot1::kan taz1::hph ura4::internal-telo:LEU2*	This study
9081	*pot1::kan/pot1+ aur1R:pot1-V5/aur1+ rad22::nat/rad22+*	This study
9082	*pot1::kan/pot1+ aur1R:pot1-2A-V5/aur1+ rad22::nat/rad22+*	This study
9083	*pot1::kan/pot1+ aur1R:pot1-5A-V5/aur1+ rad22::nat/rad22+*	This study
9084	*pot1::kan/pot1+ aur1R:pot1-2D-V5/aur1+ rad22::nat/rad22+*	This study
9089	*pot1::kan/pot1+ aur1R:pot1-V5/aur1+ rad3::hph/rad3+*	This study
9090	*pot1::kan/pot1+ aur1R:pot1-2A-V5/aur1+ rad3::hph/rad3+*	This study
9091	*pot1::kan/pot1+ aur1R:pot1-2D-V5/aur1+ rad3::hph/rad3+*	This study
9127	*cdc25-22 pot1::kan aur1R:pot1-wt-V5*	This study
9128	*cdc25-22 pot1::kan aur1R:pot1-2A-V5*	This study
9129	*cdc25-22 pot1::kan aur1R:pot1-2D-V5*	This study

JCF	Relevant genotype	Source
9130	*cdc25-22 pot1::kan aur1R:pot1-5A-V5*	This study
9143	*rap1::nat/rap1+ pot1::kan/pot1+ aur1R:pot1-wt-V5/aur1+*	This study
9144	*rap1::nat/rap1+ pot1::kan/pot1+ aur1R:pot1-2A-V5/aur1+*	This study
9145	*rap1::nat/rap1+ pot1::kan/pot1+ aur1R:pot1-2D-V5/aur1+*	This study
9146	*rap1::nat/rap1+ pot1::kan/pot1+ aur1R:pot1-5A-V5/aur1+*	This study
9147	*poz1::hph/poz1+ pot1::kan/pot1+ aur1R:pot1-wt-V5/aur1+*	This study
9148	*poz1::hph/poz1+ pot1::kan/pot1+ aur1R:pot1-2A-V5/aur1+*	This study
9149	*poz1::hph/poz1+ pot1::kan/pot1+ aur1R:pot1-2D-V5/aur1+*	This study
9150	*poz1::hph/poz1+ pot1::kan/pot1+ aur1R:pot1-5A-V5/aur1+*	This study

2.1.2 Media

Media	Components
YE	0.5% Difco yeast extract, 3% dextrose
YES	0.5% Difco yeast extract, 3% dextrose, 250 mg/ml uracil, adenine, histidine, leucine
ME	3% Bacto-malt extract (pH5)
Minimal	14.7 mM potassium hydrogen phthalate, 15 mM Na_2HPO_4, 93.5 mM NH_4Cl, 2% w/v glucose, salt stock, vitamin stock, mineral stock
Minimal –N	14.7 mM potassium hydrogen phthalate, 15 mM Na_2HPO_4, 2% w/v glucose, salt stock, vitamin stock, mineral stock

2.1.3 Vegetative growth conditions

To obtain vegetative growth, strains were grown at 32ºC in rich media as liquid culture or on 2% agar plates unless otherwise stated. Serial passages on plates were performed by selecting single colonies and re-streaking onto a new plate, with the exception of patching experiments. Antibiotic selections were applied by addition of the following chemicals (Bahler et al., 1998, Sato et al., 2005, Hashida-Okado et al., 1998):

Resistance	Components
aur	0.5µg/ml aureobasidin A (Takara Bio)
hph	300µg/ml hygromycin B (Roche)
kan	200µg/ml geneticin G418 (Gibco)
nat	100µg/ml nourseothricin (Werner Bio-agents)

2.1.4 Growth curve and dilution assay

Growth curves are obtained by measuring OD_{595} of an exponentially growing culture every hour. An OD_{595} of 0.1 equals approximately $1x10^6$ cells/ml for *wt* cells.

Dilution assays were performed with log phase culture at a starting concentration of $1x10^7$ cells/ml (OD_{595} =1.0) and diluted in 5-fold increments. Each dilution was then spotted onto agar plates with desired selection or agents.

2.2 Strain construction

2.2.1 Mating and sporulation

To induce meiosis, haploid cells of the opposite mating type, or diploid cells in the case of azygotic meiosis, were patched and mixed on ME plate, and incubated at 30ºC for 2 days (except for temperature sensitive strains for which mating were carried out at 25ºC). Spores were released in 0.5% Helix Pomatia Juice (Pall Biosepra) and resuspended in distilled water. Approximately 200-500 spores were plated on selective plates on obtain the desired genotype.

2.2.2 Transformation for tagging, deletion, or insertion

Constructs of gene C-terminal tagging or deletion with antibiotic and auxotrophic markers were performed using the one-step PCR technique (Bahler et al., 1998, Sato et al., 2005). Insertion of sequences at *aur1* locus was performed using pCST159 plasmid as described in the literature (Chikashige et al., 2006). Yeasts were transformed using the LiAc method:

1. Spin down 5ml of OD 0.5 culture, 3min at 3k rpm.

2. Resuspend cell pellet in 1ml distilled water, and transfer to 1.5ml eppendorf tube. Wash cells with 500µl LiTE.

3. Resuspend cell pellet in 100µl LiTE, add 10µl transformation DNA (digested plasmid or PCR product). Mix gently by pipetting, incubate at room temperature for 10min.

4. Add 260µl PLATE, mix gently by pipetting. Incubate at 32ºC (or 25ºC for temperature sensitive strains) for 30-60min.

5. Add 43µl DMSO, mix gently by pipetting. Heat shock at 42ºC for 5min.

6. Cool down samples at room temperature for 1min. Flash spin, wash 2X with 1ml water.

7. Resuspend pellet in 200µl water. Plate cells on YES, and incubate at 32ºC overnight.

8. Replica onto selective plate the next day. Verify genotype of selected colonies by PCR.

Solutions

Li-TE

0.1M LiAc pH7.5
10mM Tris-HCl pH7.5
1mM EDTA

PLATE

40% PEG-4000
0.1M LiAc
10mM Tris-HCl
1mM EDTA

2.3 Cell cycle analysis

2.3.1 G2 arrest using *cdc25-22* mutant

Temperature sensitive *cdc25-22* mutant strains were constructed by mating, and selected by checking cell elongation after 3h temperature shift at 36ºC.

To block cells in G2 phase, early/mid-log phase (OD 0.2-0.4) cultures grown at permissive temperature were shifted to restrictive temperature 36.5ºC for 4h, and then released by shifting temperature back to 25ºC.

At each time point, 1ml of the culture was fixed in 70% ethanol to follow synchrony by FACS or septation index.

2.3.2 G1 arrest by nitrogen starvation

To achieve best synchrony by nitrogen starvation, prototrophic strains were constructed by mating. Auxotrophic strains can be used with addition of 1/3 of normal amounts of supplements, which yields less efficient starvation and poor synchrony.

1. Grow prototrophic strains to log phase in minimal media.
2. Harvest cells by vacuum filtration or centrifugation at 3krpm, wash 3 times with minimal-N medium.
3. Resuspend cells in minimal-N media to OD=0.5. Grow for 16h at 25ºC shaker generally generates >80% synchrony. Alternatively grow for 9h at 32ºC, which generates >60% synchrony.
4. Release by re-feeding with 1x NH_4Cl. At 32ºC, S phase starts at 2.5h and finishes by 3.5h.

2.3.3 FACS analysis

1. Spin down 1ml OD 0.5 culture, resuspend cells in 1ml cold 70% ethanol. Sample can be kept at 4°C before processing.

2. Vortex well before processing. Add 0.5ml to 1ml 50mM NaCitrate. Vortex and spin down, 1min at 13k rpm.

3. Resuspend cell pellet in 1ml 50mM NiCitrate, spin down, 1min at 13k rpm.

4. Resuspend cells in 0.5ml 50mM NaCitrate containing 0.1mg/ml RNase A, incubate for at least 2h at 37°C.

5. Dilute Propidium iodide (PI) stock 1:62.5 to 16µg/ml in 50mM NaCitrate. Add 0.5ml to each sample. Cells can be stored at 4°C in dark for up to a week before processing.

6. Before processing, sonicate samples at 10 microamplicons for 6sec. Votex, dilute 30-100µl of sample in 600µl of 50mM NaCitrate in FACS tubes, and votex again.

7. Measure samples on FACS machine.

2.4 Microscopic analysis

2.4.1 Cell length measurement

For analysis of cell length distributions, exponentially growing cells were harvested and photographed under a Zeiss Axioplan 2 microscope. Cell length was measured in Volocity Image Analysis Software.

2.4.2 Septation Index

To score the septation index, cell cycle progression samples fixed in 70% ethanol were spun down and rehydrated with water. 0.1mg/ml calcofluor solution was added to the sample on a coverslip and incubated for 2 min at room temperature. Samples were then observed under a Zeiss Axioplan 2 microscope to count the percentage of cells with septum. The peak of septation corresponds to S phase of the cell cycle.

2.4.3 Immuno-fluorescence

1. Spin down 10ml of OD0.5 culture, resuspend in 0.77ml PEM. Add 0.23ml para-formaldehyde (from freshly-opened ampule, stock solution 16%) to a final concentration of 3.7%, mix and incubate on wheel at room temperature for 10-15min.

2. Wash cells 3X with 1ml PEM (10sec to 2min, 12K rpm). Resuspend in 1ml PEMS with 1mg/ml Zymolyase-100T (AMSBio). Incubate for 90 minutes at 37°C, mix occasionally.

3. Resuspend in PEMS + 1% Triton-X100. Wait 30sec or up to 5min. Spin down and wash 3X with PEM.

4. For FISH only: Resuspend in PEMBAL + 0.2mg/ml RNase A, incubate at 37°C 2 hours. Rotate fixed cells in PEMBAL at room temp for 30 minutes to block.

5. Spin down and resuspend in 40-300 µl PEMBAL + 1st antibody. Rotate overnight at room temp. Concentration of antibodies used in this study: mouse α-V5 (AbD serotec) 1:500, rabbit α-Rhp51 (AbCam) 1:1000, rabbit α-Taz1 (lab stock) 1:500.

6. Wash 4X 15min with PEMBAL. Resuspend in 40-300 µl PEMBAL + 2nd antibody, rotate with foil wrapped at room temp for 2h. Concentration of antibodies used in this study: Alexa Fluor series antibodies (Invitrogen) anti-mouse 488, anti-rabbit 546 at 1:2000.

7. Wash 3X 15min with PEMBAL, resuspend in 0.3ml PEMBAL. Samples can be stored at 4°C for years at this stage.

8. Cells are analyzed under DeltaVision Microscopy Imaging System. To stain DNA with DAPI, add 0.5µl sample to 2.5µl mounting media (Vector Laboratories) on a coverslip.

Solutions

PEM

100mM PIPES, pH 6.9 (pH with NaOH to dissolve)
1mM EDTA
1mM MgSO4

PEMS

PEM
1.2M Sorbitol

PEMBAL

PEM
1% BSA
0.1% Sodium azide
100mM L-Lysine hydrochloride
Filter sterilize

2.5 DNA analysis techniques

2.5.1 Genomic DNA extraction

1. Grow cells to OD1.0, spin down, and wash with 1ml smash prop buffer. Pellet can be stored at -20°C.

2. Add 400µl smash prep buffer, 400µl of glass beads (not to reach the surface) and 400µl phenol:chloroform:isoamyl alcohol 25:24:1 (v/v). Votex on Disrupter for 5min at 4ºC.

3. Centrifuge at 13k rpm for 10min. Transfer the aqueous layer to new 1.5ml eppendorf tube.

4. Add 2.5X volume pre-chilled 96% ethanol, votex and incubate at -20°C for at least 2h. Alternatively, incubate at -80°C for 15min, votexing every 15min (less yield).

5. Centrifuge at 4°C, 13k rpm for 10min. Remove supernatant.

6. Wash the pellet with 1 ml 70% ethanol for 30min at room temperature.

7. Centrifuge at 13k rpm for 5min. Air-dry the pellets at room temperature until no liquid can be seen at the bottom.

8. Re-suspend pellet in 50 µl 0.5X TE-RNase, votex to dissolve, incubate at 37°C for 20min. The genomic DNA can be stored at -20°C indefinitely.

Solution

Smash prep buffer

2% Triton X-100
1mM EDTA
1% SDS
10mM Tris-Cl
100mM NaCl

2.5.2 Southern blotting for telomere length analysis

1. Genomic DNA extract is digested with *EcoRI* or *ApaI* restriction enzymes (NEB) overnight at 37°C or 25°C, respectively. To ensure equal loading, check DNA concentration on a gel before digestion.

2. Make 25cm-long, 1% agarose gel in 1x TBE containing 0.01mg/ml ethidium bromide. Load up to 30µl of sample per well, electrophorese at 100V for 5h or until required separation is achieved.

3. After visualizing under UV lamp, incubate gels in 0.25M HCl for 15min on a gently shaking platform to nick the DNA, followed by 30min in Blot 1 to denature, and 30min in Blot 2 to neutralize.

4. Prepare Hybond-N membrane by incubating in Blot 2 for 5min.

5. Set up dry transfer. On top of a 10cm-thick stack of paper tower and Whatman paper, lay the membrane and the gel sequentially. Cover the top of the gel with Saran wrap and a glass plate. Transfer overnight.

6. Auto-crosslink the DNA to the membrane with Stratagene UV crosslinker 2400. Pre-hybridize membrane in Church-Gilbert buffer for at least 1h at 65°C.

7. Prepare probe by labelling 25ng of double-stranded fragment (telomeric probe: synthetic telomere fragment or restriction digest of pIRT2-telo plasmid; subtelomeric probe: ApaI STE fragment of pNSU70 plasmid) using random primer labelling kit with 5µl α-^{32}P dCTP. Purify labelled probe using G-25 spin columns. Boil the labelled probe at 95ºC to denature the DNA immediately before use.

8. Add probe to the hybridization tube, mix with Church-Gilbert solution before it touches the membrane. Use half of the probe per blot. Incubate on wheel overnight at 65°C.

9. Wash membrane 2X 30min with washing buffer at 65°C. Wrap it in Saran, overlay with Storage phosphor screen (Amersham) to expose overnight or for a few days.

10. Read the screen using STORM840 PhosphoImage scanner.

Solutions

Blot 1

100mM NaOH
1.5M NaCl

Blot 2

20mM NaOH

1M NH_4Ac

Church-Gilbert solution

1% BSA

1mM EDTA

7% SDS

0.5M $NaHPO_4$ pH7.2

Washing buffer

2x SSC

0.1% SDS

2.5.3 In-gel hybridization

1. Genomic DNA extract is digested with *EcoRV* or *NsiI* restriction enzymes (NEB) overnight at 37°C. A control treatment by *E. coli* Exonuclease I (NEB) for 10min at 37ºC can be used before the restriction enzyme to test whether the ssDNA signal is located at the ends. To ensure equal loading, check DNA concentration on a gel before digestion. For easy handling, a separate set of samples is recommended for each probe.

2. Prepare 0.5% agarose gel in 0.5xTAE with 0.01mg/ml ethidium bromide (EB). Load digested DNA, heat denatured plasmid containing telomere signal 9pNSU70 or pIRT2-telo could be used) as ssDNA control, and native plasmids as dsDNA control. Electrophoresis at 100V for 1h or until desired separation is achieved. Picture gel under UV lamp.

3. Place the gel on a Hybond-N+ nylon membrane (Amersham) in 20xSSC, transfer it on top of 2 layers of Whatman paper on the Hoefer Slab Gel Dryer (Amersham). Be cautious as the gel is slippery. Cover the top with Saran wrap. Place a glass board on top to help even distribution of the force.

4. Vacuum dry the gel at 50ºC for 30 min up to an hour, changing direction as required, until the gel is completely dry. The dry gel should feel like a thin layer of membrane. Any lump will cause high background.

5. With the gel overlaid on top of the Nylon membrane, pre-hybridize it in Church-Gilbert buffer at 42ºC for at least 2 hours.

6. Prepare radioactively labelled single-stranded probe of C-rich and G-rich telomeric sequences with γ-^{32}P dATP and T4 polynucleotide kinase. 5µl of 10µM G- or C-strand ssDNA is used for each probe.

7. To detect native signal, add probe to the hybridization tube, and incubate at 42ºC overnight. Use G-rich probe to detect the background, and C-rich probe to detect the overhang signal. Wash the gel with plenty of Washing buffer for at least 8 hours at 42ºC. Longer washes up to one week are essential for low background signal.

8. Separate the gel from the membrane very carefully; try not to tear the gel. Wrap the gel in Saran wrap after gently absorbing excess buffer with tissue. Overlay the gel with Storage phosphor screen (Amersham) and expose for 1-7 days. Single stranded signal can be very weak and takes long time to obtain good quality exposure.

9. To denature the double-stranded DNA in the gel, soak the gel overlaid with the membrane in the denaturing solution for 25min, and the in neutralizing solution for 10min at room temperature. Pre-hyb again before dsDNA signal detection.

10. To detect the total telomere DNA, hybridize the gel overlaid on the membrane again with G-rich and C-rich probes. Wash at 42ºC for at least 8 hours, and wrap the gel with Saran wrap and expose with Storage phosphor screen overnight.

Solutions

Church-Gilbert solution

1% BSA
1mM EDTA
7% SDS
0.5M $NaHPO_4$ pH7.2

Washing buffer

2x SSC
0.1% SDS

Denaturing solution

0.5M NaOH
150mM NaCl

Neutralizing solution

0.5M Tris-Cl pH8.0
150mM NaCl

2.6 Protein analysis techniques

2.6.1 Protein extraction with TCA

1. Spin down 15ml of OD0.5 culture. Resuspend cell pellet in 1ml 20% TCA, transfer to 1.5ml screw cap tube. Samples can be kept at 4°C for a few hours.

2. Flash spin for 10sec at 12k rpm. Wash with 1ml 1M Tris-Base.

3. Spin down. Resuspend pellet in 100µl 2X LDS loading buffer (NuPage) with 200mM DTT (fresh). Boil for 3min at 100°C block.

4. Add 100µl glass beads, boil for 1min. Votex for 1min, boil again.

5. Losen the tube cap to reduce pressure. Puncture a hole at the bottom of the tube, place it on top of a new 1.5ml Eppendorf tube, and spin at 5k rpm for 15sec to recover the lysate.

6. Centrifuge at 13k rpm for 10min, move supernatant to a new tube. Samples can be kept at -20°C for a few days, or at -80°C indefinitely.

7. Boil samples before loading. Use 5-15µl per sample on SDS-PAGE for Western Blot analysis.

2.6.2 Mitotic protein extraction for 2DGE

1. Spin down 50ml log-phase culture. Wash cells 3X with 50 ml cold water.

2. Transfer cell pellet to 1.5 screw tube, spin shortly to remove all remaining liquid. Cells can be frozen in liquid nitrogen and stored in -80°C.

3. Add 100µl sample preparation solution, and 30µl of glass beads. Fast Prep, 6.5 degree for 45 sec in cold room.

4. Transfer the cell lysate to new 1.5ml eppendorf. Centrifuge at 4°C, 13k rpm for 10min, and transfer supernatant to new 1.5 eppendorf.

5. Measure the protein concentration of each sample (2µl) using 2D Quant Kit (Amersham). Use 0-50µg BSA to make standard curve.

6. Dilute up to 200µg of protein in up to 150µl DeStreak Rehydration Solution with 0.5% IPG buffer per sample.

Solution

Sample preparation solution

8M urea
4% CHAPS
2% IPG buffer (GE Healthcare)
40mM DTT

1x protease inhibitor cocktail (CalBiochem), added fresh
1% nuclease mix (Ettan), added fresh

2.6.3 Protein 2DGE first dimension

1. Rehydrate Immobiline DryStrip (GE Healthcare): remove protective plastic from the anodic end, place strips gel-side down in the appropriate volume of DeStreak Rehydration Solution with 0.5% IPG buffer. Rehydrate for 10-20h at room temperature. Immobiline DryStrip pH 4-7 24cm strips are used in this study.

2. Place the Manifold on Ettan IPGphor II, and pour 108ml PlusOne DryStrip Cover Fluid in all channels.

3. Transfer IPG strips to the Manifold, placing them face up according to marker position on the IPGphor. Make sure that the strips are not floating on top of the cover fluid.

4. Place cups properly on the opposite end of the strip compared to the pI of protein of interest. Place moist electrode pads on the ends of the strips, and position the electrodes on top of the pads.

5. Load the 2DGE samples into the cups. Run desired programme overnight.

6. Immediately after the programme stops, take the strips out of the Manifold. Either process to 2DGE second dimension immediately, or store them in a equilibration tube at -80ºC to avoid de-focusing.

2.6.4 Protein 2DGE second dimension

1. Equilibrate strips at room temperature for 15min in SDS equilibration buffer with 10mg/ml DTT, and again for 15min in SDS equilibration buffer with 25-40mg/ml iodoacetamide.

2. Cut strips to an appropriate length for the second dimension NuPage 4-12% Bis-Tris Zoom acrylamide gradient gel. Rinse strips in MOPS SDS Running buffer (Invitrogen) before insertion into the IPG well.

3. Electrophorese at 100V for 2h or until desired separation is achieved.

Solution

SDS equilibration solution

6M urea
75mM Tris-HCl pH8.8
29.3% glycerol
2% SDS
0.002% bromophenol blue

2.6.5 Western blotting

1. After SDS-PAGE of protein samples or 2DGE second dimension, proteins are transferred to a PVDF membrane (Bio-Rad) using Mini Trans-Blot Cells, 200mA for 45min, or 20mA overnight at 4ºC.

2. Membranes can be stained with Ponceau S (Sigma-aldrich) to confirm successful transfer of protein, or proceed directly to blocking.

3. Block membrane in PBST (0.1% TWEEN-20) with 5% milk or BSA for 1h at room temperature, or overnight at 4ºC.

4. Primary antibody is added to the blocking solution and incubated for 1h at room temperature, or overnight at 4ºC. Concentration of antibodies used in this study: mouse α-V5 (AbD serotec) at 1:4000, mouse α-Myc (Cell Signalling) at 1:4000, rabbit α-Cdc2 (Santa Cruz Biotechnology) at 1:1000, mouse α-HA (Covance) at 1:1000.

5. Wash 3x 10min in PBST. Incubate with secondary antibody for 30min at room temperature. Concentration of antibodies used: Sheep ECL α-mouse

IgG Horseradish peroxidase linked (GE Healthcare) at 1:5000, Donkey ECL α-rabbit IgG Horseradish peroxidase linked (GE Healthcare) at 1:4000.

6. Wash 3x 10min in PBST. Signal can be detected using ECL Plus Western Blotting Detection System (GE Healthcare).

2.6.6 Immunoprecipitation

1. For analytical scale analysis, spin down 50ml of OD0.5 culture. Scale up accordingly for preparatory analysis by mass spectrometry.

2. Wash once with 10ml stop buffer. Resuspend cell pellet in 1ml ice-cold lysis buffer with PMSF and transfer to screw-cap tube. Flash spin to remove all supernatant. Cell pellet can be stored at -80ºC.

3. Resuspend cell pellet in 100µl of cold lysis buffer with PMSF and protease inhibitor cocktail. Add 100µl glass beads, Fast Prep 5.5 degree for 45sec.

4. Add 200µl lysis buffer with PMSF and protease inhibitor, puncture a hole in the bottom of the tube. Spin at 5k rpm to recover cell lysate. Spin lysate at 4ºC,13k rpm for 10min. Transfer supernatant to new eppendorf tube. Mix 15µl of extract with 15µl 2X LDS buffer as Input for Western Blotting.

5. Prepare Dynabeads: use 50µl Dynabeads Pan-Mouse IgG (Invitrogen) per IP. Pull down beads with magnet, wash 3x 1ml lysis buffer. Resuspend beads in original volume lysis buffer with antibody (for anti-V5 antibody use 10µl per IP), rotate on wheel at room temperature for 30min. Wash 3x 1ml lysis buffer. Resuspend in original volume of lysis buffer with PMSF and protease inhibitor.

6. Mix 150µl extract with 50µl antibody-coupled beads. Rotate on wheel at 4ºC for 2h. Pull down beads with magnet. Wash 3x with 1ml lysis buffer.

7. For Western Blotting analysis: add 30µl 2X LSD buffer with DTT. Boil all samples for 5min to elute. For mass spectrometry analysis: wash again with lysis buffer with no TX-100, elute in 2% SDS for 10min at 65ºC.

Solutions

Stop buffer (prepare fresh)

150mM NaCl
50mM NaF
10mM EDTA
1mM NaN_3

Lysis buffer

50mM Tris-Cl pH7.5
150mM NaCl
50mM NaF
1% TX-100
10% Glyceral
Add before use 1mM PMSF, 1x protease inhibitor cocktail, 2mM $NaVO_3$.

2.7 DNA-Protein interaction analysis

2.7.1 Chromatin IP

1. Pour 45ml of log phase culture into 50ml Flacon tubes containing 1.4ml 37% formaldehyde, mix by inversion immediately. Incubate on a wheel for 15min at room temperature. Wash 3X with 30ml cold PBS.

2. Transfer cells to a screw-cap tube, centrifuge at 13k rpm to remove all liquid. Sample can be snap frozen in liquid nitrogen and stored at -80°C for a few months.

3. Prepare beads: use 100µl Dynabeads Pan-Mouse IgG (Invitrogen) per sample, wash 2X with 5ml PBS, wash once with lysis buffer. Resuspend beads in its original volume in lysis buffer with antibody (for anti-V5 antibody, use 10µl per sample). Incubate for 2h at room temperature, or alternatively

over night at 4°C. Wash 3X in 1ml of lysis buffer without PMSF. Resuspend in original volume.

4. Wash pellet in 500µl cold lysis buffer with PMSF/Cocktail Inhibitor/$NaVO_3$. Resuspend in 500µl, add 500µl glass beads, Fast Prep for 3X 30sec at speed 6.5, rest samples on ice in between.

5. Puncture a hole in the bottom, centrifuge to recover sample to a new 1.5ml Eppendorf tube. Spin at 14k rpm at 4°C for 30min. Remove supernatant carefully. A light yellow layer if cross-linked chromatin is visible above the cell debris. Resuspend in 900µl lysis buffer, transfer to 15ml Falcon tube.

6. Sonicate with Bioruptor at 4ºC, 30sec ON / 1min OFF on High setting for 8min. Transfer lysate to 1.5ml Eppendorf tube. Spin at 13k rpm for 10min at 4°C. Transfer 800µl supernatant to a new 1.5ml tube. Move 10µl to PCR tubes and Eppendorf tubes as INPUT for ChIP and WB, respectively.

7. For IP, take 600µl per sample to mix with 100µl of antibody-coupled beads. Incubate at 4°C on wheel for 2h. Make SDS, Hi Salt, T/L, and T/E solution while beads are rotating.

8. Pull down samples. Wash at room temperature as following:

    a. 2x 1 ml SDS buffer, rotate for 4min. Pull down and remove supernatant.

    b. 1x 1 ml Hi Salt buffer, rotate for 4min. Pull down.

    c. 1x 1 ml T/L buffer, rotate for 4min. Pull down.

    d. 2x 1 ml T/E buffer, mix briefly by inversion, pull down, and remove all supernatant carefully.

9. Add 145µl TE + 1% SDS to beads, vortex. Elute at 65˚C for 10min. Transfer 120µl supernatant as IP to PCR tubes. Take 10µl for Western blots.

10. Add 110µl TE with 1% SDS to 10µl INPUT. Reverse crosslink both IP and INPUT samples at 65˚C overnight. Purify DNA with Qiagen PCR Purification Kit. Elute DNA in 60µl 0.5x EB.

11. Samples can be stored at -20ºC for months before analysis by q-PCR or dot blot.

Solutions

Lysis buffer

50mM HEPES pH 7.5
140mM NaCl
1mM EDTA pH 8.0
1% IGEPAL CA-630
0.1% sodium deoxycholate
Add prior to use: 1mM PMSF, 1X Cocktail Inhibitor, 2mM $NaVO_3$.

SDS buffer

50mM HEPES pH7.5
140mM NaCl
1mM EDTA pH 8.0
0.025% SDS

Hi Salt buffer

50mM HEPES pH7.5
1M NaCl
1mM EDTA pH8.0

T/L buffer

20mM Tris-HCl pH7.5
250mM LiCl
1mM EDTA
Filter sterile, add 0.5% IPEGAL-CA630 and 0.5% sodium deoxycholate.

T/E buffer

20mM Tris-HCl
0.1mM EDTA pH8.0

2.7.2 Quantitative-PCR

Co-immunoprecipitation of cross-linked DNA was monitored using quantitative PCR. Standard protocol of Platinum SYBR Green qPCR SuperMix Kit (Invitrogen) was used to amplify the signal. Each sample was amplified in triplicate. Relative enrichment was determined by normalizing subtelomeric signal (TELO) to the signal of a control non-telomeric region (Act1).

Chapter 3. DNA damage response at telomeres of Pot1 phospho-mutants

3.1 Aim of the study

The telomeric ssDNA binding protein Pot1 is important for both telomere length regulation and inhibition of DNA damage signal at telomeres, although the molecular mechanism is not well understood. In fission yeast, the function of Pot1 cannot be studied by removal of the protein, as Pot1 is essential for telomere protection and gene deletion leads to rapid telomere loss. It has been reported that Pot1 is required to prevent activation of the Rad3-dependent checkpoint pathway (Carneiro et al., 2010). However, as the *pot1Δ* strains assessed in these studies had presumably lost the telomeres and existed as circular survivors, the checkpoint responses could not be induced by de-protected telomeres. Rather, they could be consequence of chromosome circularization. Other studies used over-expression of Pot1 truncation mutants to show that certain regions of Pot1 are important for its function, which helped further our understanding (Bunch et al., 2005). However, the results were a complex interplay between altered levels and the effects of the various truncations; moreover, a number of manipulations led to telomere loss as seen for the *pot1*-null.

A set of C-terminally tagged Pot1-V5 phosphorylation mutants was constructed in the Cooper Laboratory during mapping of the Pot1 phosphorylation sites (Kuznetsov, 2008). The putative phosphorylation sites were mutated either to Ala (*pot1-A-V5*) or Asp (*pot1-D-V5*) to remove or mimic the phosphorylation modification at these sites. The mutant alleles were integrated using pCST159 *aur1R* plasmid at the *aur1*$^+$ locus under the endogenous promoter and terminator of *pot1*$^+$. The endogenous copy of *pot1*$^+$ was then replaced with antibiotic markers and selected against to generate an effective genotype of *pot1-V5* phosphorylation mutant. In this Chapter we describe the characterization of these *pot1-V5* mutants with respect to telomere protection and length regulation, and inhibition of DDR, and show that they act as partial loss-of-function mutants that induce DNA damage response at telomeres. The roles of DDR response at telomeres of Pot1

phosphorylation mutants were also examined, and we conclude that Rad51, as well as the Rad3^{ATR} Chk1 pathway, are important for telomere maintenance in these mutant backgrounds, potentially shedding light on the redundant mechanisms that underlie telomere stability in wt cells.

3.2 *pot1-V5* phospho-mutants are partially functional in telomere maintenance

3.2.1 *pot1-V5* phospho-mutants are defective in telomere length regulation

Pot1 plays key roles in telomere length regulation in fission yeast. Expression of mutant forms of Pot1 often leads to altered telomere lengths (Bunch et al., 2005, Pitt and Cooper, 2010). To determine whether the phosphorylation mutations of *pot1-V5* have an effect on telomere length control, we looked at the telomere length of a range of clones of each mutant. For each mutant, eight colonies, each derived from germination of the spores of a heterozygous *pot1-V5 mutant/pot1*$^{+}$ diploid) of different starting size were propagated before their telomeres were analyzed by Southern blotting.

The telomere length of the parental diploid cells is similar to that of *wt* (~300bp); this can result from low expression level of tagged alleles in the presence of a *wt* copy of *pot1*$^{+}$ (see section 5.2), and/or the recessive effects of the mutants. Assuming that telomere attrition does not occur during meiosis in the heterozygous situation or during spore dormancy, it would represent the starting telomere length of the spores. Antibiotic selection for mutant alleles led to an immediate 3-fold increase of telomere length to 0.8-1kb in cells harbouring the C-terminal V5-tagged, but otherwise wild type, Pot1; this telomere length remains stable through several passages (Figure 3.1). This is similar to the effect seen with the *pot1-GFP* tagged allele; the occurrence of telomere lengthening in any C-terminally tagged version of Pot1 that we have tested suggests that the C-terminus is important for telomere length control (see section 5.2). Compared to *pot1-wt-V5*, telomeres of both *pot1-A-V5* and *pot1-D-V5* mutants are more heterogeneous in length and contain more

slow-migrating signal, representing on average a further 0.1-0.5kb elongation. Interestingly, the telomere length distribution was fairly equal across different colonies of the phospho-deficient *pot1-A-V5* mutants. In contrast, varying length was observed in different *pot1-D-V5* colonies; this variation is not dependent on the passage number or the starting size of the colony (data not shown). Nonetheless, we noticed that all *pot1-D-V5* colonies tested contained elongated telomeres compared to *pot1-wt-V5*, which disagrees with previous observations in which *pot1-D-V5* yielded normal-length telomeres (Kuznetsov, 2008). We concluded that both phospho-deficient and phospho-mimic mutants of *pot1-V5* induce a telomere elongation phenotype, although to varying degrees.

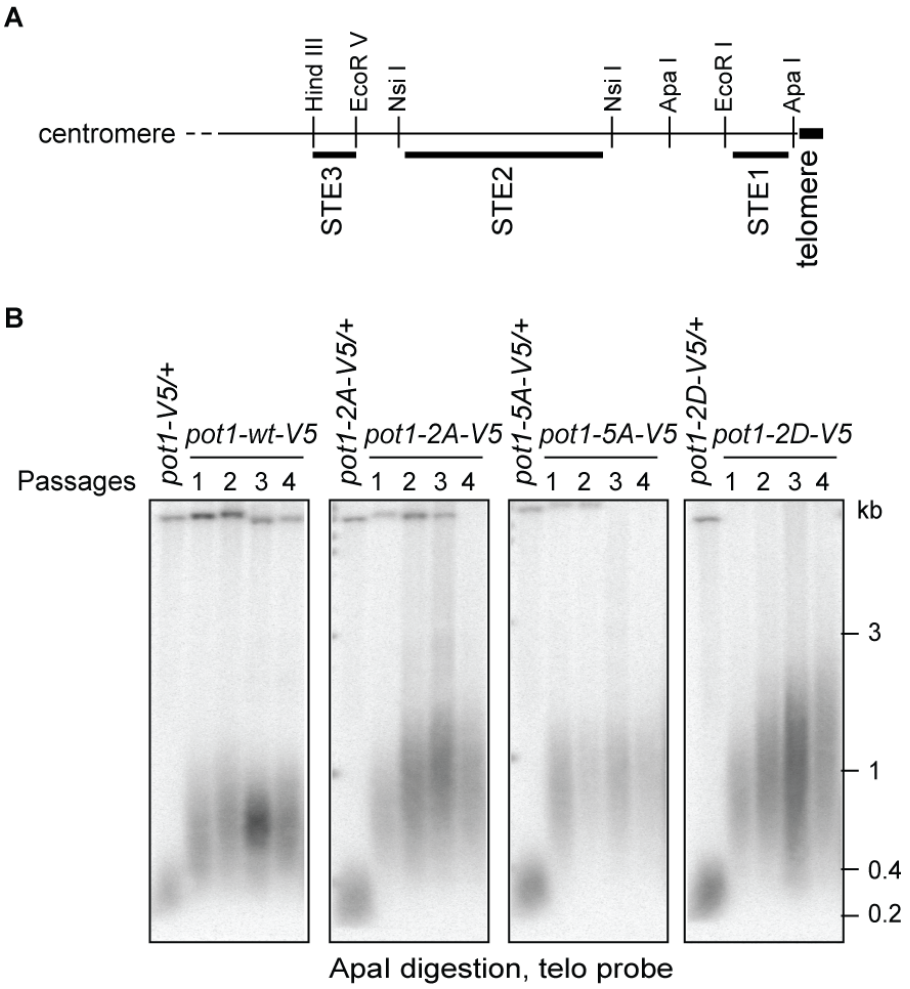

Figure 3.1 phospho-mutants of *pot1-V5* lead to telomere elongation

A. Restriction enzyme map of representative telomeric and subtelomeric region. Adapted from (Nakamura et al., 1998). **B**. Representative Southern blot showing telomere length of *pot1-V5* phospho-mutants. Pot1 mutants were antibiotic selected for respective genotypes, and followed for four passages after sporulation of heterozygous diploids (1st lanes). Numbers on top indicate the number of passages on rich medium (typically 36 generations per passage). The bands at the top of the gel are strain specific STE signal.

3.2.2 *pot1-V5* phospho-mutants induce hyper-recombination at telomeres

In addition to its role in telomere length regulation, Pot1 is also involved in inhibition of DNA repair activities at telomeres, including homologous recombination. In both human and yeasts, telomere recombination is normally repressed and is active only at telomeres made dysfunctional through disruption of shelterin or by telomere length crisis. It has been shown in mice that disruption of Pot1a leads to increased telomere sister chromatid exchange (T-SCE) at telomeres and formation of T-circles, a by-product of recombination (Hockemeyer et al., 2006, Wu et al., 2006). In budding yeast, deficiency of the telomeric ssDNA-binding protein Cdc13 also induces recombination-based telomere maintenance (Grandin et al., 2001, Grandin and Charbonneau, 2003).

We set out to investigate the effect of the phospho-mutants on recombination at the telomeres. It is difficult to measure recombination at telomeric sequences, as both recombination-based mechanisms and telomerase action can lead to net change in the number of telomeric repeats. In contrast, the subtelomeric elements (STE) cannot be acted upon by telomerase, and changes of subtelomeric pattern over time are likely to represent the effect of recombination at telomeres rather than abnormal telomerase activity; moreover, we have shown that in a *taz1Δ* background in which changes in the subtelomeric restriction pattern are seen, these changes depend on Rad51. Therefore, we followed the change in STE pattern after *ApaI* digestion over time (Figure 3.2). As expected, the *wt* allele in the *pot1-V5* background maintains a stable STE pattern over serial re-streaks. In contrast, both the phospho-deficient and the phospho-mimic mutants of *pot1-V5* display changing patterns between each re-streak, suggesting constant recombination activity at subtelomeric regions. In summary, both the phospho-deficient and the phospho-mimic mutants are deficient in inhibition of HR activities at the telomeres.

Note that in many cases, the STE bands become homogenized after a few re-streaks. This could result from a mechanism similar to break-induced replication (BIR), in which a chromosome end that has lost its telomere utilizes the homologous sequence in the STE region of another chromosome as a template for

replication. If this were true, the initiating event should be the loss of telomeres at some, but not all, the chromosome ends. This is consistent with further analysis of these mutants showing that spontaneous telomere loss occurs frequently in these mutants (see below).

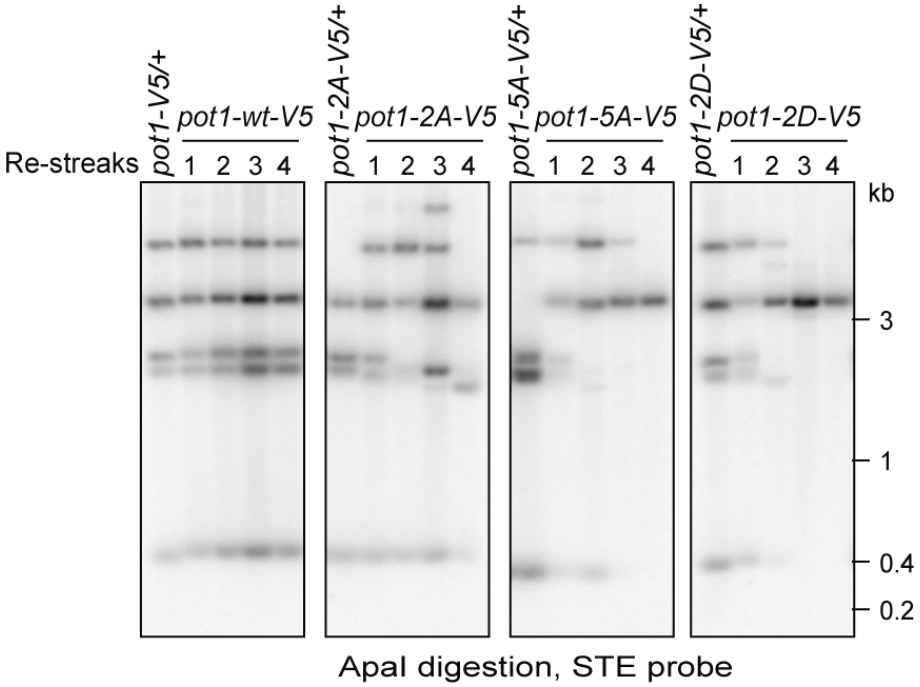

Figure 3.2 Hyper-recombination of *pot1-V5* phospho-mutant telomeres

The blot in Figure 3.1B is stripped and probed for the ApaI-released fragment of the subtelomeric element STE1 (see Figure 3.1A for restriction map). Appearance of additional bands and disappearance of starting bands indicate subtelomeric recombination.

3.2.3 Stochastic telomere loss occurs in *pot1-A-V5* mutants

During strain propagation, we noticed that colony size is more variable in the *pot1-A-V5* mutants compared to *pot1-wt-V5* and *pot1-D-V5* mutants. When randomly plated on solid medium, about 10% of the *pot1-A-V5* cells form small colonies that contain sick, senescent cells, while the percentage of these remains well below 1% in *pot1-wt-V5* and *pot1-D-V5* background (Figure 3.3A). A fraction of these slow growing colonies are hypersensitive to the DNA damaging agent MMS (Figure

3.3B). A closer look at these cells under the microscope revealed chromosomal bridges and segregation defects (Figure 3.3C).

The growth and chromosome segregation defects we observed in these slow growing colonies were reminiscent of circular survivors generated from telomerase deficient *trt1Δ* strains (Jain et al., 2010). Southern blot analysis using a telomere probe confirmed loss of telomere signal in some, but not all, of the cells derived from these colonies, indicating that some of these cells survive with circularized chromosomes. We estimated the frequency of spontaneous chromosomal circularization to be around 1% in the *pot1-A*-V5 mutants (i.e. around 1 in 10 colonies we examined by Southern blot did not display any telomere signal), while it remained undetectable in the *pot1-wt*-V5 and *pot1-D*-V5 mutants by the assays used in this study. However, it should be noted that the loss of telomere is detectable on Southern blot only when all the telomeres in the cell are lost; therefore, the percentage of telomere loss occurring at individual telomeres is likely to be much higher than 1%. In fact, as unrepaired DSBs cause cell cycle arrest, the occurrence of small colonies could be taken as an indication of loss or uncapping of individual telomeres. Recovery of these telomeres can be achieved via recombination-based mechanisms that use the STE and telomeric sequences at a different chromosome, which could explain the constantly changing STE pattern seen in Figure 3.2.

Taken together, our data suggest that the phosphorylation mutants of *pot1-V5* are partially functional mutants of *pot1*$^{+}$. While the majority of the cells harbouring the mutant alleles manage to maintain chromosome linearity, telomere length regulation and protection against recombination are compromised in all the phosphorylation mutants. The *pot1-A-V5* mutants seemed to display a more severe phenotype, with a small fraction sustaining completely defective telomere protection and losing telomeres spontaneously. This phenotype is reminiscent of that in some human cancer cell lines, where spontaneous telomere loss occurs at a high rate despite telomerase expression (Nakamura et al., 2009). The outcome of spontaneous telomere loss is reminiscent of DSB repair near the telomeric region (Zschenker et al., 2009), hinting at a defect in DDR suppression.

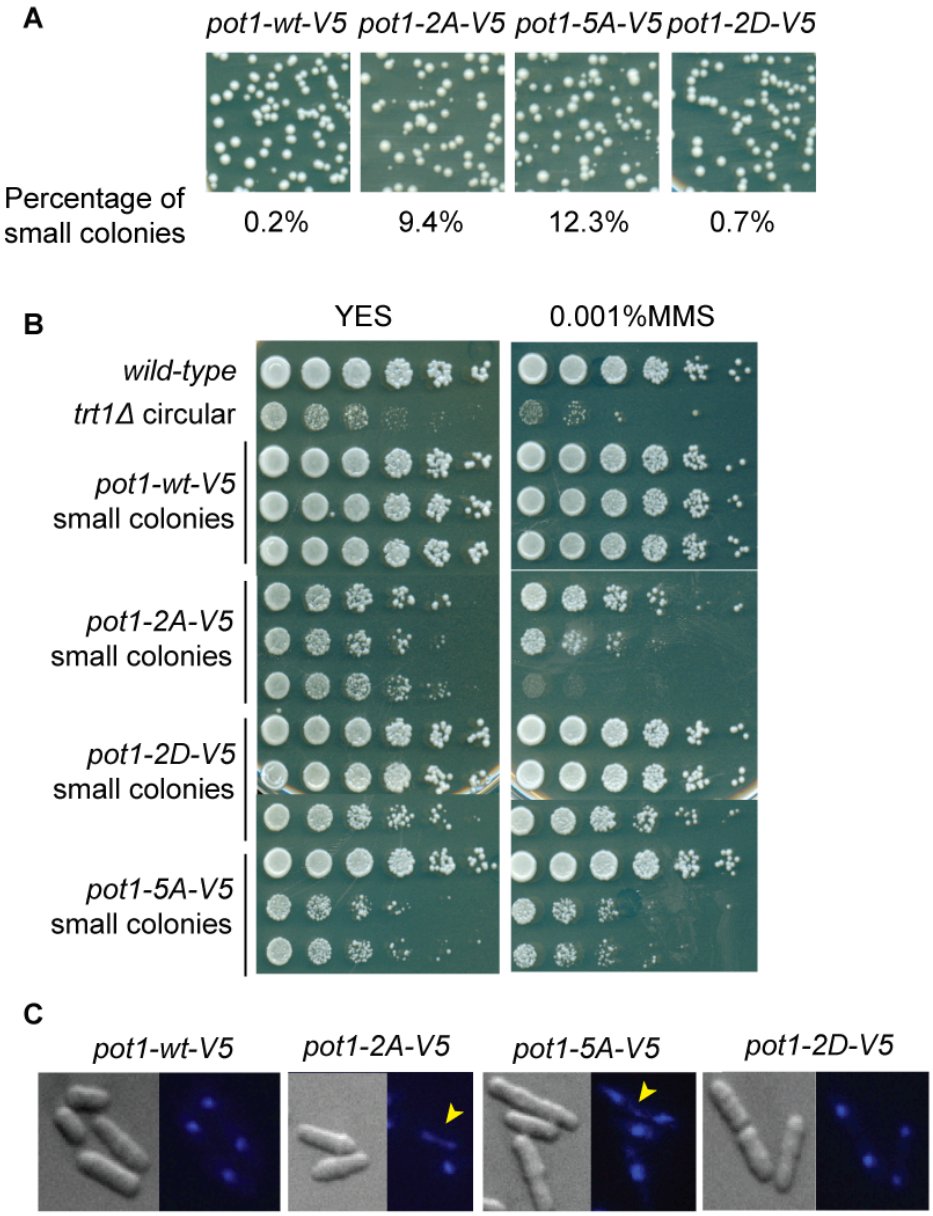

Figure 3.3 Elevated rate of senescence in *pot1-A-V5* mutants

A. Plating assay shows that senescent colonies arise spontaneously in *pot1-A-V5* mutants. Approximately 1000 cells from a log phase culture were plated on rich medium in duplicates, and the percentage of small colonies was calculated. Numbers below indicates the percentage of small colonies for each mutant (*n*=2000). **B**. Dilution assay on YES +/- MMS media, showing severe growth defect and occasional MMS-sensitivity in *pot1-A-V5* mutants. 5-fold dilutions were performed with starting concentration of $1x10^7$ cells/ml (OD_{600} = 1). Cells were spotted onto YES and MMS plates, and incubated at 32ºC for 2 days. Three independent colonies are shown for each genotype. **C**. DAPI staining of *pot1-V5* phospho-mutants. Arrowheads indicate chromosome bridges between nuclei in dividing *pot1-A-V5* mutant cells.

3.3 *pot1-V5* phospho-mutants fail to repress DNA damage response at telomeres

3.3.1 Checkpoint activation by Pot1-V5 phospho-mutants

The dramatic phenotype of elevated senescence in the phospho-deficient *pot1-A-V5* mutants prompted us to examine their cellular and population growth. Cell length of all the *pot1*-V5 phospho-mutants was measured in log phase cultures, which contain predominantly G2 phase cells. In fission yeast, cell elongation indicates cell cycle arrest or delay by an activated checkpoint. As expected, and in concurrence with the small colony phenotype, the *pot1-A-V5* mutants contain more elongated cells compared to *pot1-wt-V5*, suggesting checkpoint activation in these mutants (Figure 3.4). Surprisingly, the phospho-mimic *pot1-D-V5* mutant cells display a very wide distribution of cell length, and the average length of a population varies depending on the clone assessed. This could explain a previous observation in the lab that the *pot1-D-V5* mutant does not activate a checkpoint or lead to cell elongation (Kuznetsov, 2008), as the sample was derived from one single clone. Nevertheless, a large fraction of the *pot1-D-V5* mutant cells are indeed elongated, despite the low percentage of small colonies observed for in this strain.

In line with the cell elongation and checkpoint activation induced by the *pot1-V5* phosphorylation mutants, population growth is also affected. At 32ºC in rich medium, the doubling times of both *wt* and *pot1-V5* strains are around 2h, meaning that population growth is not affected by the C-terminal V5-tagging. In strains harboring the phospho-deficient *pot1-A-V5* mutants, however, doubling time varies greatly between 2.5-4h depending on the clone inoculated, notwithstanding identical genotypes. Consistent with the wide distribution of cell length, the *pot1-D-V5* mutant cultures inoculated from different colonies also display different growth curves and doubling times, although they more closely resemble *wt* than *pot1-A-V5*, with the doubling times average at 2.3h. Hence, while both *pot1-A-V5* and *pot1-D-V5* mutants lead to checkpoint activation, the phospho-deficient *pot1-A-V5* phenotypes appeared to be more penetrant.

It should be noted that the percentage of cells displaying an elongation phenotype is higher than the rate of spontaneous chromosome circularization and the occurrence of small colonies for both *pot1-A*-V5 and *pot1-D-V5* mutants. In addition, the doubling time of *pot1*Δ circular chromosome-containing strains is around 3h, which is significantly shorter than some of the *pot1-A-V5* mutants. Therefore, the cell elongation and delayed doubling time are not simply readouts of chromosomal circularization in these strains. These observations suggest that the phospho-mutants of *pot1-V5* are not complete loss-of-function *null* alleles of *pot1*, and that even when chromosome linearity can be maintained in these strains, the Pot1-V5 mutant proteins are defective in suppressing checkpoint activation at telomeres.

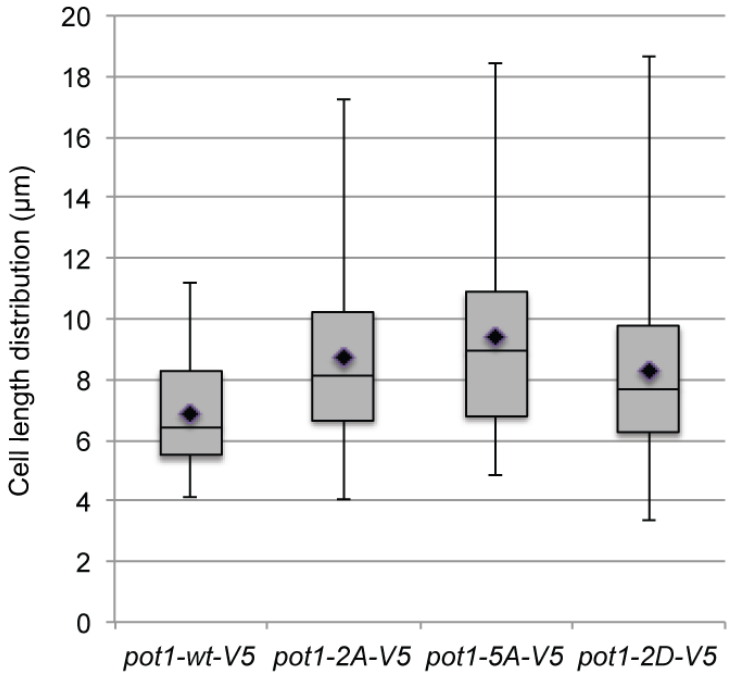

Mean doubling time (h)	1.9	2.8	2.9	2.3

Figure 3.4 Cell elongation and delayed doubling in *pot1-V5* phospho-mutants

Box plot depicting the cell length distribution of *pot1*-V5 phosphorylation mutants. Minimum of 300 cells were measured for each genotype in three independent experiments. The grey box includes 50% of the cell length observed, starting from 25th percentile to 75th percentile. The minimum and maximum length observed for each genotype is marked by whisker lines, and the median is represented by the line within the box. Average cell length of each genotype is indicated by the diamond mark.

3.3.2 DNA repair protein Rad51 accumulates at mutant telomeres

Chromosomal circularization is too rare to account for the high frequency of checkpoint activation in cells harbouring *pot1-V5* phosphorylation mutants. In order to determine the localization of DDR signal, we utilized fluorescence microscopy to visualize Rad51 (previously Rhp51), a central HR repair protein, *in situ*.

As tagging of Rad51 abolishes its function (Catlett and Forsburg, 2003, Akamatsu et al., 2007), we performed indirect immunofluorescence (IF) using an antibody against *sp*Rad51 protein. Asynchronous logarithmically growing cultures of *pot1-V5* mutant cells were fixed in 70% ethanol, and were subject to dual immunofluorescence staining against Rad51 and Pot1-V5, which is used as a marker of the telomeres (see section 4.2). As expected, we observed few discrete Rad51 foci in *wt* or *pot1-V5* cells, which can be observed in 16-17% of nuclei and most likely correspond to sites of replication (note that telomeres are replicated in late S/G2 in a *wt* background). The Rad51 foci in *pot1*-V5 cells rarely co-localize with Pot1-V5 signal at the telomeres. In contrast, in cells harbouring phosphorylation mutants of Pot1-V5, close to 50% of the cells contain one or more clear foci of Rad51 in the nucleus, a 3-fold increase over *wt* and *pot1-V5* cells. Moreover, the rate of Rad51/Pot1-V5 foci co-localization more than doubled, from 7% in *pot1-V5* to 18-34% in the phosphorylation mutants.

The localization of Rad51 to the telomeres demonstrates that the telomeres in *pot1-V5* phosphorylation mutants elicit a DNA damage response. The fact that the mutant forms of Pot1-V5 are seen to co-localize with Rad51 foci indicates that DDR is induced while the mutant Pot1 protein is present at the telomeres, instead of localizing exclusively to chromosome ends that have lost the telomere sequence or are defective in Pot1 recruitment. Taken together, these results suggest that both phospho-mimic and phospho-deficient mutants of *pot1-V5* are defective in suppression of DDR at telomeres; this defect is not due to loss of Pot1 from the telomeres.

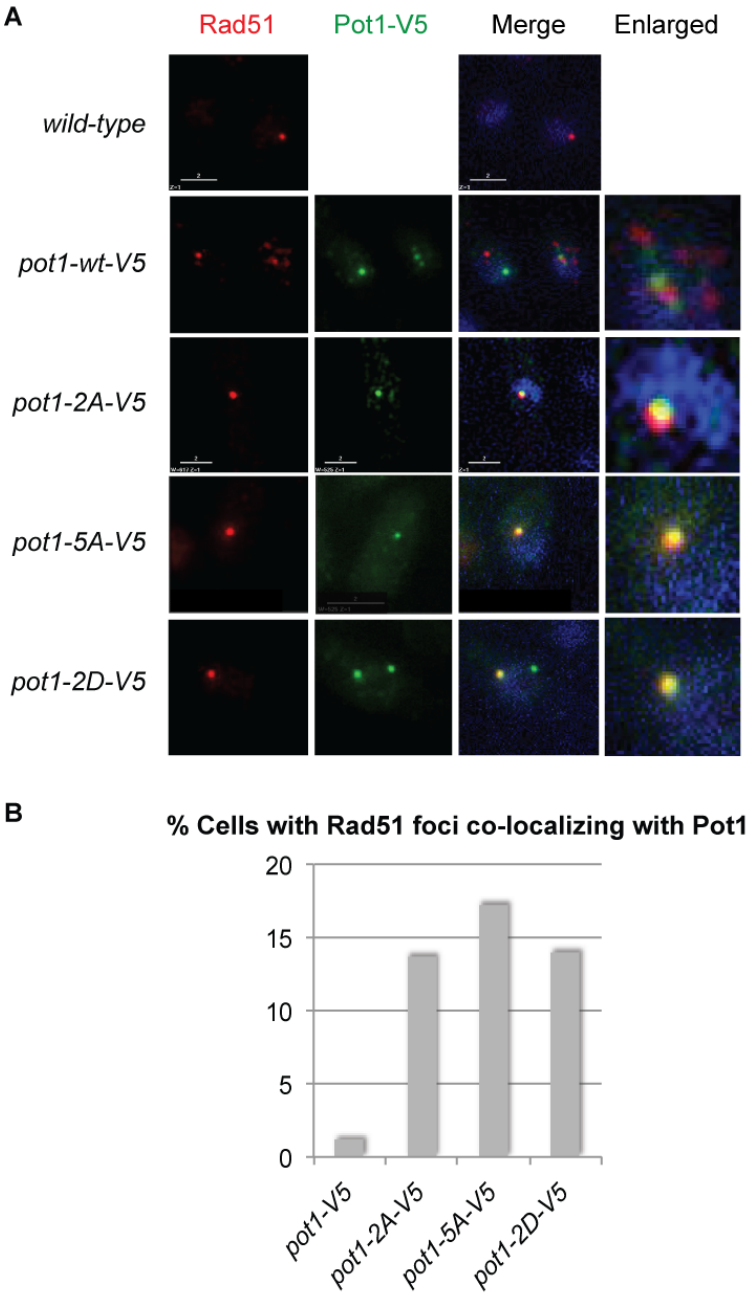

Figure 3.5 *pot1-V5* phospho-mutants induce formation of Rad51 foci

A. Dual immunofluorescence staining against Rad51 (red) and Pot1-V5 (green) in *pot1-V5* phosphorylation mutants, DNA stained with DAPI to indicate the nuclei (blue). See text for experimental procedure. Images are flattened *z*-stacks taken with DeltaVision Microscopy Imaging System. Scale bar: 2µm. **B**. Quantitation of the percentage of cells with Rad51 foci co-localizing with Pot1-V5 foci (*n*>100).

3.4 DNA damage checkpoint is required for telomere maintenance in pot1-V5 phospho-mutants

3.4.1 Rad51 is required for telomere maintenance in pot1-V5 phospho-mutants

We have shown that Pot1-V5 phospho-mutants are defective in inhibiting homologous recombination at the telomeres, and that recombination protein Rad51 strongly localizes to the mutant telomeres. Now we would like to know what the role of Rad51 is at these telomeres. The two extreme scenarios relating to its recombinase function are: 1, if Rad51 is only recruited due to loss of HR inhibition, then removal of Rad51 would leave the telomeres intact, and a stable STE pattern should be observed instead. 2, if the mutations completely abolish telomerase-mediated telomere elongation, i.e. telomeres are maintained solely by recombination-based mechanisms; in this case, disruption of the HR pathway would lead to loss of telomere signal. Alternatively, Rad51 may play a role other than recombination at these telomeres, e.g., protecting the 3' overhang or restricting its generation (Schlacher et al., 2012).

To explore the function of Rad51 at the mutant telomeres, we examined the *rad51Δ pot1-V5* phosphorylation mutant following sporulation of double-heterozygous diploids. Compared with *rad51Δ* or *rad51Δ pot1-V5*, double mutants of *rad51Δ* combined with either *pot1-A-V5* or *pot1-D-V5* took longer to form colonies after germination, and the cells were much sicker (not shown). When we followed telomere length in these mutants, we found that while the telomere hybridization pattern in *pot1-V5* is not affected by *rad51Δ*, neither *pot1-A-V5* nor *pot1-D-V5* were able to stably maintain the telomeres in the absence of Rad51 (Figure 3.6A). We conclude that Rad51 is required for telomere maintenance in *pot1-V5* phosphorylation mutants, in agreement with previous observations (Kuznetsov, 2008).

We also noticed that the kinetics of telomere loss differ between the putative phospho-mutant and phosphor-mimic alleles. In *rad51Δ pot1-2A/5A-V5* double mutants, telomere signal became fainter but not shorter over time, which is

indicative of a growing fraction of telomeres undergoing sudden, complete telomere loss within the population. In contrast, *rad51Δ pot1-2D-V5* loses telomere signal completely before the first re-streak (~3 days after germination), suggesting rapid loss of telomeres similar to that observed in *pot1Δ.* The cells that have lost all the telomeres were no longer able to maintain their chromosomal linearity, but exist as circular survivors, as evidenced by the appearance of fusion bands on PFGE (pulse-field gel electrophoresis) (Figure 3.6C). Note that the *rad51Δ pot1-2A-V5* cultures contain both fused and un-fused chromosome ends, indicating a mixed population at the time of examination (~7 days after germination).

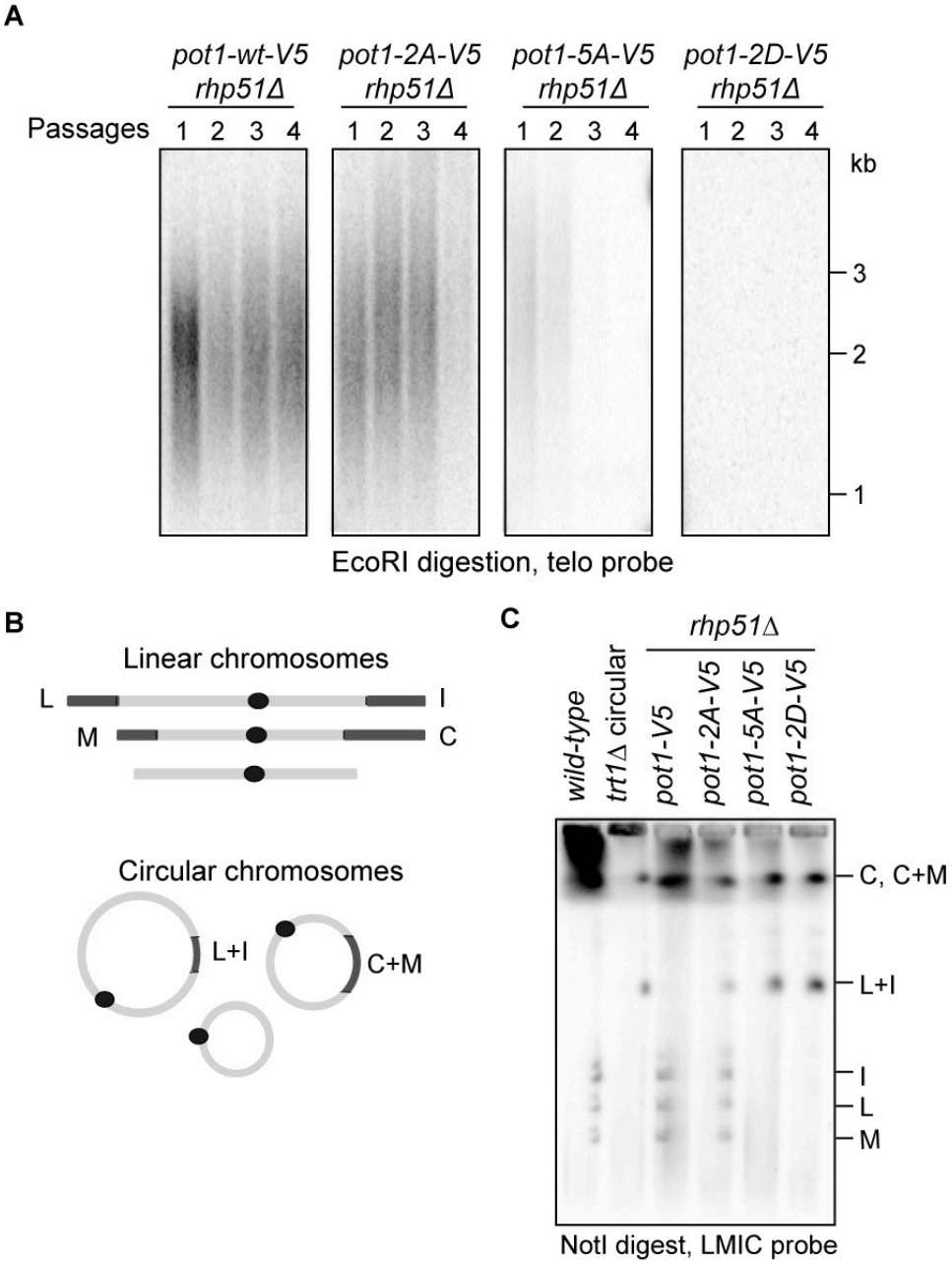

Figure 3.6 Rad51 is required for telomere maintenance in *pot1-V5* phospho-mutants

A. Genomic DNA of *rad51 pot1-V5* phospho double mutant over 4 passages was *EcoRI* digested and probed with telomere probe to follow telomere length after sporulation of double-heterozygous diploid strains. Numbers on top indicate the number of passages. **B**. Schematic diagram of relative position of LMIC probes. **C**. Pulse-field gel electrophoresis of log phase cultures corresponding to passage 2 used in Southern blotting, wt used as a control for linear chromosome protected by telomeres, *trt1*Δ circular strain as a control with intra-chromosomally fused ends.

3.4.2 The role of Rad22 in Rad51-dependent telomere protection

The requirement for Rad51 for telomere maintenance in *pot1-V5* phospho-mutant cells raised the possibility that a homologous recombination-based mechanism is required to maintain the mutant telomeres, which prompted us to examine the dependence on the HR pathway. We decided to look at their dependence on Rad22, a fission yeast homolog of Rad52. In budding yeast, Rad52 is essential for nearly all forms of recombination, whereas in fission yeast, Rad22 function is partly overlapping with a second Rad52 homolog, Rti1 (van den Bosch et al., 2002). Nonetheless, it has been shown that Rti1 has very limited function in recombination, and Rad22 alone is responsible for Rad51-dependent recombination, which establishes Rad22 as the central recombination protein in fission yeast (Doe et al., 2004).

We constructed double-heterozygous diploid strains of the *pot1-V5* phospho-mutants *rad22Δ*, sporulated them and selected for corresponding genotypes upon germination. Surprisingly, *rad22Δ* does not affect the telomere maintenance in any of the mutants, nor in *wt* or *pot1-V5* background (Figure 3.8B). The independence is not due to suppression of *rad22Δ* phenotypes by mutations of the reported suppressor gene *fbh1*, which allows Rad51-mediated strand exchange in the absence of Rad22 (Osman et al., 2005), as we have sequenced *fbh1* gene, including its promoter and terminator in full in all the progeny analysed, and no mutations were detected (data not shown). In addition, unlike the *rad22Δ*-suppressed strains reported in the literature, which were rescued from severe growth defects, the double mutants of *rad22Δ pot1-V5* phospho-mutants grow extremely slowly (Figure 3.8A). Therefore, it is unlikely that the *rad22*Δ strains analyzed in this study contained *fbh1* suppressor mutations.

In summary, our current results suggest that Rad22 is not required for telomere maintenance in *pot1-V5* phosphorylation mutants. Since Rad22 is normally required for loading of Rad51 onto the ssDNA to replace RPA, other mediators of Rad51 loading, including Rad55-57 and Swi5-Sfr1 complexes (Akamatsu et al., 2007, Akamatsu et al., 2003), may be required to participate in this process. Alternatively, this result would imply that the protective function of Rad51 at the

phospho-mutant telomeres does not involve its role in recombination *per se*. Rather, Rad51 might be involved in binding and protecting telomeric ssDNA when Pot1 is not fully functional.

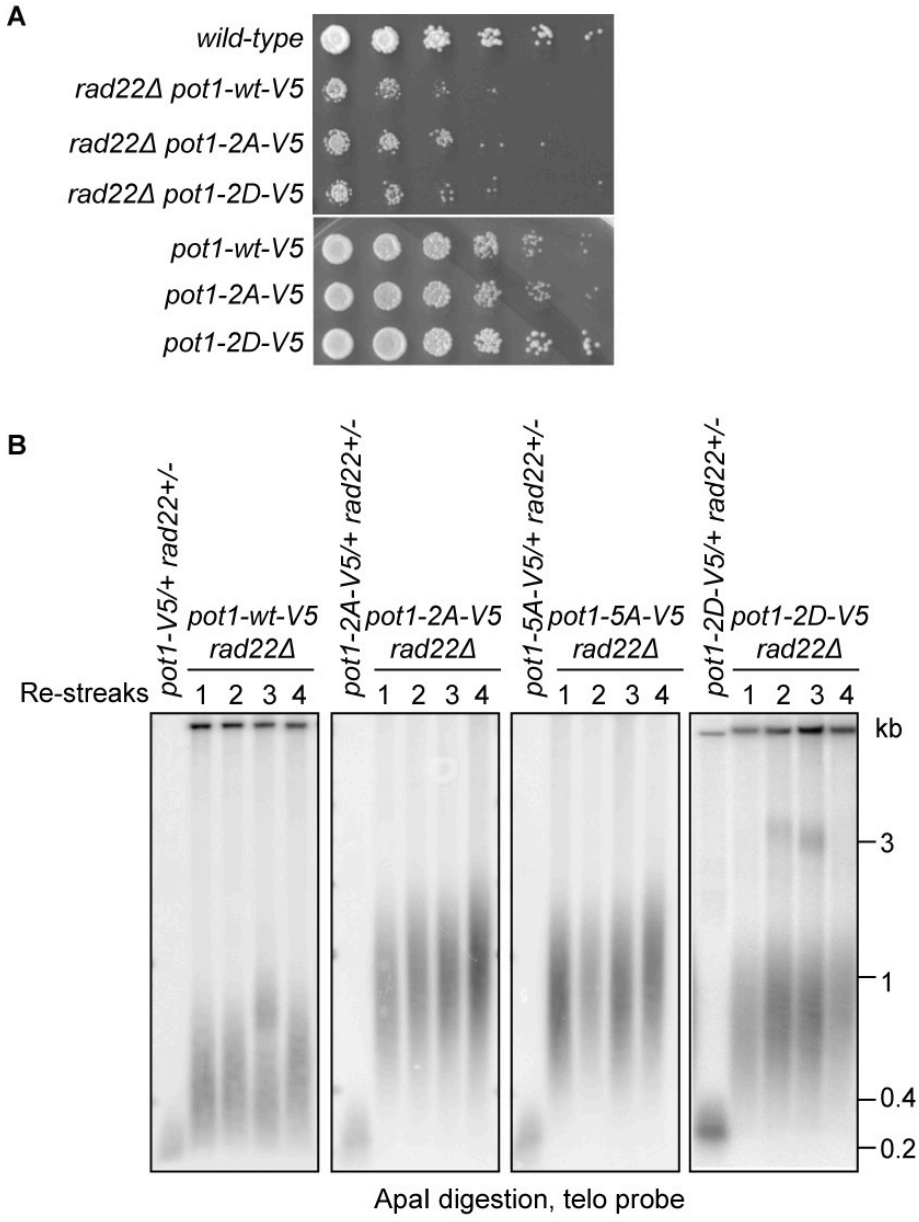

Figure 3.7 Rad22 is not required for telomere maintenance

A. Dilution assay of *pot1-V5* phosphorylation mutants in the presence or absence of *rad22*Δ, showing that the *rad22*Δ strains have growth defect. **B**. Telomere length of *rad22*Δ *pot1-V5* phosphorylation mutants are followed for four passages after sporulation of double-heterozygous diploids, showing telomere maintenance is not affected by the *pot1-V5* phosphorylation mutants.

3.4.3 The Rad3-Chk1 checkpoint pathway is required for telomere protection at mutant telomeres

The recruitment, and indeed requirement for, Rad51 at *pot1-V5* mutant telomeres suggests that some aspects of a DNA damage response are involved in telomere protection in the *pot1-V5* phospho-mutant background. To determine which aspects of DDR are involved, we conducted additional analyses combining the *pot1-V5* phosphorylation mutants with components of DDR pathways. Double-heterozygous diploid strains were constructed and sporulated, and their progeny followed over time.

Intriguingly, these experiments revealed that the DDR sensor kinase $Rad3^{ATR}$ and the transducer kinase Chk1 are required for telomere maintenance in both *pot1-A-V5* and *pot1-D-V5* mutants, while they have little or no effect on telomeres in *wt* and *pot1-V5* backgrounds. Loss of telomere signal is very rapid in all the *rad3Δ* or *chk1Δ* double mutants analysed, as no signal is observed on the Southern blot after the first passage (~3 days after germination). In contrast, no telomere loss phenotype was observed in $cds1^+$ or $tel1^+$ deletion mutants in any of the *pot1-V5* phospho-mutant phenotypes (data not shown), suggesting that the dependence is specific for the pathway involving Rad3 and Chk1. The telomere maintenance defect observed in these mutants is different from the accelerated *est* phenotype in *rad3Δ tel1Δ* double mutant, which requires more than 5 days for telomere signal to disappear (Moser et al., 2009b). Instead, it reminds us of the rapid telomere loss in *pot1Δ* strains that lose protection against telomere resection (Pitt and Cooper, 2010). Therefore, the dependence on Rad3 is presumably not due to its redundant role in phosphorylating Ccq1 and recruitment of telomerase (Moser et al., 2009b). It appears that the *pot1-V5* phosphorylation mutants confer a telomere protection defect, which confers a requirement for the checkpoint proteins Rad3 and Chk1.

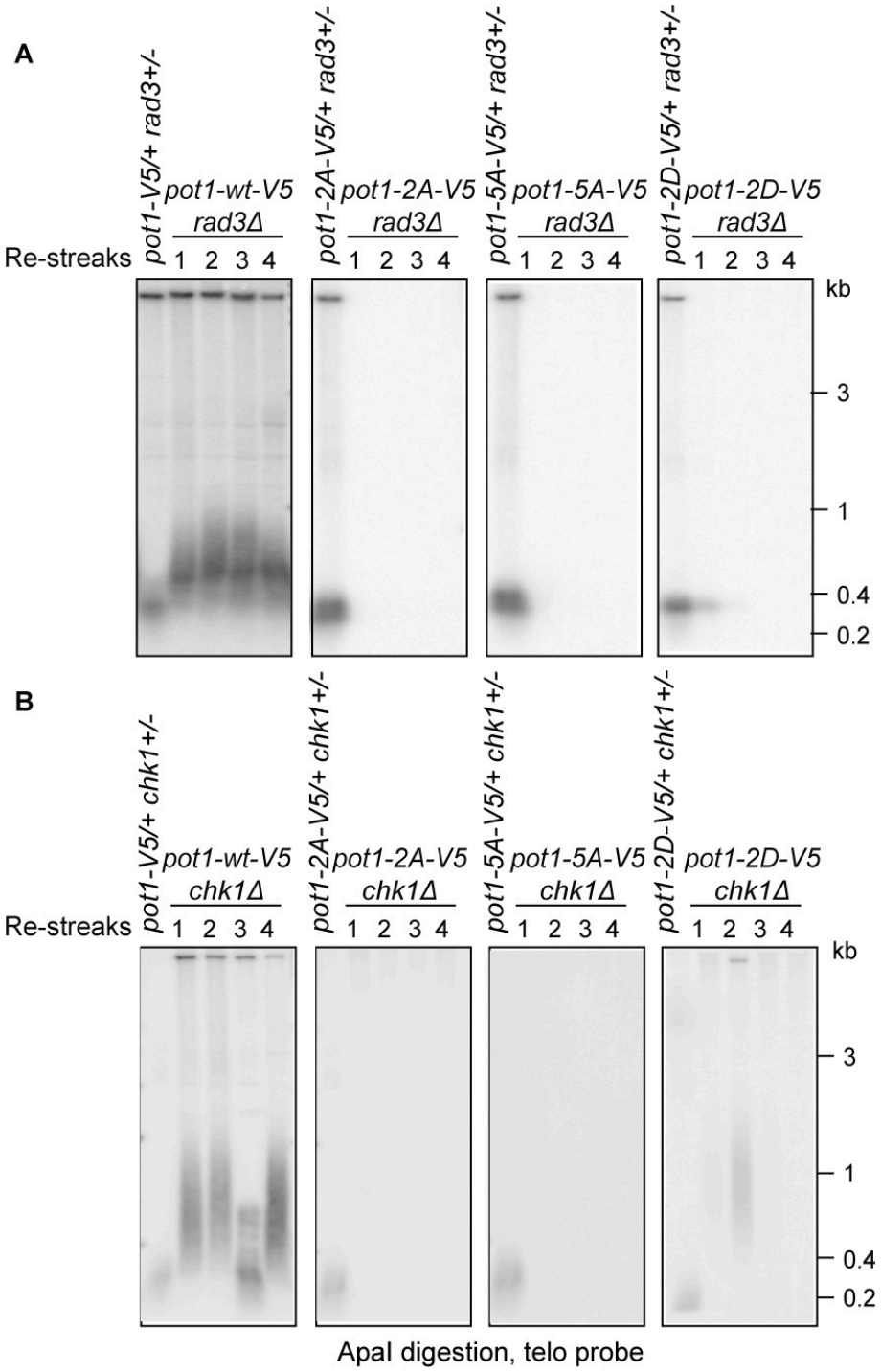

Figure 3.8 Chk1 and Rad3 are required for telomere maintenance in *pot1-V5* phosphorylation mutants

Telomere length was followed for four passages after sporulation from double-heterozygous diploid strains of *pot1-V5* phosphorylation mutants in combination with deletions of checkpoint kinases *rad3*$^{+}$ (**A**) and *chk1*$^{+}$ (**B**). Numbers on top indicate the number of passage.

3.5 Summary

Our results uncovered surprising roles for a number of DDR proteins at telomeres of the *pot1-V5* phospho-mutant strains. Components of the ATR checkpoint pathway, Rad3 and Chk1, are required for telomere protection in these mutants; Rad51, the RecA family recombinase capable of binding the ssDNA tail, is also required. In contrast, Rad22, a pivotal recombination protein that promotes strand invasion, is not essential for this protection, suggesting HR-independent roles of Rad51 in telomere protection in these mutants.

The dependence of these mutants on Rad51 and the Chk1 checkpoint pathway is reminiscent of that observed in later generations of *ccq1Δ* cells, which sustain chromosomal linearity by maintaining extremely short chromosomes via homologous recombination (Tomita and Cooper, 2008). However, there are some interesting differences between them. Firstly, while the *ccq1Δ* cells are perfectly capable of inhibiting chromosome end fusion before they hit the critically short telomere stage (~10 days after germination), the *pot1-V5* phospho-mutants already require the checkpoint pathway when they still have robust telomere signal immediately after germination. Secondly, *ccq1Δ* cells are defective in telomerase recruitment, meaning that at the critically short stage they would have to depend fully on the HR pathway; in contrast, telomeres of the *pot1-V5* phospho-mutants still engage telomerase (see section 4.2). It therefore seems likely that Rad51-Rad3-Chk1 dependency in *pot1-V5* phospho-mutants is achieved by a different mechanism than that seen for *ccq1Δ* cells.

A role for Rad51-like proteins in telomere maintenance has also been reported in mammals. It has been shown that in mammalian cells, the Rad51 paralog RAD51D forms clear foci at telomeres in the absence of DNA-damaging agents, and its removal leads to telomere dysfunction including telomere shortening and elevated levels of end-to-end fusions even in the presence of telomerase (Tarsounas et al., 2004)0 #6323}. While Rad51 foci are not observed at *wt* telomeres in fission yeast, the *pot1-V5* mutant background might provide us with a tool to study Rad51 functions at chromosome ends.

Taken together, our results showed that the telomeres of the *pot1-V5* phosphorylation mutants bear certain defect in telomere protection. They fail to suppress DDR at telomeres, which leads to recruitment of the HR repair protein Rad51 and activation of checkpoint. The DDR pathway in turn is required for telomere protection at the mutant telomeres. Removal of several components of the DDR pathway leads to cellular senescence immediately after their removal, and chromosome circularization often within the first passage. Therefore, proper Pot1 phosphorylation and the DDR pathway redundantly protect the telomeres from chromosome end fusions that are independent on Chk1 and Rad3. We attempted to address the cause of telomere dysfunction in the *pot1-V5* phospho-mutants, which is elaborated in Chapter 4.

Chapter 4. Molecular mechanism of the telomere protection defects of *pot1-V5* phospho-mutants

4.1 Introduction

Pot1 has been shown to be involved in many different, and sometimes conflicting, aspects of telomere maintenance, including length maintenance, suppression of ATR signalling, and protection against rampant resection and chromosomal fusion. The molecular mechanism underlying each aspect of its function is only starting to be understood. For instance, human POT1 acts as both a positive and a negative regulator of telomerase-mediated telomere maintenance, as both over-expression and RNAi-mediated knockdown of POT1 lead to telomere elongation (Colgin et al., 2003, Ye et al., 2004). It is proposed that POT1 can inhibit telomerase action by sequestering the single-stranded ends via bridging to the dsDNA region of the telomere (Palm and de Lange, 2008). As the loading of POT1 is facilitated by its interaction with the telomeric dsDNA-binding complex, this mechanism also enforces a negative feedback loop on telomere elongation (Loayza and De Lange, 2003). On the other hand, the POT1-TPP1 complex stimulates telomerase activity and processivity (Wang et al., 2007), providing positive regulation of telomerase-mediated telomere maintenance.

In fission yeast, a large portion of Pot1 including both the N-terminal OB-folds and the C-terminal domain is required for its function, as truncations of either terminus lead to a null phenotype (Bunch et al., 2005). The dominant and striking phenotype of telomere loss in *pot1*-null mutants complicates the investigation into its role in other aspects. Phenotypic analysis showed that the *pot1-V5* phosphorylation mutants are partially functional alleles of $pot1^{+}$. While they manage to maintain linear chromosomes to different extents in *pot1-A-V5* versus *pot1-D-V5*, these mutants are defective in inhibition of DNA damage checkpoint. The defect in DDR suppression leads to accumulation of the HR repair protein Rad51 and checkpoint activation. They also have defects in telomere protection, which result in a requirement of DDR proteins for telomere protection. How these mutations in the N-terminal OB-fold affect Pot1 function is not clear. Here, we investigate the

molecular mechanism underlying the effects of the *pot1-V5* putative phosphorylation mutations.

4.2 Pot1-V5 phospho-mutants are located at the telomeres

4.2.1 Pot1 phospho-mutants localize to the telomeres

Pot1 presumably has two telomeric binding modes, one via Tpz1 and the dsDNA-binding complex and one via ss interaction. Its various functions, including telomerase recruitment and resection inhibition, likely require Pot1 to act *in cis* at individual chromosome ends via either and/or both binding modes. Pot1 localization to telomeres is thus an important aspect of its function. As the putative phosphorylation sites reside in the N-terminal OB-fold of Pot1, which mediates telomeric ssDNA binding, mutations of these sites might affect its recruitment to the telomeres. We therefore investigated the binding of Pot1-V5 phosphorylation mutants to the telomeres *in vivo* utilizing IF and ChIP techniques.

Cellular localization of the mutants was determined by dual IF analysis. Asynchronous cultures of *pot1-V5* phosphorylation mutants were fixed in 70% ethanol, and the cells were subject to IF staining against Pot1-V5 and the telomere marker Taz1. In most cells, 1 to 3 clear foci of Taz1 and Pot1-V5 can be observed to co-localize in the nucleus (stained with DAPI) in *pot1-V5* as well as *pot1-A-V5* and *pot1-D-V5* strains (Figure 4.1). Therefore, both Pot1-V5 and its phosphorylation mutants have the ability to localize to the telomeres.

Quantitation of the IF shows that the rate of co-localization, i.e. percentage of Taz1 foci accompanied by a Pot1-V5 focus, was similar in the *pot1-V5* phospho-mutant cells compared with in *pot1-V5* cells (around 60-80%). It should be noted that even in *pot1*-V5 background, around 20% of Taz1 foci are not companied by a Pot1-V5 signal, which could reflect the limitation of the IF and/or microscopy technique. We conclude that the cellular localization of the Pot1-V5 is not clearly affected by the phospho-mutations in the N-terminal OB-fold.

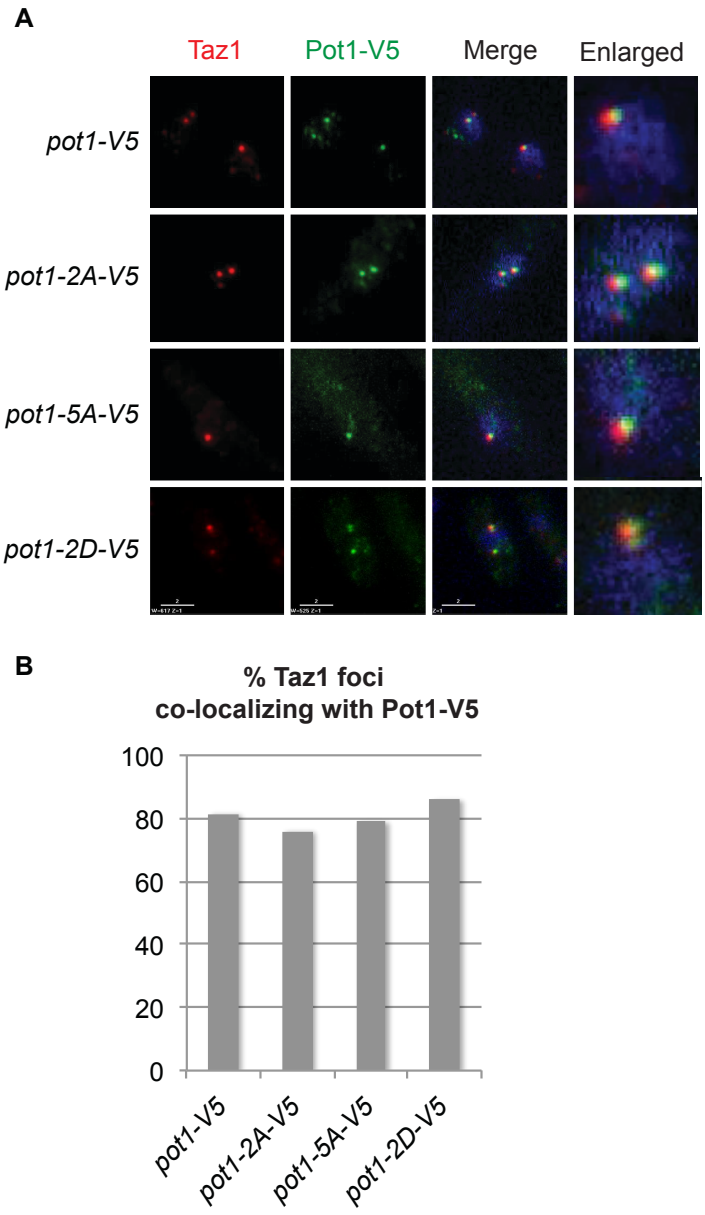

Figure 4.1 Cellular localization of Pot1-V5 phospho-mutants

A. Representative image of dual immunofluorescence staining against Taz1 (red) and Pot1-V5 (green) in *pot1-V5* phospho-mutants, DNA stained with DAPI (blue). See text for experimental procedure. Images are flattened on *z*-stacks. Scale bar: 2µm. **B**. Quantitation of Pot1-V5 co-localization with Taz1, showing the percentage of Taz1 focus accompanied by a Pot1 focus in fixed samples of asynchronous log phase cultures (*n*>100).

In order to provide quantitative assessment on the telomere recruitment of Pot1-V5 phosphorylation mutants, we performed ChIP against V5 in *pot1-V5* phospho-mutant backgrounds. Asynchronous log phase cultures were treated with 1% formaldehyde to cross-link genomic DNA with its associating proteins. Extracted chromatin was sonicated, and immunoprecipitated using α-V5 antibodies. Binding of Pot1-V5 mutants with telomeres was detected by quantitative-PCR for subtelomere (STE1) regions or dot blot for the telomere region itself.

Using q-PCR, relative enrichment of the STE1 region and the internal *act1*$^+$ region in *wt* and in *pot1-V5* phospho-mutants was determined as follows. The enrichment (expressed as IP/Input) in *pot1-V5* phospho-mutants after α-V5 IP was normalized to that in an untagged negative control. The value of relative enrichment of STE1 and *act1*$^+$ in the untagged *wt* strain is therefore 1, which represents the background of the assay. The relative enrichment of *act1*$^+$ is low in all Pot1-V5 IPs, consistent with the expectation that Pot1 is not recruited to internal genomic regions. In contrast, we observed significant enrichment of STE1 signal after Pot1-V5 IP in all tagged strains, although the level is slightly reduced in *pot1-V5* phospho-mutant backgrounds (Figure 4.2A).

As the telomeres are long and heterogeneous in the mutant backgrounds, sonication of the chromatin could break the DNA between the Pot1 binding site and the STE1 region if Pot1 binds the extreme chromosome terminus, thereby introducing errors when the binding is measured by qPCR at STE1 (Dehe et al., 2012). We therefore performed dot blot Southern analysis to detect Pot1 binding to telomeres directly. The ChIP samples were spotted onto a membrane, UV-crosslinked and hybridized with telomere probes (Figure 4.2B). Quantitation of the dot blot reveals similar trend of enrichment (IP/Input) with the qPCR result, showing strong enrichment of telomere signal in all Pot1-V5 IPs, with slight reduction in the phospho-mutant backgrounds. To sum up, the ChIP analyses suggest that Pot1 recruitment to telomere is not abolished, but are slightly affected, by the phospho-mutations in the N-terminal OB-fold.

The above analyses produced consistent results over three experimental repeats. It should be noted, however, that these analyses were performed using the same

clone of each *pot1-V5* mutant. Interestingly, when the analysis was performed on different *pot1-A-V5* clones, varying and often higher-than-normal levels of telomere enrichment can be observed; these variations were not observed in the *pot1-D-V5* background (Shaikh, unpublished data). Given that many of the phenotypes of *pot1-A-V5* mutants are clone dependent (see section 3.2), binding of Pot1-A-V5 to telomeres may indeed contribute its functionality. Hence, we regard our data on Pot1 binding as preliminary and in need of further exploration.

Taken together, our data showed that the Pot1-V5 phospho-mutants do localize to the telomeres. While the recruitment appeared unaffected by the mutations at the cytological level, the binding efficiency varies in *pot1-A-V5* background when assessed by ChIP. Whether the variation is biologically significant is not clear yet. Further investigation is required to establish a possible correlation between recruitment level and the phenotypes in the *pot1-V5* phospho-mutant backgrounds.

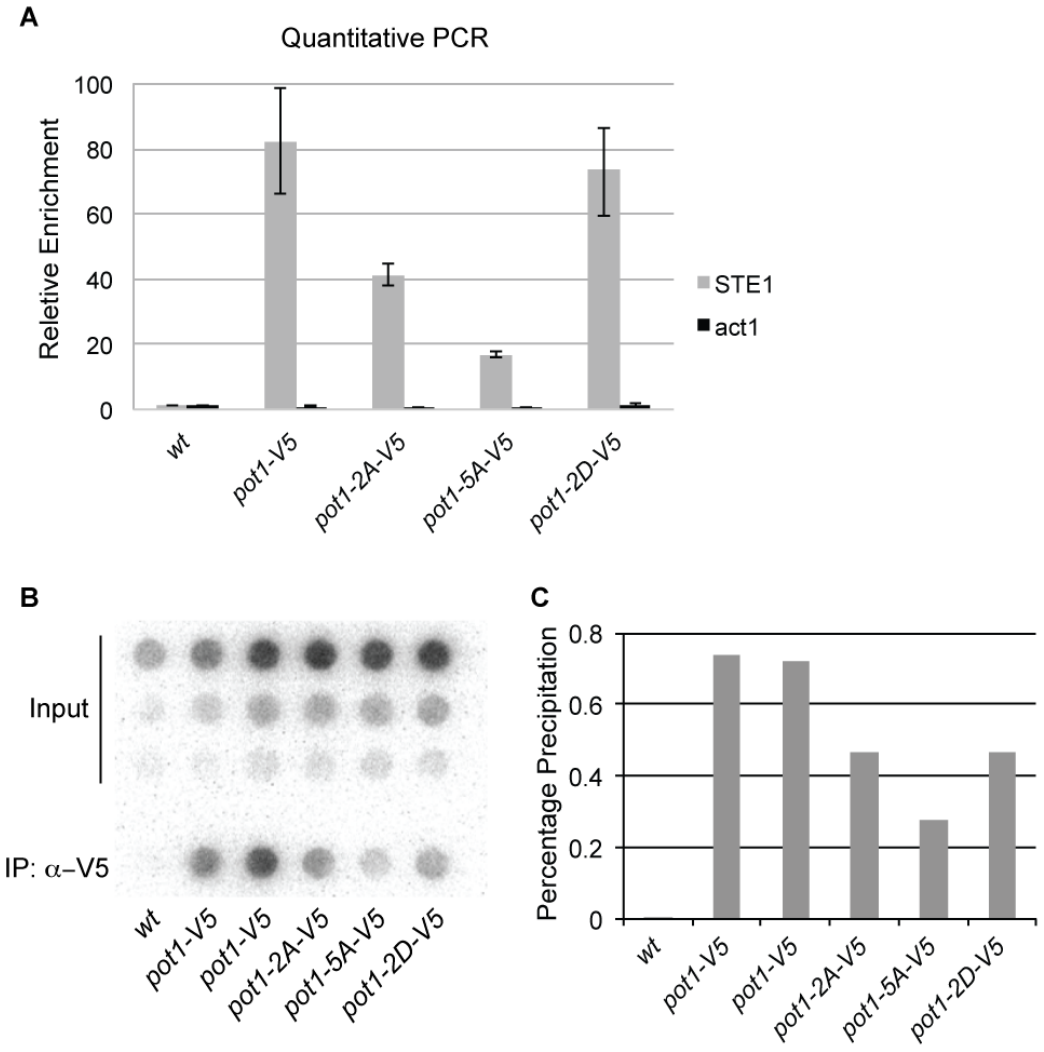

Figure 4.2 Pot1-V5 phospho-mutants are enriched at telomere DNA by ChIP

A. Levels of STE1 and *act1*$^{+}$ enrichment in V5 IPs in *wt* (negative control) and *pot1-V5* phospho-mutant backgrounds as determined by q-PCR. Error bars represent standard deviation of three ChIP experiments. **B**. Dot blot analysis of telomeric enrichment in ChIP samples, representative of 3 independent experiments. The blots were hybridized with synthetic telomere probes, and exposed using PhosphoImager. Inputs were loaded in series of 10-fold dilution to avoid saturation of the signal. Three repeats show similar trends. **C**. Quantitation of the dot blot in **B**, which is analysed using ImageQuant Array Analysis software.

4.2.2 Attempts to distinguish between binding to ds and ssDNA

Pot1 can be recruited to the telomeres either by direct binding to telomeric single-stranded overhang via its OB-folds, or by indirect interaction with the dsDNA binding complex Taz1-Rap1 via Poz1 (Miyoshi et al., 2008). Binding via ssDNA is likely only a small portion of the total amount recruited, because telomeric overhang is short compared to the dsDNA region. This is evidenced by the weak signal of the overhang, which is detectable by in-gel hybridization technique only in synchronized S phase culture in wt cells (Tomita et al., 2004). Additionally, a series of Taz1-interacting C-terminal fragments of Pot1 co-localize with Taz1-GFP at telomeres by IF, while expression of the N-terminal OB-folds forms no discrete foci, suggesting that Pot1 localization to telomeres is mediated predominantly by its interaction with the Taz1 complex (Bunch et al., 2005). Therefore, if the recruitment of Pot1 to dsDNA remains unaffected while the binding to ssDNA is reduced, it may not be reflected when assessing total recruitment.

As the phospho-mutations are in the ssDNA-binding OB-fold, it is conceivable that they might affect binding to telomeric ssDNA only. Techniques such as ChIP and IF at *wt* telomeres do not allow us to distinguish between the two binding modes. Previously, an electrophoresis mobility shift assay (EMSA) using recombinant Pot1 N-terminal OB-fold showed that the phospho-mutations do not drastically affect the ability of the OB-fold to associate with telomeric ssDNA sequences *in vitro* (Kuznetsov, 2008). However, the ssDNA-binding ability *in vivo* involves the Pot1 binding partner Tpz1, and might be affected by other modifications; moreover, the subtle differences seen by EMSA in vitro may become important in vivo. Therefore, it is important to address the effect of the phosphorylation mutations on Pot1 ssDNA binding *in vivo*.

Since recruitment of Pot1 to telomeric dsDNA largely depends on the dsDNA binding complex Taz1-Rap1, removal of either of these two proteins should abolish or reduce the binding of Pot1 to the dsDNA region, which would allow us to measure the ssDNA-binding ability of Pot1. Therefore, we constructed double-heterozygous diploid strains with *pot1-V5* phospho-mutants in *taz1*$^{+/\Delta}$ and *rap1*$^{+/\Delta}$ backgrounds. Spores were germinated on selective media to obtain the desired

genotype with phospho-mutants in *taz1Δ* or *rap1Δ* backgrounds, which were then characterized. Surprisingly, the phospho-deficient *pot1-A-V5* mutants lose telomeres rapidly in the absence of either component of the dsDNA-binding complex. The telomere maintenance dependence of *pot1-A-V5* mutants on the Taz1-Rap1 complex is described in section 4.4. These strains are therefore not suitable for the telomeric ssDNA-binding analysis. A different strategy needs to be developed to assess the *in vivo* ssDNA-binding abilities of the phosphorylation mutants.

4.3 Telomerase is required for telomere maintenance in all *pot1-V5* mutants

4.3.1 Telomerase is recruited to *pot1-V5* phospho-mutant telomeres

Our observation that telomere maintenance depends on Rad51 in *pot1-V5* phosphorylation mutants (see section 3.4) can be subject to various interpretations. One explanation relies on a telomerase-independent mechanism of telomere maintenance. If the mutants are defective in telomerase action, e.g. if they confer reduced telomerase recruitment or processivity, then telomere maintenance in these mutants could depend solely on homologous recombination. In that case, the HR protein Rad51 should be required for telomere maintenance.

Indeed, a previous observation in the laboratory supported this hypothesis. It showed that the *pot1-A-V5* mutants were not affected by telomerase deletion, and were able to maintain stable long telomeres in the absence of telomerase (Kuznetsov, 2008). This result could imply that in *pot1-A-V5* mutants, even though telomerase is present, it is not active at the telomeres.

We attempted to verify this assumption and pinpoint which step in telomerase action went awry. For telomerase to act, it first has to be recruited to its substrate, the chromosome ends. To test whether telomerase recruitment is impaired in the *pot1-A-V5* mutant, we performed ChIP against tagged telomerase subunits in *pot1-V5* phospho-mutant backgrounds. Using PCR-based gene targeting, we constructed double-heterozygous diploid strains of *pot1-V5* phosphorylation mutants with either the catalytic subunit Trt1 or the regulatory subunit Est1 tagged at the respective C-termini. The strains were random sporulated, and germinated on selective media. Crosslinked chromatin extracted from asynchronous cultures were immunoprecipitated using an antibody against the tag, and associating DNA analysed by quantitative PCR.

Both telomerase subunits, Trt1-myc and Est1-HA, were shown to be enriched at the telomeric region compared to a non-telomeric internal control region (*act1* gene) in the *wt* background as well as the phosphorylation mutants. In fact, Trt1-myc

recruitment was higher in both *pot1-V5* phospho-mutants, coinciding with the elongated telomere in these strains. While further confirmation is required, our preliminary data suggest that recruitment of telomerase was not abolished by the phospho-mutations in the OB-fold of Pot1.

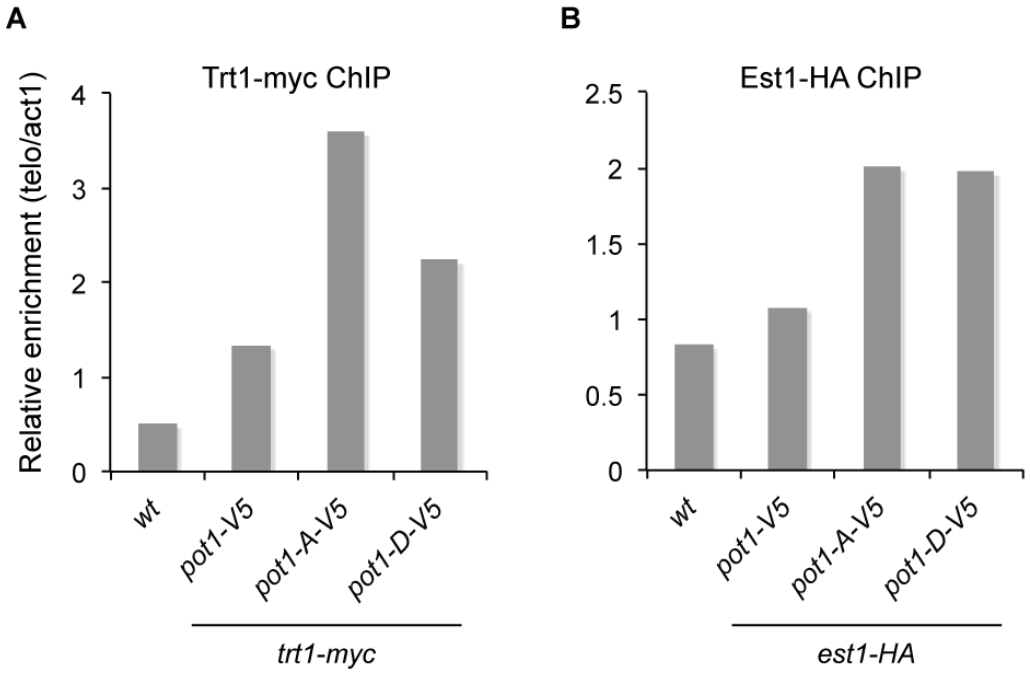

Figure 4.3 Telomerase subunits are recruited to *pot1-A-V5* telomeres

A. Levels of Trt1-myc enrichment at telomere sequence over background (telo/*act1*). Quantitative PCR using primers in STE1 (telo) and act1 gene was performed on α-myc IP derived from asynchronous cultures of *wt* (untagged control) and *trt1-myc pot1-V5* phospho-mutants. The result shown is representative of three independent repeats. **B**. Level of Est1-HA enrichment at telomere over background. Samples are α-HA IP from asynchronous cultures of *wt* (untagged control) and *est1-HA pot1-V5* phospho-mutants. The result shown is representative of two independent repeats.

4.3.2 Telomere maintenance in *pot1-V5* phospho-mutants depends on Trt1

The fact that telomerase is recruited at high levels to the telomeres in *pot1-V5* phospho-mutants seemed to contradict a previous observation that telomere maintenance is independent of telomerase in the *pot1-A-V5* mutants (Kuznetsov, 2008). We therefore performed a more detailed analysis on the telomere maintenance dependence of the mutant strains.

To investigate the effect of telomerase removal, we followed the cellular and telomeric phenotypes of the *pot1-V5* phospho-mutants over time after removal of telomerase. *trt1Δ pot1-V5* phospho-mutant double-heterozygous diploid strains were sporulated and germinated on selective media, and were propagated in rich media for several single colony passages. Colonies of *trt1Δ pot1-A-V5* mutants grew very slowly upon antibiotic selection, suggesting that they senesced immediately, while the *trt1Δ pot1-wt-V5* and *trt1Δ pot1-D-V5* strains did not senesce until the 4th or 5th passage (Figure 4.4A). Consistent with previous observations, telomeres of *pot1-V5* and *pot1-D-V5* gradually shortened and eventually disappeared in the absence of telomerase, showing a classic *est* (ever shorter telomeres) phenotype. However, the telomere phenotype of *pot1-A-V5 trt1Δ* mutants was confusingly different. In contrast to the previous result, telomeres of the *pot1-2A-V5* mutant strain also shorten over time and disappeared at even earlier passage than the *pot1-wt-V5 trt1Δ* strain, while telomeres of *pot1-5A-V5 trt1Δ* exhibited an elongated phenotype after the first passage (~5 days after germination), suggesting a recombinational mode of telomere maintenance and, in this case, resembling the former results (Figure 4.4B). Therefore, it appears that telomerase does affect telomere maintenance in the *pot1-V5* phospho-deficient mutants, at least in the *pot1-2A-V5* background.

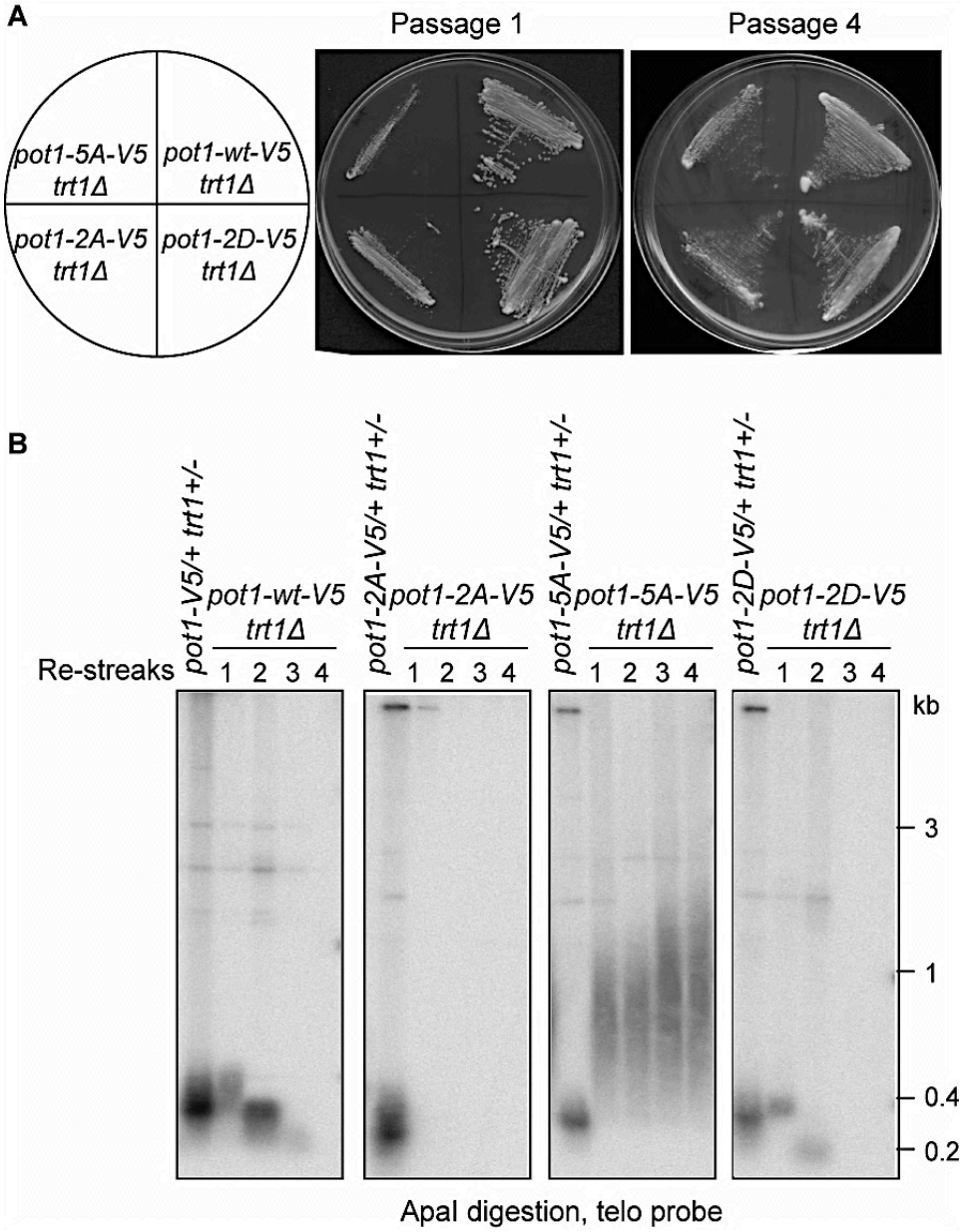

Figure 4.4 Early senescence and telomerase dependency of *pot1-A-V5* mutants

A. Plates of *trt1*Δ *pot1*-V5 phospho-mutants passage 1 and 4 after sporulation of double-heterozygous diploid strains. *pot1-A-V5* mutants show phenotypes of senescence characterized by slow growth and irregular-shaped colonies at the 1st passage, while wt and *pot1-D*-V5 mutants senesce only at the 4th passage. **B**. Telomere length of each mutant was followed for 4 passages after telomerase removal. Numbers on top indicate the number of passages after germination. The blot shown is representative of 3 independent repeats.

To confirm the telomerase dependence in a different setting, we also constructed *trt1Δ pot1-V5* phosphorylation mutants by deleting *trt1*$^{+}$ in individual haploid *pot1-V5* mutant strains. Unlike the progeny of the double-heterozygous diploid strains, which have *wt* length telomere at the beginning of the time course, the double mutants made from haploid gene-replacement start with longer telomeres. This allows better resolution of telomere shortening over time, although the inherent selection involved in obtaining transformant colonies from haploid knockout experiments may complicate interpretation.

Following antibiotic selection, gene replacement was individually verified by PCR, and 2 confirmed clones of each genotype were propagated and analysed. In contrast to the early senescence of *trt1Δ pot1-A-V5* mutant strains starting from double-heterozygous diploids, the haploid-deletion *trt1*△ *pot1-A-V5* mutants grew well at the first few passages after *trt1Δ* transformation. Similar to *trt1Δ pot1-V5* and *trt1Δ pot1-D-V5* strains, they started to senesce only at the 4th re-streak, which is characterized by formation of small, rough-edged colonies (Figure 4.5A). In other words, senescence is delayed in the haploid-deletion *trt1*△ *pot1-A-V5* mutants where the starting telomere length is longer than heterozygous diploid strains.

Southern blots following changes in telomere length in the double mutants confirmed the *est* phenotype in all *trt1Δ pot1-V5* phospho-mutant strains. Note that as the starting length of the telomeres is long in the haploid *trt1Δ pot1-V5* mutants, they retained robust, albeit shorter, telomere signal until the 4th passage (Figure 4.5B). Therefore, the timing of the sickness or senescence observed in *trt1Δ pot1-V5* phospho-mutants corresponds to the time at which telomeres reach critically short length. These data suggest that in the haploid scenario, telomerase is involved in telomere maintenance in *pot1-V5* phospho-mutants.

Interestingly, compared to *trt1Δ pot1-wt-V5* or *trt1Δ pot1-D-V5* strains, the rate of telomere shortening is faster in *trt1Δ pot1-A-V5* mutants (Figure 4.6B). The *pot1-wt-V5* and *pot1-D-V5* strains undergo telomere shortening at approximately 100bp per passage (~3 days), or around 3bp per cell division, which is similar to the rate of telomere shortening in telomerase-deficient *wt* cells. In contrast, the *pot1-A-V5* mutants exhibited a net decrease of 400-600bp within one passage, which

corresponds to around 10-15bp telomere loss per division, suggesting that telomere erosion is faster in *pot1-A-V5* mutants than in the *wt-pot1-V5* or *pot1-D-V5* backgrounds.

Accelerated telomere erosion could explain the lack of visible telomere shortening in the *trt1Δ pot1-5A-V5* mutants derived from heterozygous diploid strains. As the starting telomere length is only 300bp in the heterozygous diploids, an attrition rate of 400-600bp per passage means that the telomeres of *trt1Δ pot1-5A-V5* could become critically short before the 1st passage after germination, forcing the cells into telomerase-independent survival mode (see section 4.3.3). If linear survivors arise immediately, their long telomeres could be difficult to distinguish from those utilizing telomerase. In addition, the fact that linear survivors arise much more frequently in *trt1*Δ *pot1-A-V5* than in *trt1*Δ (see section 4.3.4) could facilitate the 'immediate' switch.

To sum up, we demonstrated that telomerase is recruited to and active at the telomeres of *pot1-V5* phospho-mutants, irrespective of the initial telomere length before telomerase removal. In addition, our data suggest that telomere erosion is accelerated in *pot1-A-V5* phospho-deficient mutants. These results contradict the observation made in the previous study, which suggested that telomeres fail to shorten in *pot1-A-V5 trt1Δ* strains derived from double-heterozygous diploids (Kuznetsov, 2008). We analysed in detail the procedures used in these two studies to explain how such striking differences could result (see below).

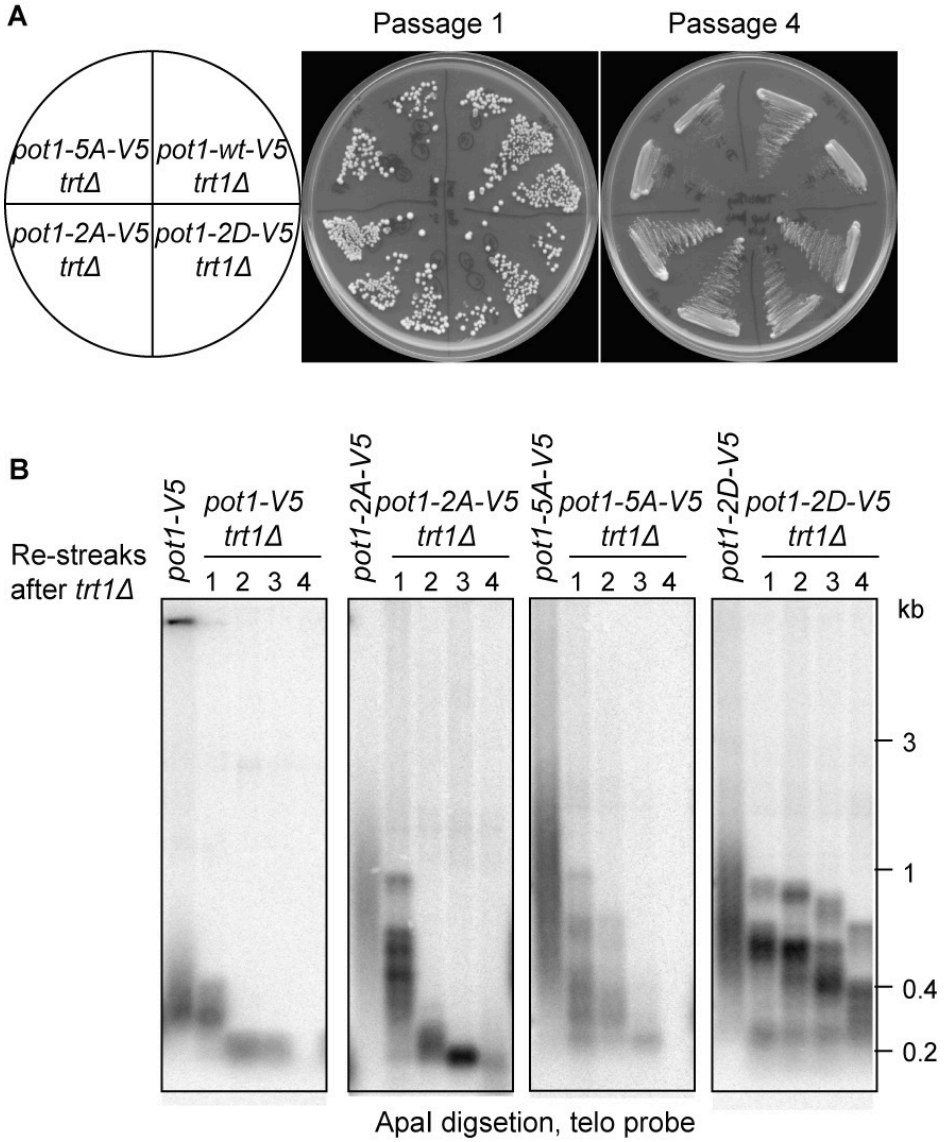

Figure 4.5 Accelerated telomere erosion in *pot1-A-V5* background after telomerase removal from haploid mutant cells

A. Plates of *trt1*Δ *pot1*-V5 phospho-mutants passage 1 and 4 after deletion of *trt1*$^{+}$ by gene targeting in haploid *pot1-V5* phosphorylation mutants. None of the mutants show senescence phenotypes at the 1st passage. **B**. Telomere length of each mutant was followed for 4 passages after telomerase deletion. Numbers on top indicate the number of passages after transformation.

4.3.3 Single colony vs. patching passage

Why did the previous study (Kuznetsov, 2008) show telomerase-independence of the *pot1-A-V5* strain? This was a question we struggled to answer until we noticed a difference in the experimental procedure between this and the previous study. While we performed serial passages to follow the telomere phenotypes by picking and re-streaking single colonies, the previous study passaged the strains by repeatedly patching them on plates. In a senescence experiment, the latter method is known to enrich for fast growing survivors, as they outgrow the more frequent but slower growing circular survivors (Jain et al., 2010); basically, growing in patches is equivalent to growing in liquid.

We demonstrated that telomere erosion is accelerated in *pot1-A-V5* phospho-deficient strains. In the *pot1-A-V5 trt1Δ* double mutants generated from heterozygous diploids, telomeres become critically short very soon after germination. At this point, the cells are forced to adapt to one of the three telomerase-minus survival modes: circularizing all chromosomes, maintaining linear chromosomes by homologous recombination, and HAATI (heterochromatin amplification-mediated and telomerase-independent). In a single colony passage scenario, it is likely that the most frequent form of survivor – circular survivors – is picked at random. However, in a patching scenario, the rare but fast growing linear or HAATI survivors generated soon after germination are likely to take over the population, thus explaining the lack of telomerase-dependence.

To support this hypothesis, we repeated the *trt1Δ* experiment by patching and followed telomere length over time. As expected, the *trt1Δ pot1-V5* cells undergo telomere shortening before linear survivors arise. In contrast, a clear telomere shortening phenotype is not observed in *trt1Δ pot1-2A-V5* or *trt1Δ pot1-2D-V5* strains, which instead seemed to be enriching for linear survivors with *wild-type* length or more elongated telomeres soon after the 1st and 2nd passage, respectively (Figure 4.6). The phenotypes of *trt1Δ pot1-V5* phospho-mutants thus recapitulate the result of the previous study, supporting our hypothesis that patching passage creates the illusion that telomerase is not active or required at *pot1-A-V5* telomeres.

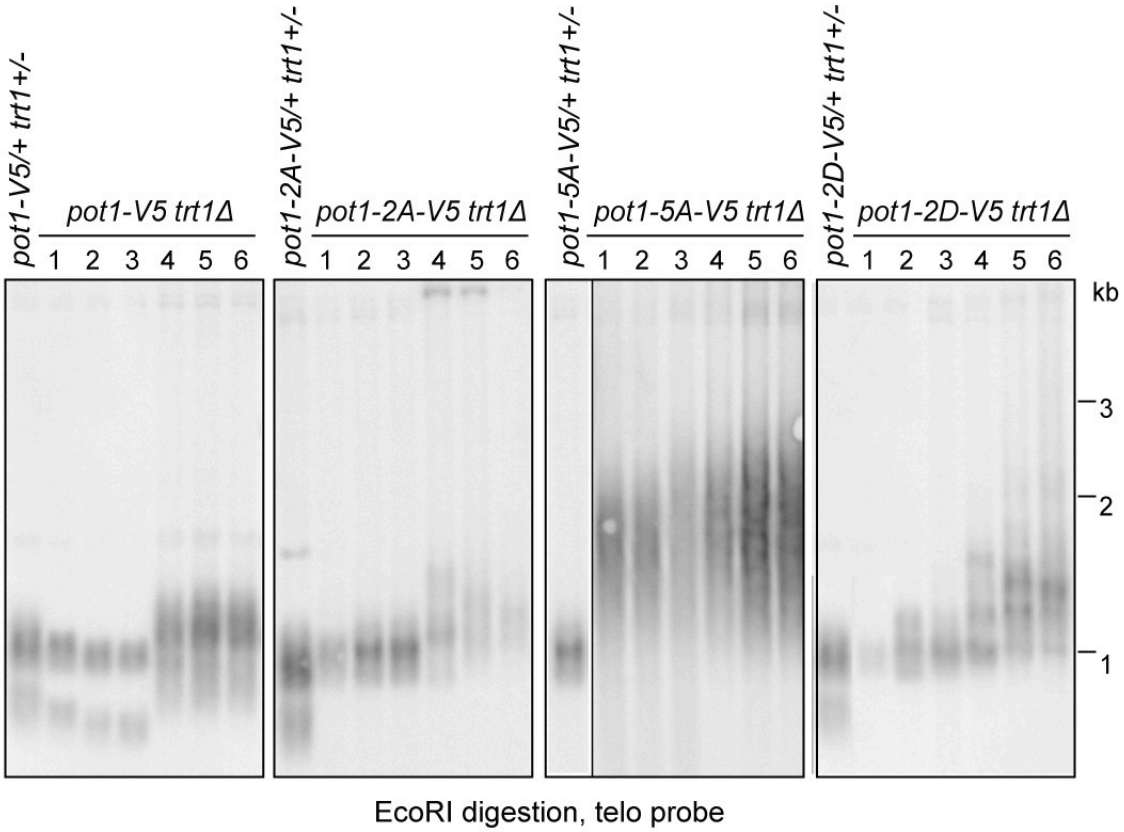

Figure 4.6 Patching passage of telomerase-null mutants enrich for linear survivors

Southern blotting showing telomere length changes over 6 patching passages after germination. A clear *est* phenotype was not observed in the *trt1*Δ *pot1-V5* phospho-mutant strains. The first lanes represent telomere length of the diploid parent strains, and the numbers on top indicate the number of patching passages after germination. *EcoRI* digestion and pIRT2-telo probe were used to facilitate detection of short telomere fragments.

4.3.4 Choice of survival mode by patching passage after telomerase removal

The *trt1Δ pot1-2D-V5* mutant also forms linear survivors in the patching experiment shown above, which differs from the result of the previous study (Kuznetsov, 2008). Does this mean the patching conditions still differ between the two studies, or that linear survivor forms only in a portion of the patches?

To answer this question, we performed patching passages on multiple colonies derived from the double-heterozygous diploid mutants, and looked at the ratio of survivors formed. 22 patches of each *trt1Δ pot1-V5* phosphorylation mutant genotype were propagated on plate for 10 passages (~20 days) before they were replicated onto 0.001% MMS plates to check for hyper-sensitivity. The patches highly sensitive to MMS likely contain mainly circular survivors, while those that are less MMS sensitive are enriched for either HAATI or linear survivors (Jain et al., 2010). Subsequently, representative patches of both categories were grown up in liquid culture. The DNA was extracted in agarose plugs, fragments containing chromosomal ends were released with *NotI* digestion, and the chromosomal end structure was analysed by PFGE to distinguish between the three forms of survivors. Linear chromosome ends enter the gel and show distinct bands of L, M, I fragments (see Figure 3.6 for relative position of the digestion fragments); circular survivors with fused chromosome ends show fusion bands corresponding to the size of L+I fragment; chromosome ends of HAATI survivors contain complex structures and do not enter the gel (Jain et al., 2010).

Surprisingly, HAATI formation seemed to be impaired by V5-tagging of wild-type *pot1*$^{+}$. Compared to patches of a *trt1Δ pot1*$^{+}$ strain, patches of *trt1Δ pot1-V5* strains are mostly hypersensitive to low concentration of MMS (0.0001%), with only a small number of patches showing MMS resistance; the same is true for *trt1*∆ *pot1-A-V5* and *trt1*∆ *pot1-D-V5* strains (Figure 4.7A). The circular nature of MMS-sensitive patches was confirmed on PFGE, as they display fused bands of chromosome ends (Figure 4.7C). The reason why HAATI and/or linear survivors do not arise as frequent in *trt1*∆ *pot1-V5* mutants as in *trt1Δ pot1*$^{+}$ strains is not yet understood. One possibility is that the C-terminal tagging might affect the

interaction between Pot1 and Tpz1-Ccq1, which was proposed to recruit Pot1 to the heterochromatic termini in HAATI survivors.

Meanwhile, we performed PFGE on representative MMS-resistant patches in all genotypes to determine which fast growing survivor – HAATI or linear survivors – was dominant in the various *pot1-V5* mutant settings. Interestingly, the MMS-resistant patches of *trt1*Δ *pot1-V5* mutant were enriched for HAATI, evidenced by the lack of discrete terminal LMI bands after *NotI*. In contrast, the MMS-resistant patches of *trt1*Δ *pot1-A-V5* or *pot1-D-V5* phospho-mutants contained predominantly linear survivors, which lacked the complex terminal structure in HAATI and generated PFGE pattern similar to *wt* strains after *NotI* digestion (Figure 4.7C). Elevated telomere recombination in the phospho-mutants might prompt the cells to adapt a recombination-based survival mode. Alternatively, impaired HAATI formation by V5 tagging may have facilitated enrichment for linear survival mode in the *pot1-V5* phospho-mutants.

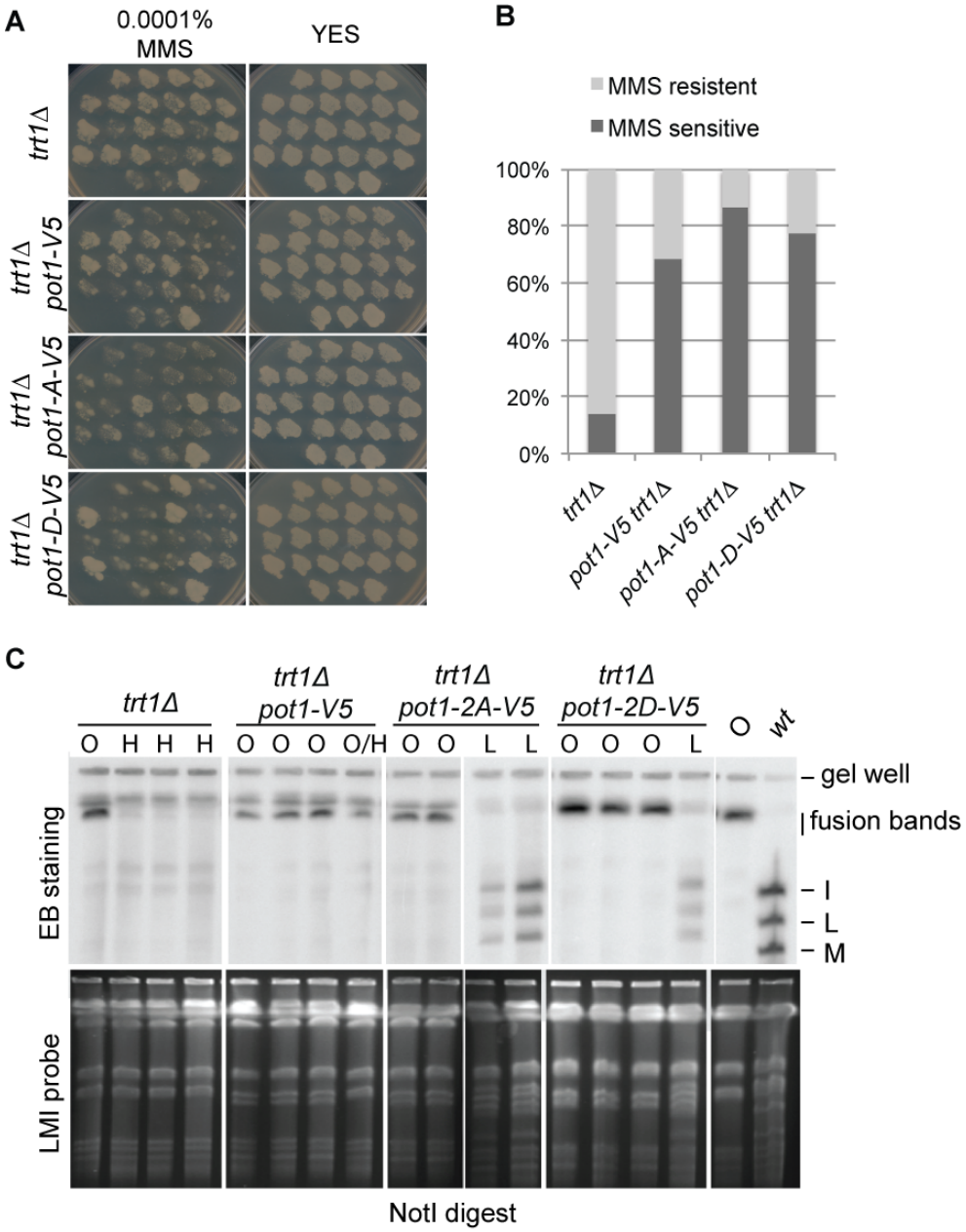

Figure 4.7 Survivor formation by patching passage after *trt1*$^{+}$ deletion

A. MMS sensitivity assay of patches of *trt1*Δ and *trt1*Δ *pot1-V5* phospho-mutants. 22 clones of each genotype were propagated by patching passage, and then replica onto YES plate ± MMS. The last three patches on each plate are circular, circular, and *wt* controls. **B**. Percentage of MMS-sensitive and resistant patches for each genotype. **C**. PFGE analysis of representative patches after *NotI* digestion. For *trt1*Δ, 1 MMS-sensitive and 3 MMS-resistant patches were analysed; for *trt1*Δ *pot1-V5* phospho-mutants, 2 MMS-sensitive and 2 MMS-resistant patches were analysed. MMS-sensitive patches in all mutants were confirmed circular (indicated as O). MMS-resistant patches in *trt1*Δ and *trt1*Δ *pot1-V5* were likely HAATI (H), while those in *trt1 pot1-A/D-V5* more likely formed linear survivors (L).

4.4 Telomeric dsDNA-binding complex is required for telomere maintenance in *pot1-A-V5* mutants

In our attempt to assess single-stranded telomeric binding of Pot1-V5 phosphorylation mutants (section 4.2), we found that the phospho-deficient *pot1-A-V5* mutants lose telomere signal upon disruption of the telomeric dsDNA-binding protein Taz1. Double-heterozygous diploid strains with *pot1-V5* phosphorylation mutants in *taz1*$^{+/\Delta}$ background were sporulated and germinated on selective media. Formation of single colonies following spore germination is much slower in the *pot1-A*-V5 mutants compared to *pot1-wt-V5* and *pot1-D-V5* mutants, and the colonies that managed to emerge contained only slow growing, senescent cells. When the telomeres of these cells were analysed on Southern blot after the first passage, no telomere signal can be detected (Figure 4.8A). Therefore, telomere maintenance in *pot1-A-V5* mutants depends on Taz1.

The same experiment was performed in *rap1*Δ background. After sporulation of double-heterozygous diploid strains, *rap1*Δ *pot1-A-V5* mutants formed colonies much smaller than *rap1*Δ *pot1-V5* and *rap1*Δ *pot1-D-V5* mutants. Senescent phenotypes were also observed in *rap1*Δ *pot1-A-V5* mutants when the strains were propagated on rich medium (Figure 4.8B). Due to technical problems, we could not measure changes in telomere length by Southern blotting at this time. Instead, colony PCR was performed using primer sets at STE1 region to verify the presence of the telomere, and at *act1*$^{+}$ region as control. While *rap1*Δ *pot1-V5* and *rap1*Δ *pot1-D-V5* mutant showed strong STE1 signal similar to *wt*, the signal was absent in *rap1*Δ *pot1-A-V5* colonies (Figure 4.8C), suggesting the loss of telomere in these strains. Telomere maintenance in *pot1-A-V5* mutants thus depends on Rap1 as well.

Therefore, we concluded that the Taz1-Rap1 dsDNA-binding complex is required for telomere maintenance in the *pot1-A-V5* phospho-deficient mutants. This result suggests the tantalizing possibility that Pot1-A-V5 binds telomeres only via the Taz1-Rap1 complex; hence, in mutants lacking this telomeric dsDNA-binding complex, a *pot1*-null phenotype arises (see below).

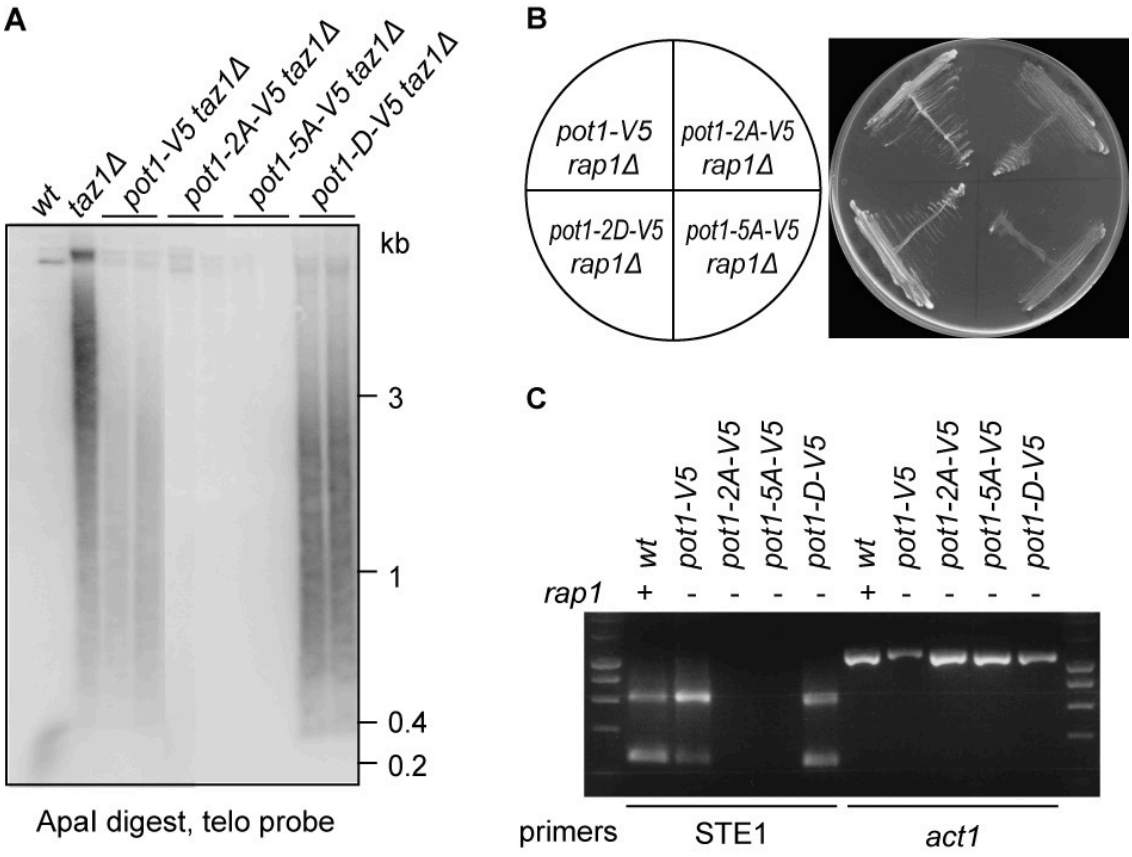

Figure 4.8 Taz1 and Rap1 are required for telomere maintenance in *pot1-A-V5* mutants

A. Southern blotting showing telomere maintenance defect in *taz1*Δ *pot1-A-V5*. For each genotype of *pot1-V5* phospho-mutants in *taz1*Δ background, two independent clones were subject to Southern blotting and probed for telomere signal. Samples were taken five days after sporulation of double-heterozygous diploid strains. **B**. Passage 1 of *rap1*Δ *pot1*-V5 phospho-mutants after sporulation of double-heterozygous diploid strains. Picture was taken after incubating at 32ºC for 1 day. **C**. Colony PCR of *rap1*Δ *pot1*-V5 phospho-mutants using primer sets targeting STE1 and *act1*$^{+}$ regions, respectively. The *wt* strain was used as control.

4.5 Synthetic lethality by disrupting recruitment of Pot1-A-V5 mutants to telomeric dsDNA

To understand the mechanism behind the Taz1 and Rap1 dependence in *pot1-A-V5* background, we looked for functions that are shared between Taz1 and Rap1. One of the defects shared between *rap1*Δ and *taz1*Δ telomeres is loss of inhibition to chromosome end-to-end fusion due to low Taz1 occupancy (Miller et al., 2006). However, the telomere fusion induced by Taz1 deficiency employs non-homologous end joining pathway, which, in fission yeast, occurs mainly in nitrogen-starved G1 arrest culture (Ferreira and Cooper, 2004). The telomere fusion phenotype observed in *pot1-A-V5 taz1*Δ and *pot1-A-V5 rap1*Δ is therefore unlikely the consequence of an elevation in NHEJ activity.

Another shared function of Taz1 and Rap1 is that both proteins are required to recruit the Pot1 sub-complex to the telomeric dsDNA-binding complex (Miyoshi et al. 2008). We therefore investigated whether the bridging of Pot1 to telomeric dsDNA region is required for telomere maintenance in the *pot1-A-V5* mutants. The fission yeast shelterin component Poz1 is proposed to be a crucial part of the bridging structure, which interacts with the telomeric dsDNA- binding complex via Rap1, and with the ssDNA-binding complex via Tpz1. To test whether bridging to the dsDNA is indeed required for telomere maintenance *pot1-A*-V5 mutants, we examined the phenotype of *poz1*$^{+}$ removal in the *pot1-V5* phospho-mutants. Double-heterozygous diploid strains of *poz1*Δ *pot1-V5* phosphorylation mutants were constructed by gene targeting, and verified by PCR. The strains were then sporulated and plated on antibiotic selection media. Both *pot1-V5 poz1*Δ and *pot1-D-V5 poz1*Δ mutants formed the predicted number of colonies, which grew well for at least 3 passages (not shown). In contrast, the *poz1*Δ *pot1-A-V5* mutant spores fail to form any haploid colonies on selective media (Figure 4.9); the few colonies formed on *poz1*Δ *pot1-A-V5* plates derived from diploid mating, and still contained a *wt* copy of *poz1*$^{+}$. Therefore, we conclude that there is a synthetic lethal interaction between *pot1-A-V5* and *poz1*Δ.

In summary, our data showed that recruitment to telomeric dsDNA is essential for Pot1-A-V5 to function, suggesting defective recruitment via the ssDNA. Such ideas reinforce the need to test ds versus ss telomere binding by the various phospho-mutant Pot1 forms, as described above.

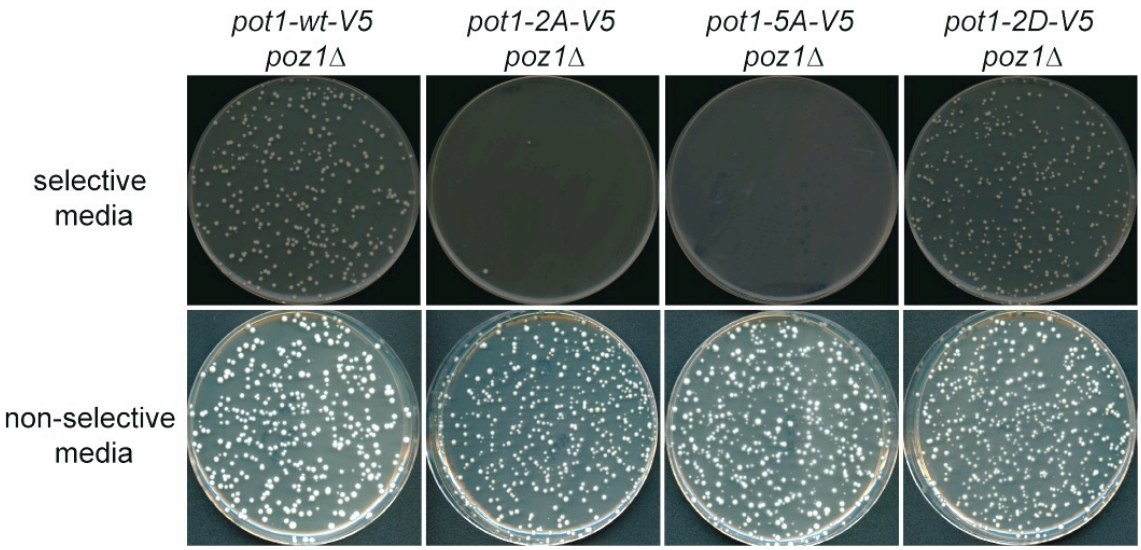

Figure 4.9 Synthetic lethality of *poz1*Δ *pot1-A-V5* double mutants

Random sporulation of *poz1*Δ *pot1-V5* phospho-mutants. Pictures were taken 4 days after approximately 1000 spores were plated on selective media. No *poz1*Δ *pot1-A-V5* colony formation was observed till 6 days after plating the spores.

4.6 Telomeric ssDNA is deregulated in *pot1-A-V5* phospho-deficient mutants

One of the most dramatic phenotypes of *pot1* deficiency in fission yeast is rampant 5'-strand resection during late S phase, generating excess single-stranded overhang, a substrate for ATR-mediated checkpoint activation (Pitt and Cooper, 2010). As our data presented above suggest that Pot1-A-V5 mutants are defective in ssDNA binding, we asked whether they also affect telomeric resection by assessing presence of overhang signal in these mutants. We took advantage of the in-gel hybridization technique performed under non-denaturing condition, thus allowing detection of endogenous ssDNA. As overhang signal is low in asynchronized cells, we constructed double mutants by mating the *pot1-V5* mutant strains with a *cdc25-22* cell cycle mutant. Growing the culture at restrictive temperature 36ºC for 4 hours successfully arrested these cells; upon release to the permissive temperature of 25ºC, they progress synchronously through the cell cycle (Figure 4.10A).

In *wt* cells, telomeric overhang signal is low through most of the cell cycle but becomes discernible in late S phase, which corresponds to the period of telomere replication and end processing. The same pattern is observed in *pot1-D-V5* mutant strain. Notably, however, a different pattern emerges for the *pot1-A-V5* mutant strains. While the overhang signal does increase transiently in late S phase, there is a persistent, high-mobility ssDNA signal throughout the cell cycle (Figure 4.10B, red arrowhead).It is not yet clear whether this ssDNA represents overhangs at the very ends of the chromosomes, or internal bubbles that may result from unresolved replication or recombination intermediates. Hence, further experiments probing such gels with a probe hybridizing to the C-strand as well as treatment with *E. coli* Exo I (which digests specifically 3' overhangs) are needed to interpret this data.

In summary, it appears that while all mutants generate overhang in a regulated manner, the phospho-deficient *pot1-A-V5* mutants exhibit additional unregulated ssDNA signal through the cell cycle.

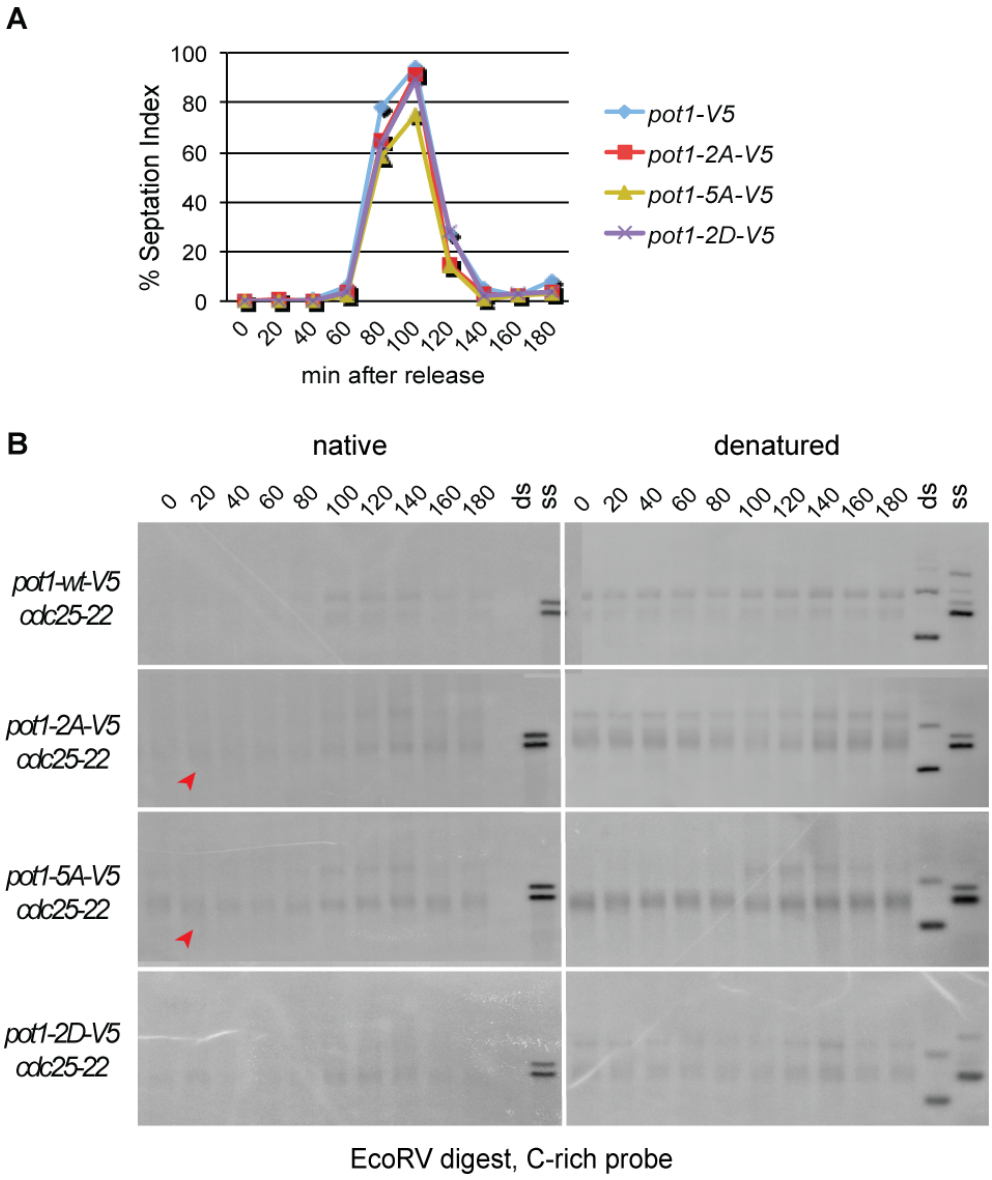

Figure 4.10 ssDNA generation through the cell cycle

A. Septation index of *cdc25-22 pot1-V5* phospho-mutants. Samples at *time 0* were taken after 3.5h arrest at 37ºC restrictive temperature, after which the cultures were shifted back to 25ºC permissive temperature. Time between 80-120min correspond to S phase. **B**. In-gel hybridizaiton using C-rich single-stranded probe hybridizing to the telomeric G-rich strand. Numbers on top indicates time after release at 25ºC; the 1st sample was taken upon release from G2 arrest, samples were then taken every 20min. dsDNA and ssDNA controls are native and denatured telomere sequence-containing plasmid (pIRT2-telo). Native signal represents native single strand in the form of overhang and/or metabolic intermediates, where red arrowheads indicate persistent signal. Denatured signal represents total telomeric DNA after in-gel denaturation.

4.7 Summary

Following the phenotypic analyses described in Chapter 3, we attempted to investigate the molecular mechanisms behind the defects conferred by *pot1-V5* phosphorylation mutants. Telomeric association of the mutants as examined by IF and ChIP analyses showed that the Pot1-V5 phospho-mutants were still recruited to the telomere, although recruitment via direct binding to the ssDNA was not determined.

The genetic interactions between the *pot1-V5* phosphorylation mutants and several telomeric components were examined. Contrary to previous findings, the phospho-deficient *pot1-A-V5* mutant engage telomerase to elongate the telomeres, rather than switching automatically to recombination-based maintenance. Additionally, our results uncovered some unique telomere maintenance requirements of the *pot1-A-V5* mutants. Recruitment of Pot1 via the telomeric dsDNA-binding complex was required for telomere maintenance in the *pot1-A-V5* background, highlighting the importance of the coordinated interaction between the ds and ssDNA-binding complexes. Importantly, ssDNA generation was also deregulated in the *pot1-A-V5* background, suggesting that the phosphorylation in the N-terminal OB-fold ensures proper Pot1 function in regulating generation of telomeric ssDNA.

Our data presented in Chapter 3 and 4 showed that the *pot1-D-V5* mutant displayed a range of moderate defects, some being similar to those seen in *pot1-A-V5* mutants. These observations argue against the previous assumption that the S/T to D mutations fully mimic the phosphorylation of Pot1-V5, although cycles requiring both phosphorylation and dephosphorylation could still explain our results. Alternatively, the mutations may actually impair physiological phosphorylation of the sites, thus conferring phenotypes similar to those of the phospho-deficient mutant alleles. A concurrent goal of my thesis work was to address directly whether Pot1 is phosphorylated in vivo and whether the studies mutations exert their effects through altered phosphorylation. These efforts are described in the next section.

Chapter 5. Miscellaneous information

5.1 Mass spectrometry analysis of Pot1

Pot1 phosphorylation was initially discovered in a strain harbouring a C-terminally tagged allele of *pot1*$^{+}$, and was detected using an α-V5 antibody after 2DGE. While the phosphorylation spot pattern of Pot1-V5 has be confirmed (Figure 5.1A), the intrinsic limitation of the tagging and Western blotting techniques left us with two concerns. First, does the phosphorylation actually occur in the N-terminal OB-fold? 2DGE could not give a definite answer to this question because the correlation between the loss of phosphorylation and the mutations can be subject to different interpretations: either phosphorylation actually occurs at those residues, or the mutation disrupts interaction of Pot1 with the protein kinase, which is required for phosphorylation of Pot1 at a different locus. Another possible explanation of the loss of phosphorylation is that the mutants induced sickness and thereby a global change of phosphorylation pattern; in this case, the observed phosphorylation changes would not be attributable to DDK-mediated regulation of Pot1 phosphorylation. Moreover, we wished to ask whether the C-terminal V5-tag affects the phosphorylation status of Pot1. This is a concern because the V5-tagging has mild telomere phenotypes, and the tagged and untagged phosphorylation mutants display different sets of phenotypes in terms of telomere maintenance and protection (see section 5.2). Although unlikely, there is the possibility that the phosphorylation observed in the *pot1-V5* mutants actually depends on the presence of the V5 tag.

In order to answer these questions and eventually determine the phosphorylation status of *wt* Pot1, we set out to separate the protein without the C-terminal tag by raising antibodies against Pot1. Mass spectrometry was employed to visualize the modification status of the protein samples. Unfortunately, we have not been able to confirm the phosphorylation via mass spectrometry to this point since the putatively modified peptide is large and contains hydrophobic residues so it fails to ‘fly’ (see below). Nonetheless, interesting aspects of Pot1 and its interacting proteins were observed in this study.

5.1.1 Generation of Pot1 antibodies

To detect and isolate untagged forms of Pot1, antibodies against either custom-designed Pot1 peptides or the full-length protein were generated from different sources, and were individually tested both for Western Blot and for IP. Among the 15 antibodies generated, a mouse polyclonal antibody generated against full length Pot1 using the DNA Immunization technique (InCellArt) proved effective when used in IP against Pot1-V5 under native conditions, and the efficiency was similar to that of α-V5 antibody (Figure 5.1B). Unfortunately, however, it did not work in IP after denaturation of the lysate, or in Western Blot after SDS-PAGE (data not shown), suggesting that the epitope is conformational and occurs as a result of higher order structure. This antibody was thus not suitable for analysis of protein phosphorylation using 2DGE.

We also tried to generate a phospho-specific antibody from a synthetic phospho-peptide (BioGenes) modified at T68, a putative phosphorylation site of Pot1 that is located at a loop region of the N-terminal OB-fold, in an attempt to confirm phosphorylation at this residue directly. Unfortunately, no phospho-specific antibody could be purified from the immunized animals, and the non-phospho-specific antibody purified did not detect a Pot1 band by Western blotting (data not shown).

5.1.2 C-terminal V5-tagging of Pot1 does not dramatically affect its protein interaction

We went on to investigate the difference between *wt* and V5-tagged Pot1 with the antibodies generated. In collaboration with the Protein Analysis and Proteomics group in London Research Institute, we performed large-scale immunoprecipitation against V5-tagged or un-tagged Pot1 from native cell lysates using the polyclonal α-Pot1 antibody (Figure 5.1C). Samples were subject to trypsin digestion followed by liquid chromatography with tandem mass spectrometry (LC-MS/MS). Common protein modifications such as oxidation, phosphorylation, acetylation, and methylation were included in the search against the fission yeast protein database.

A total of more than one hundred fission yeast proteins were identified in this analysis in both tagged and un-tagged samples. A selection of identified proteins is available in Table 5.1, sorted by the number of assigned spectra as an indication of their enrichment in the sample. Components of the single-stranded telomere-binding complex, which includes Tpz1, Ccq1 and Poz1, were identified in abundance. Rap1, the dsDNA binding protein, which has been shown to interact with Poz1 (Miyoshi et al., 2008), was also identified. Meanwhile, the Taz1-Rif1 complex, which interacts with the Pot1 sub-complex indirectly via the Poz1-Rap1 bridge, was not in the list. Together, this result points to the validity of the protein-protein interactions identified in this analysis, as well as the selectivity of the technique.

Interestingly, while the V5-tagged Pot1 display a different set of phenotypes compared to untagged Pot1, the protein interaction profile is remarkably similar between the two. Many of the proteins identified were pulled down in comparable quantities, including the telomere proteins Tpz1, Poz1 and Rap1, the chaperone protein Hsp90, and the cell cycle regulator Cdc48. This is consistent with the fact that *pot1-V5* is largely functional at the telomeres.

Nevertheless, interactions with several candidates appeared to be altered by the V5-tagging. For example, the level of the telomerase recruiter Ccq1, which is recruited to telomeric ssDNA via interaction with Pot1-Tpz1, was lower in the Pot1-V5 IP. Although this is not expected from the telomere elongation phenotypes observed in *pot1-V5* cells, it does imply that the V5 tag can affect regulation of telomerase action by Pot1 at the telomeres (see section 5.2). Another interesting protein is Rad24, which functions in DNA damage checkpoint and was enriched by more than three-fold in the IP against Pot1-V5 compared to that against Pot1. It requires further investigation to determine the physiological significance of these differences in protein interaction profile.

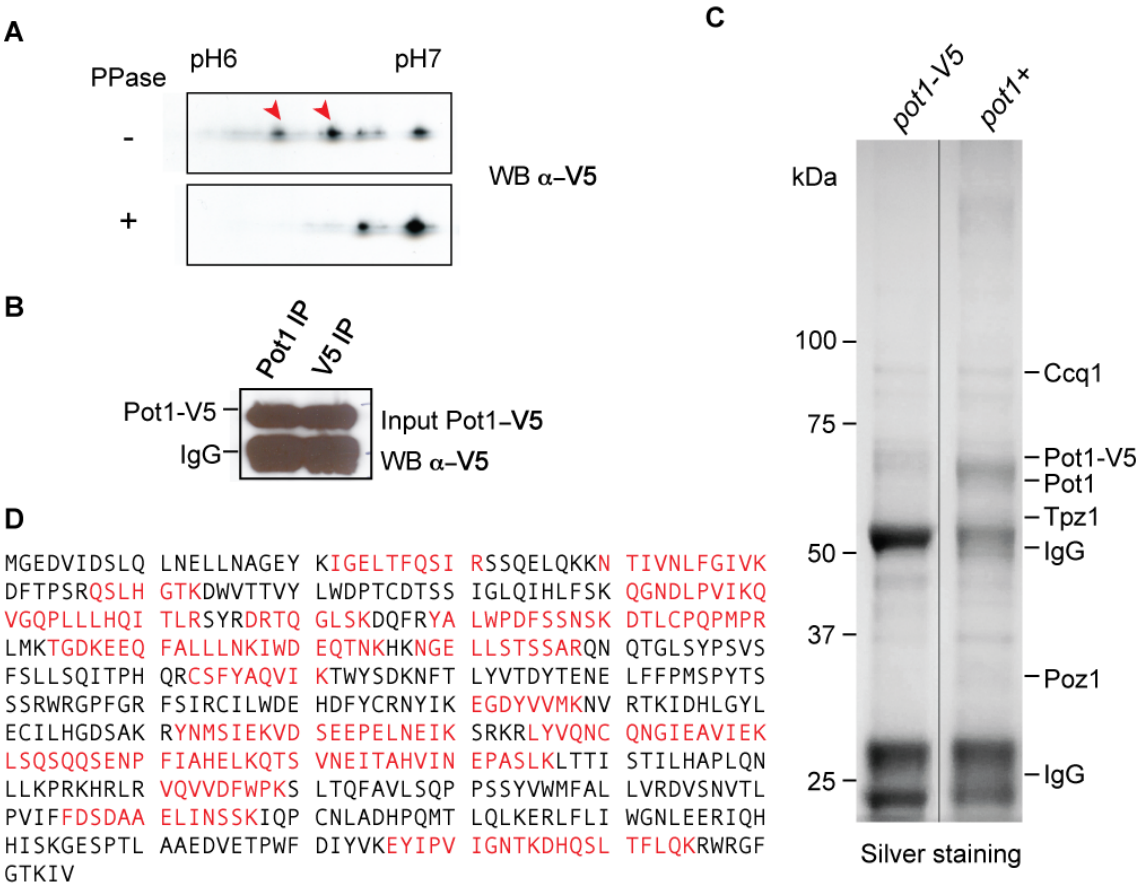

Figure 5.1 Mass spectrometry analysis of Pot1 and Pot1-V5

A. Pot1-V5 phosphorylation pattern after 2DGE. Samples derived from asynchronous *pot1-V5* culture were treated with λ phosphatase (+) or mock treatment (-). Red arrowheads indicate phosphorylated spots of Pot1. **B**.Western blotting showing IP efficiency of α-Pot1 antiserum. Cell lysate of a *pot1-V5* strain used as input for the IP against Pot1 (left) and V5-tag (right). Pot1-V5 in the pull down was detected by α-V5 antibody. **C**. Lanes excided from a silver-stained gel of a large-scale purification. Left: α-V5 IP in *pot1-V5* lysate. Right: α-Pot1 IP in *wt* lysate. Bands corresponding to known Pot1-interacting proteins are indicated on the right. **D**. Sequence coverage of Pot1 by LC-MS/MS analysis after Trypsin digestion. Identified peptides are marked in red. The peptide containing T68 T75 is not identified by mass spectrometry.

Protein	General role	Pot1-V5 IP	Pot1 IP
Ccq1	Telomere maintenance	225	304
Tpz1	Telomere protection	206	169
Pot1	Telomere protection	169	136
Ef1a-A	Translation elongation	79	113
Hsp90	Heat shock protein	91	89
Nop58	rRNA processing	93	248
Act1	Actin protein	58	118
Poz1	Telomere maintenance	91	78
Pyk1	Pyruvate kinase, glycolysis	75	62
Ded1	Translation initiation	39	86
RS3	Ribosomal protein	55	41
YB68	Dynamin-like protein	0	61
Rap1	Telomere binding protein	25	32
Cdc48	Cell cycle regulation	23	24
Rad24	DNA damage checkpoint	37	9
Egd2	Cotranslational protein folding	17	17
Uba1	Ubiquitin activating E1	9	14
Alp7	Microtubule protein	16	0
Gtp1	GTP-binding (predicted)	5	2

Table 5.1 Selected proteins identified by mass spectrometry in Pot1 and Pot1-V5 IP

Numbers in the IP columns indicate the number of spectrum identified in the analysis.

In a previous study in the laboratory, potential Pot1 interaction partners were identified using a yeast two-hybrid screen (Kuznetsov, 2008). Two out of the six "strong" hits from the yeast two-hybrid screen were also identified by mass spectrometry as Pot1 interacting proteins: Tpz1, the shelterin component and ssDNA binding partner of Pot1, and Gtp1, a predicted GTP binding protein that has not been linked to telomere. The interaction partner that led to discovery of the phosphorylation modification, Dfp1, was not identified. No "medium" or "weak" hits were identified in this study.

This selective overlap between the two independent experiments, as well as the fact that many shelterin components were identified in the analysis, points to the validity of the mass spectrometry technique in identifying Pot1 interaction. On the other hand, many of the mass spectrometry hits are involved in metabolic pathways and/or are very abundant, such as mitochondrial proteins, chaperones, and the translation machinery. This highlights the biased tendency toward proteins expressed at high levels, and caution is required when interpreting the mass spectrometry results.

5.1.3 Attempts to identify Pot1 phosphorylation sites by mass spectrometry

In the above analysis we hoped to confirm phosphorylation at the putative phospho-sites on Pot1. However, a standard trypsin digestion yields a peptide that consists of 27 amino acid residues around the putative phosphorylation sites, T68 and T75, the length of which presents considerable level of difficulty to the identification of the peptide. Moreover, this peptide contains two tryptophan residues which hinder isolation. In our search using LC-MS/MS following both in-solution and in-gel digestion, we had never been able to detect the peptide of interest. Coverage in the C-terminus is also low (Figure 5.1D), making it more than impossible to rule out the presence phospho-sites at other regions of the protein.

We attempted to use other methods to investigate the phosphorylation mystery. Different digestion enzymes such as AspN were used to generate shorter peptides containing T68 and T75. Titanium dioxide (TiO_2) ligand, which selectively binds phosphorylated Ser, Thr, or Tyr, was employed to enrich for phospho-peptides

before analysis by LC-MS/MS. While the technique enabled us to identify phosphorylation sites of several other telomere proteins (see section 5.3), we have not been able to identify any phospho-peptides of Pot1 at the time of writing. Further investigation is required to tackle this problem.

5.2 C-terminal tagging complicates the phenotypes of *pot1* phosphorylation mutants

5.2.1 V5-tagging of *pot1*$^+$ exhibits mild telomere phenotypes

The V5 (also known as PK) tag is derived from the small epitope on the RNA polymerase subunit (the so-called P protein) and protein V of the paramyxovirus of Simian Virus 5. It is regularly used in biochemical studies. A V5-tagged allele of *pot1*$^+$ was shown to rescue the growth defect of *pot1*Δ *in vivo*, suggesting that the allele *pot1-V5* is functional at least in telomere protection (Bunch et al., 2005). In the initial analysis that detected the phosphorylated Pot1 protein by 2DGE, a C-terminally V5-tagged allele of *pot1*$^+$ was used to facilitate detection of the protein on Western blot after 2DGE (Kuznetsov, 2008). Subsequent mutational analysis was also performed with the V5 tag, as no α-Pot1 antibodies were available. Comparisons were always made between wt Pot1 tagged with V5, and mutant Pot1 tagged with V5. Nonetheless, characterization of the mutant alleles showed that while that the tagged alleles are largely functional in terms of telomere protection, V5-tagging of *pot1*$^+$ does slightly alter its functions.

While the tagged forms of Pot1 are expressed at high levels when the tagged allele is the only *pot1* allele in the genome, the V5-tagged protein level significantly decreases in the presence of a *pot1*$^+$ allele, e.g. in heterozygous diploid strains or when an endogenous copy of *pot1*$^+$ is available (Figure 5.2A). It is not clear whether this down-regulation of protein level is via destabilizing the tagged protein after translation or via transcriptional regulation. The reduced protein level is consistent with the lack of phenotype in heterozygous diploid strains of the *pot1-V5* phosphorylation mutants, which maintain *wt* length telomeres.

A dramatic phenotype observed in the *pot1-V5* strain is telomere elongation. Compared to *wt* telomeres, *pot1-V5* telomere length showed a roughly two- to three-fold increase to ~800 bp (see section 3.2). This elongation is dependent on telomerase activity. In the double mutant *pot1-V5 trt1*Δ strain, no initial telomere elongation is observed, and the telomeres undergo gradual shortening at a rate similar to that of a *trt1*Δ strain (see section 4.3). It therefore appears that the C-terminally V5-tagged *pot1*$^{+}$ confers enhanced telomerase activity.

Another characteristic of V5-tagged *pot1*$^{+}$ is its ability to partially reverse the telomere over-elongation phenotype of *taz1*Δ cells. Over-elongation of *taz1*Δ telomeres is the consequence of two events: firstly, replication fork stalling at telomere sequences is proposed to provide a preferred substrate for telomerase action, and secondly, loss of Taz1-mediated telomerase inhibition ensues (Dehe et al., 2012). Interestingly, other aspects of the *taz1*Δ phenotype are not affected by the V5-tagging of *pot1*$^{+}$, such as replication fork stalling, telomere entanglement and cold sensitivity (Figure 5.2 and data not shown). Therefore, the partial rescue by *pot1-V5* is not via rescue of fork stalling in the absence of Taz1, but rather points to regulation of telomerase activity.

In addition, we have shown that HAATI formation is reduced in *trt1*Δ *pot1-V5* compared with a single *trt1*Δ mutant (see section 4.3). Pot1 is required for both HAATI formation and maintenance. As the DNA-interaction domain of Pot1 is highly specific for telomeric sequence, it is proposed that Pot1 is recruited to chromosome termini in HAATI cells via interaction with Ccq1, which interacts with the heterochromatin machinery (Jain et al., 2010). An attractive hypothesis is that C-terminal tagging Pot1 may modulate its interaction with Ccq1, thus affecting both telomerase activity and HAATI formation. A semi-quantitative mass spectrometry analysis indeed showed that the number of Ccq1 peptides in the spectrum, and phospho-peptides of Ccq1, are both reduced in Pot1-V5 IP compared to Pot1 IP (see section 5.1). Whether the reduction is physiologically significant is not yet clear, and requires further investigation.

In summary, V5-tagging of *pot1*$^{+}$ appears to affect its function in telomerase regulation and perhaps other realms. The exact mechanism of the regulation is not

known yet. Current evidence suggests that *pot1-V5* can act as both a positive and a negative regulator of telomerase activity, leading to telomerase-mediated telomere elongation in the presence of Taz1, and partial rescue of *taz1*Δ telomere over-elongation.

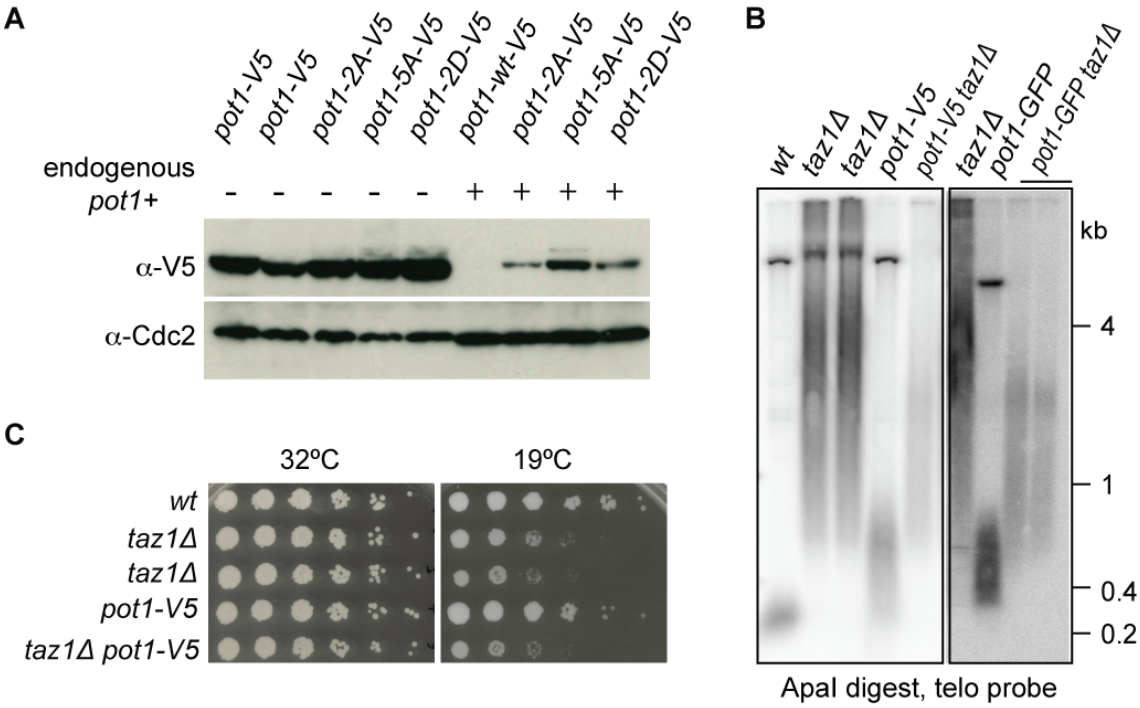

Figure 5.2 C-terminal tagging affects the function of *pot1*$^{+}$

A. C-terminal V5-tagging affects expression level of Pot1-V5 phospho-mutants in the presence of a *wt* allele. Heterozygous diploid of *pot1+/- aur1R:pot1-mutant-V5/aur1+* were sporulated, and were selected for *aur1R:pot1-mutant-V5 pot1-* (labelled endogenous pot1+ negative) and *aur1R:pot1-mutant-V5 pot1+* (labelled endogenous pot1+ positive). Cdc2 Western Blot was used as loading control. **B**. C-terminally tagged *pot1-V5* and *pot1-GFP* partially rescues telomere over-elongation of *taz1*Δ mutant. **C**. *pot1-V5* does not rescue *taz1*Δ cold sensitivity. Five-fold serial dilution of log phase cultures were spotted onto rich medium and incubated at indicated temperatures. Pictures were taken after 2 days incubation at 32ºC, and 5 days at 19ºC.

5.2.2 C-terminal V5-tag sensitizes the telomeres in *pot1*$^+$ phosphorylation mutant backgrounds

As V5-tagging of *pot1*$^+$ confers telomere phenotypes, we asked whether it might affect the function of the phosphorylation mutants. Heterozygous diploid strains of *pot1*$^+$ phosphorylation mutants without C-terminal tags were constructed by gene-targeting and plasmid integration using the same strategy as construction of the *pot1-V5* phosphorylation mutants (see section 3.1). Following sporulation and germination on selective medium, the phenotypes and telomere maintenance requirements of the untagged mutants were analyzed.

While the cells harboring the untagged phosphorylation mutants exhibited many of the characteristics of the *pot1-V5* phosphorylation mutants, some phenotypes were changed in the absence of the tag. Similar to the V5-tagged mutants, the untagged phospho-mutants activated the DNA damage checkpoint and caused cell elongation (Figure 5.3A). Telomeres in the untagged phospho-mutants are also elongated to a similar extent to the tagged mutants, showing no additive effect with the V5-tagging. The spontaneous telomere loss phenotype, which occurs in both *pot1-2A-V5* and *pot1-5A-V5*, is observed only in the *pot1-5A* mutants when the tag is absent, suggesting that *pot1-5A* is more penetrant than the *pot1-2A* mutant allele (Figure 5.3B).

Interestingly, the untagged *pot1-2A* and *pot1-2D* mutants display largely *wt* phenotypes in terms of telomere maintenance. Telomerase deletion leads to the *est* phenotype in all untagged phospho-mutants as well as in the *wt* background (Figure 5.3C). Deletion of the *rad51* did not confer any additional telomere phenotype in *pot1-2A* and *pot1-2D* mutants. While some of the *pot1-5A rad51*Δ mutants lost the telomeres, it likely resulted from the spontaneous telomere loss in *pot1-5A* mutants (Figure 5.3D). Therefore, the combination of the N-terminal OB-fold mutations and the C-terminal V5-tag confers synthetic phenotypes that were not observed in *pot1-V5* or the untagged phospho-mutants alone.

Telomere sensitization by tagging *pot1*$^+$ has been observed previously. The temperature sensitive allele *pot1-1* requires both the C-terminal GFP-tagging and

the two point mutations in the *pot1* ORF to confer the *ts* phenotype (Pitt and Cooper, 2010). Interestingly, further analysis showed that *pot1-V5* and *pot1-GFP* indeed share several characteristics, including telomere elongation, and partial rescue of *taz1*Δ telomere over-elongation but not cold sensitivity phenotypes (Figure 5.1B and not shown). Therefore, the C-terminus of Pot1 likely plays important roles in telomerase regulation, and C-terminal tagging impairs its function.

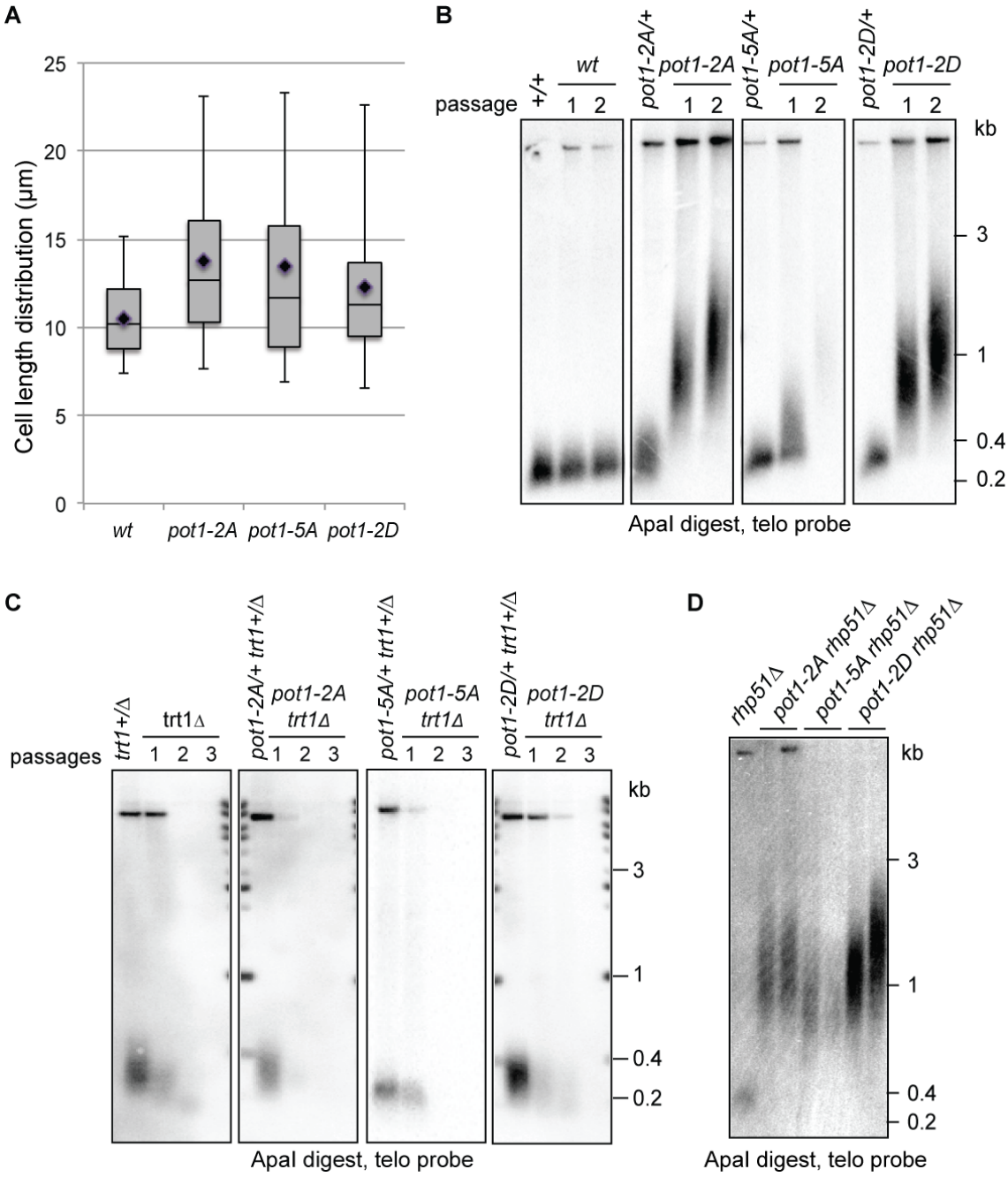

Figure 5.3 Phenotypes of the untagged phospho-mutants

A. Box plot showing the cell length distribution of *pot1* phospho-mutants (*n*=100). **B**. Telomere elongation phenotypes, showing telomere length over 2 passages after sporulation of heterozygous diploid strains. **C**. Telomere maintenance after *trt1*$^{+}$ removal, showing telomere length over 3 passages after sporulation of double heterozygous diploids strains. **D**. *rad51*$^{+}$ is not required for telomere maintenance in untagged phospho-mutants. Two independent clones were analyzed for each genotype. Samples were taken 5 days after germination of double-heterozygous diploid strains.

5.3 Phosphorylation of other components of the shelterin complex

A few interesting results came up in our attempt to identify the phospho-peptide of Pot1. With the help of TiO_2 phospho-peptide enrichment following immuno-precipitation against Pot1 and Pot1-V5 proteins, we have successfully identified phosphorylation of several other proteins, including shelterin components Tpz1 and Ccq1.

5.3.1 Tpz1 is phosphorylated in the C-terminal globular domain

Tpz1 is the fission yeast functional homolog of TPP1 in mammals and TEBPβ in *Sterkiella nova*. It is required for the formation of the Pot1 complex and the protection of telomere (Miyoshi et al., 2008). Sequence analysis predicts that Tpz1 has at least one OB-fold in the N-terminus, which, like its homologues, does not have a high affinity for telomeric ssDNA alone, but forms a stable structure with Pot1 and telomeric ssDNA and enhances Pot1 ssDNA affinity *in vitro* (Nandakumar and Cech, 2012). The C-terminal region shows high probability of forming disordered structure, which is likely a conserved feature amongst its homologues (Horvath, 2011). No modification of Tpz1 homologues has been reported.

Three phosphorylation sites, residues S342, T346, and T393, were identified in this study. Mass spectrometry showed that these sites were phosphorylated in samples of both Pot1 IP and Pot1-V5 IP. T393 resides in a globular domain in the C-terminus, which interacts with Poz1 and Ccq1 but not Pot1 (Miyoshi et al., 2008). We are attempting to understand the function of this phosphorylation by constructing mutant alleles of *tpz1* that are mutated at the phosphorylation sites. The physiological significance of the phosphorylation is still under investigation.

5.3.2 Ccq1 phosphorylation

Ccq1 is part of the Pot1 subcomplex at telomeric ssDNA in *S. pombe*. It is crucial for telomerase recruitment and repression of checkpoint signalling at telomeres (Tomita and Cooper, 2008, Carneiro et al., 2010). The C-terminal region of Ccq1 (AA 500-720) forms a coiled-coil secondary structure homologous to the centrosome component Pcp1. A protein homology/analogy recognition-based structure prediction suggests that the N-terminal region (AA 1-436) forms armadillo/heat repeats, which have been implicated in protein-protein interactions (Flory et al., 2004). Phosphorylation at T93 in the N-terminal has been shown to be essential for regulation of Ccq1-Est1 interaction (Moser et al., 2011).

Two additional phosphorylation sites were identified in this study. Phospho-S448 and S465, both of which are consensus Tel1/Rad3 phosphorylation sites, were enriched in the untagged Pot1 IP sample after TiO_2 treatment. These residues reside in a disordered region close to the HDAC2/3-like Tpz1-interacting domain of Ccq1. Interestingly, they have been proposed as potential phosphorylation site based on consensus sequence in a previous study (Moser et al., 2011). Mutation of both of these residues failed to affect Ccq1-Est1 interaction in a yeast two-hybrid experiment, suggesting that they do not act in the same pathway as T93 phosphorylation.

Surprisingly, mass spectrometry analysis did not show Ccq1 phosphorylation in the TiO_2 treated sample derived from Pot1-V5 IP, even though the peptides containing these residues were abundant before TiO_2 phospho-peptide enrichment. Although the result does not rule out the possibility that Ccq1 is still phosphorylated in *pot1-V5*, this semi-quantitative analysis suggests that the level of Ccq1 phosphorylation on S448 and S465 is reduced, if present at all. Given that the V5 tagging of Pot1 leads to phenotypes related to telomerase action and HAATI formation, both of which depend on Ccq1, this change is likely an important part of its regulation. We have constructed alleles of *ccq1* that are mutated at the phosphorylation sites, and are still working on the biological function of the phosphorylation at the time of writing.

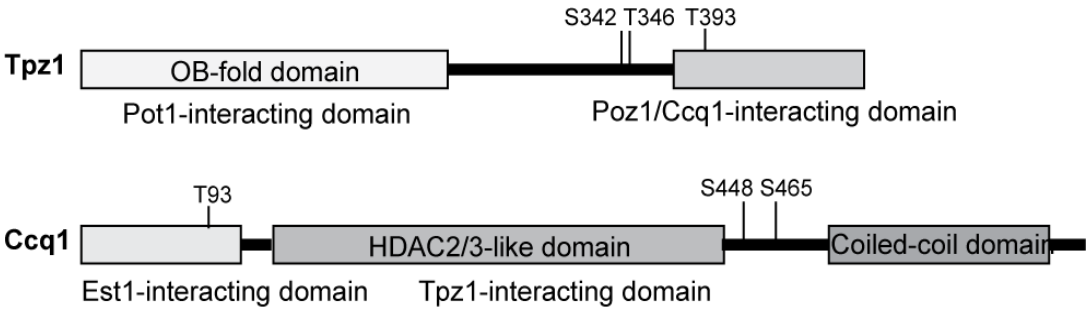

Figure 5.4 Functional domains and phosphorylation sites identified in Tpz1 and Ccq1

Schematic diagram of Tpz1 and Ccq1 functional domains (adapted from (Moser et al., 2011)). Phosphorylation sites identified in this and previous studies are indicated by black lines.

5.4 Implication of Pot1 function in telomere replication

Telomeric recruitment of Pot1 peaks in late S phase of cell cycle, which coincides with telomere duplication (Moser et al., 2009a). It has been suggested in human cells that POT1 antagonizes RPA binding to telomeres, due to its high affinity for telomere ssDNA sequences as well as local enrichment by interaction with the dsDNA-binding complex (Lazzerini Denchi and de Lange, 2007). As RPA is a key player in DNA replication, whether and how its competition with Pot1 might affect this process is not yet understood.

To investigate whether Pot1 is involved in telomere replication in fission yeast, we examined telomere replication in mutants of *pot1*$^+$ using neutral-neutral 2DGE technique. Since deletion of *pot1*$^+$ results in rapid loss of telomeres at chromosome ends, we constructed strains containing 450bp of synthetic telomere tract with a *Leu2* marker at the internal *ura4* locus in *pot1*$^+$ and *pot1*Δ backgrounds, so that fork passage through telomere sequences can be analyzed regardless of the absence of natural telomeres (Miller et al., 2006) (Figure 5.5B). The ARS3002 replication origin cluster is located 8kb centromere-proximal to the *ura4* locus, which has been shown to be mainly responsible for replication through this region (Dubey et al., 1994). Genomic DNA was gently extracted in agarose plugs to preserve any secondary structures, and digested with *NsiI* restriction enzyme to release the

fragment containing the internal telomere sequence. The fragment was separated first based on both its molecular weight and then its shape; this generates an arc shape (Y-arc) as the replication fork initiated from ARS3002 passes through the region.

The repetitive nature of the telomeric sequence poses an impediment to replication, as evidenced by accumulation of signal in the Y-arc at position corresponding to the start of the internal telomere in the *wt* background (Miller et al., 2006) (Figure 5.5C). As expected, *taz1*$^{+}$ deletion led to fork stalling at the telomere sequence, resulting in a gap in the Y-arc corresponding to the region containing the internal telomere. This gap was not observed in *pot1*Δ background, suggesting that loss of Pot1 does not lead to replication fork stalling at telomere sequences similar to that observed in *taz1*Δ background.

Surprisingly, a pronounced cone-shaped signal was observed in the *pot1*Δ background, coinciding with a reduction in the signal accumulation at the start of the internal telomere (Figure 5.5C). This cone signal is characteristic of collapsed or reversed replication forks containing cruciform intermediates (Friedman and Brewer, 1995). Our data point to the exciting possibility that Pot1 may be directly involved in stabilization of stalled replication fork as it passes through telomere sequences. Further work is required to validate these results.

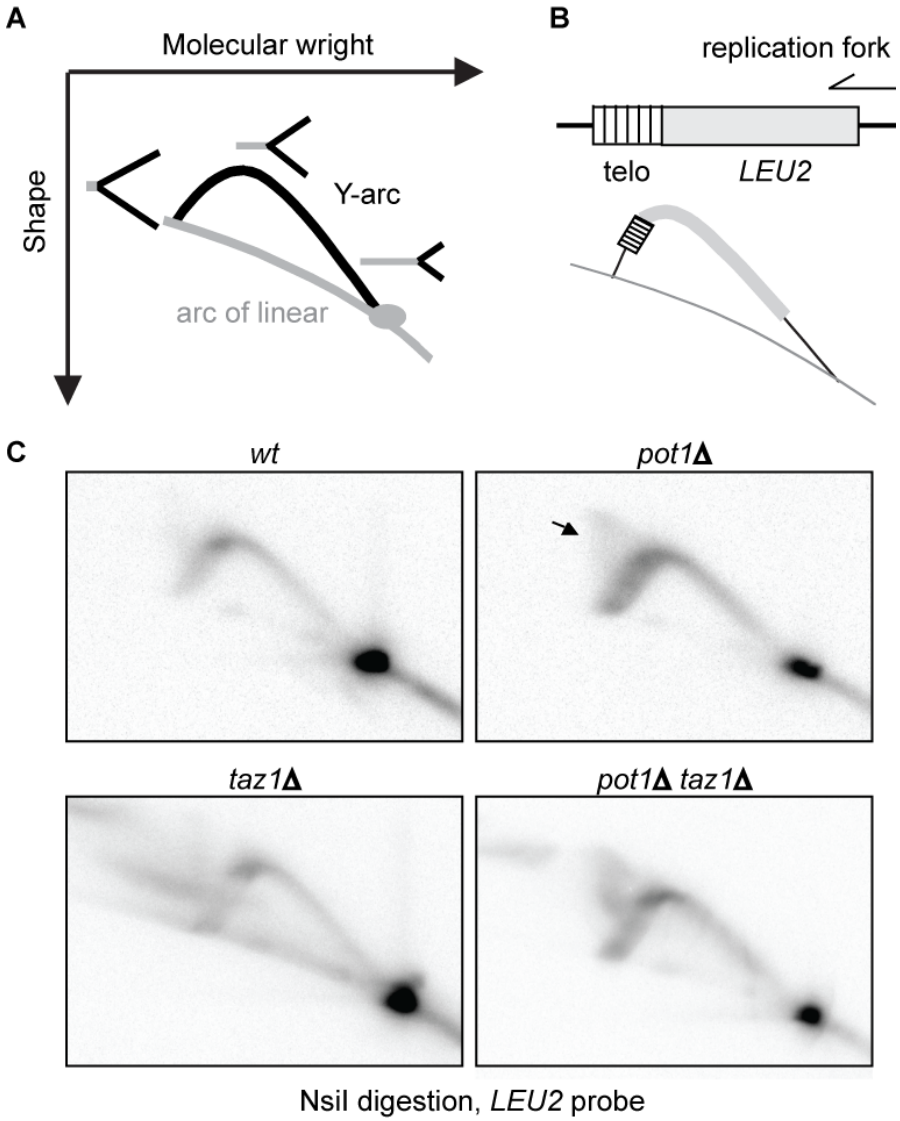

Figure 5.5 Pot1 does not directly contribute to replication fork passage

A. Illustration of the replication intermediates that makes up the Y-arc. Extension of fork expansion initially increases complexity of the molecule, generating slow migrating molecules when separated based on shape. As the fork progress to the end of the fragment, the structure resembles a linear molecule, which allows easier migration on the gel, forming the descending part of the Y-arc. **B**. The construct containing the 450bp synthetic telomere tract, and the expected 2DGE pattern using probes hybridizing to the *scLEU2* marker inside fragment. The fragment was inserted at *ura4* locus in the genome, which can be released by *NsiI* digestion. The main direction of the replication fork is indicated. **C**. 2DGE pattern of *NsiI* released internal telomere-containing fragments in different genetic backgrounds. Cone-shaped signal in *pot1*Δ is indicated by a black arrowhead.

The internal telomere tract, while informative, is different from a real telomere, not least due to the lack of a chromosome terminus. In order to look at replication through real telomeres in a *pot1* deficient background, we took advantage of the temperature sensitive *pot1-1* mutant, which allows analysis immediately after Pot1 inactivation (Pitt and Cooper, 2010). Log phase cells were synchronized by nitrogen starvation for 16h at 25ºC permissive temperature, at the end of which half of the cells remained at 25ºC as a control, and the other half were shifted to 36ºC restrictive temperature to inactivate Pot1. After release from nitrogen starvation, samples were taken every 20min for FACS analysis. The time-points corresponding to late S through early G2 phase in the first cell cycle were pooled together to ensure that the samples were at comparable stages in terms of DNA replication. Terminal fragments were released by *EcoRV* digestion and subject to DNA 2DGE analysis.

As *pot1-1* telomeres are slightly heterogeneous, a smeary Y-arc was observed in the high mobility fragments. The long, low mobility fragments, on the other hand, yielded Y-arcs with clear ascending and descending parts. The descending part of the Y-arc (large Y), which corresponds to replication intermediates close to completion, appears to be reduced (relative to the intensity of the ascending part of the Y-arc) in the Pot1-inactivated sample compared to the control sample (Figure 5.6C, black arrow). This suggests that telomere replication is impaired by Pot1 inactivation.

Interestingly, a separate arc that converges with the expected arc of linear DNA was observed in the Pot1-inactivated but not the control sample (Figure 5.6C, empty arrow). In-gel hybridization on 2DGE confirmed that this arc contained telomere G-strand, but not C-strand, ssDNA (Figure 5.7). This is consistent with the rampant 5’ strand resection following loss of Pot1 function (Pitt and Cooper, 2010), suggesting that resection of the chromosome termini can progress close to or beyond the *EcoRV* restriction site.

Collectively, our preliminary data suggest that while Pot1 is not directly involved in replication fork passage through telomere sequences, its function in inhibition of telomere resection is essential to protect the replication template. Loss of Pot1

function leads to a reduced amount of replication product in the first cell cycle after inactivation, exacerbating the telomere loss phenotype induced by excessive end resection. It is not yet clear whether the template loss affects replication of both strands or only the lagging strand, a distinction that requires further investigation.

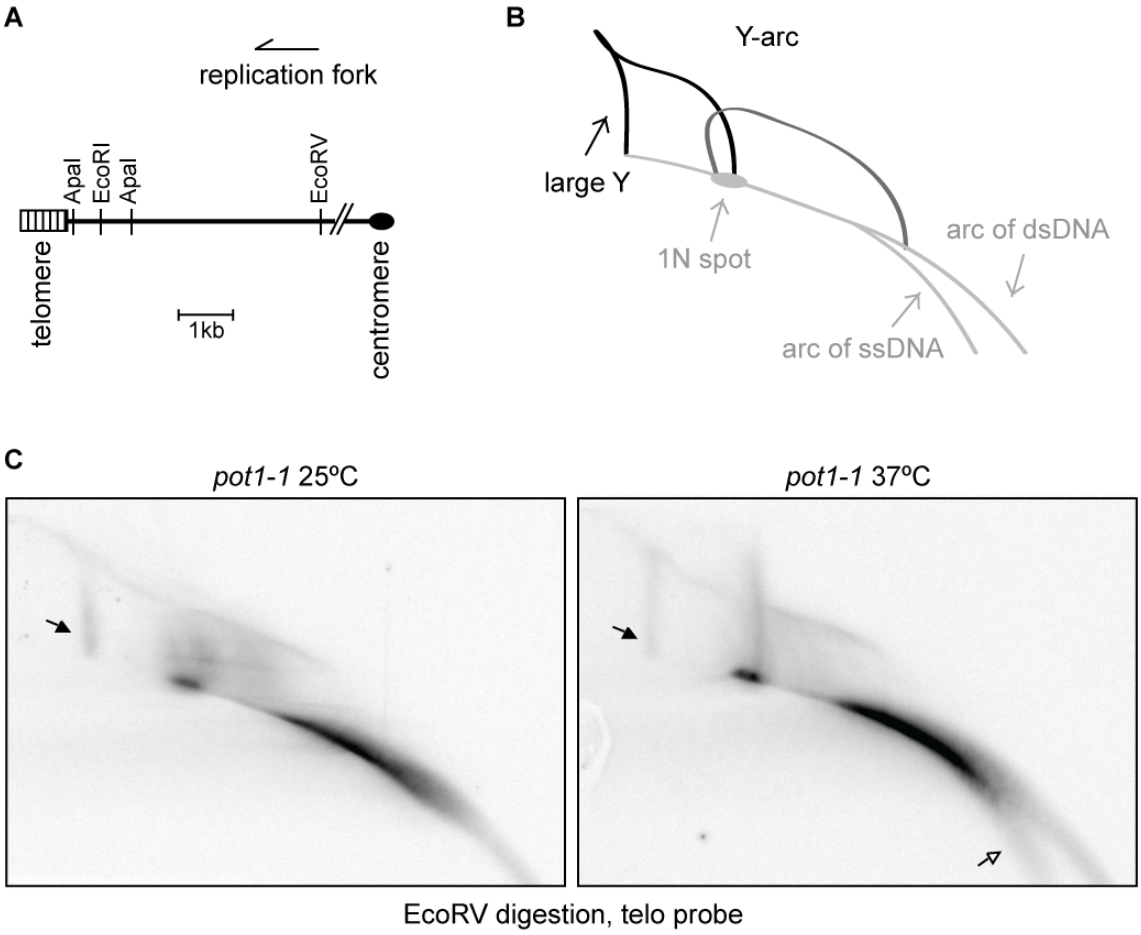

Figure 5.6 Pot1 facilitates efficient telomere replication by inhibiting resection of the template

A. Relative position of *EcoRV* restriction site in telomeric and subtelomeric regions. Direction of replication fork indicated. **B**. Schematic diagram of the 2DGE pattern of *pot1-1* telomeres after *EcoRV* digestion. The black Y-arc consists of long telomere fragments stemmed from the 1N spot, and grey Y-arc is derived from the short, heterogeneous telomere fragments. The two arcs of linear represent ds and ssDNA, respectively. **C**. 2DGE analysis of S phase-enriched samples of *pot1-1* control (25ºC) and Pot1-inactivated (37ºC). Large Y molecules indicated by black arrow. Arc of telomeric ssDNA indicated by empty arrow (see Figure 5.7).

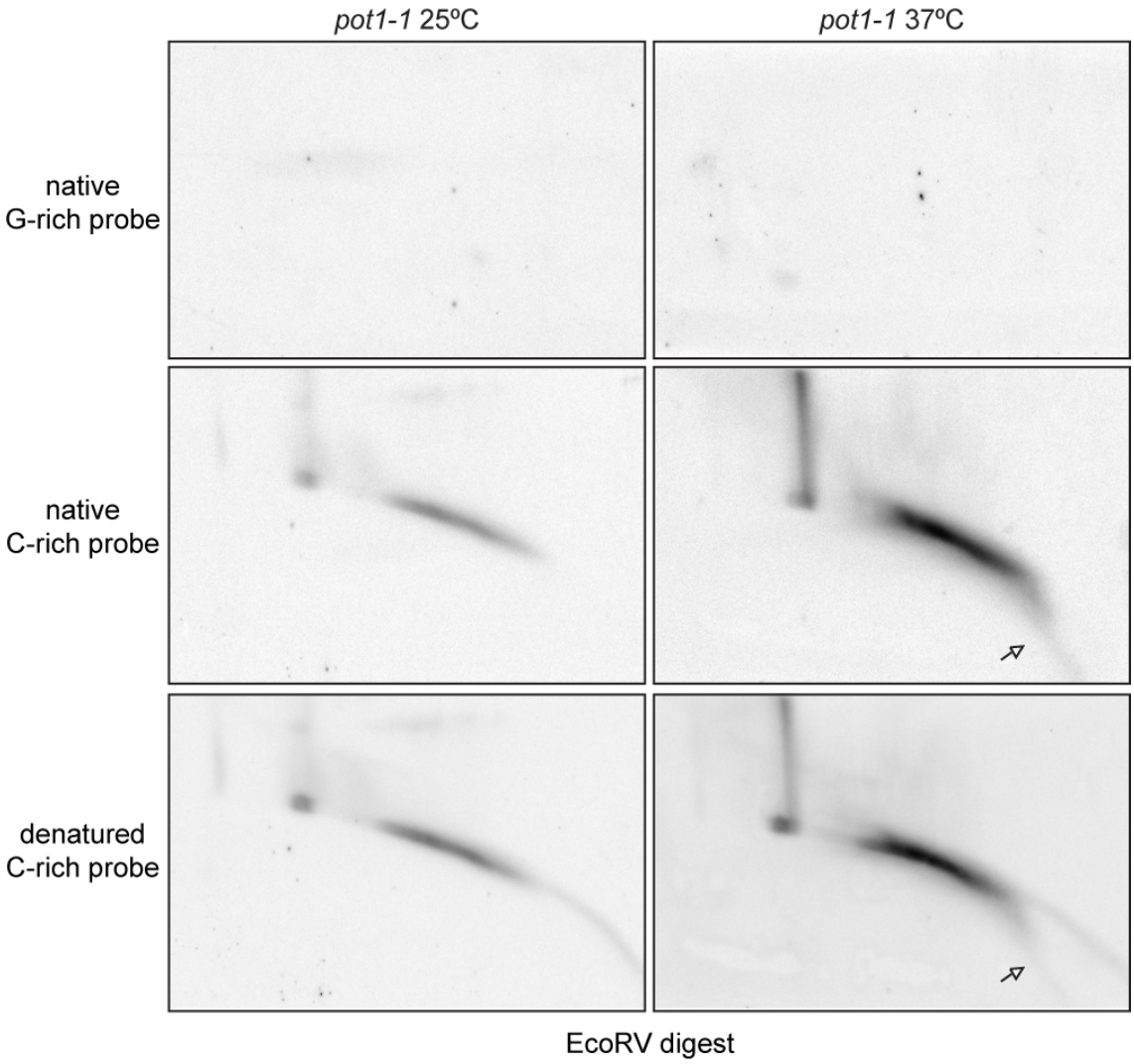

Figure 5.7 Formation of telomeric G-rich ssDNA arc after Pot1 inactivation

Samples used in Figure 5.6C were subject to in-gel hybridization after separation by 2DGE. Native signal represents naturally occurring single strand in the form of overhang and/or metabolic intermediates, where G-rich probe hybridize to the C-rich strand and *vice versa*. Denatured signal with C-rich probe represents total G-rich DNA after in-gel denaturation in 0.5M NaOH. The ssDNA arcs in both native and denatured conditions are indicated by empty arrow.

Chapter 6. Discussion

6.1 Validating the foundation

This study expanded upon previous work in the Cooper Laboratory, in which the DDK-dependent phosphorylation of Pot1-V5 in the N-terminal OB-fold was discovered (Kuznetsov, 2008). Some interesting phenotypes were described in strains harboring alleles of *pot1-V5* that are mutated at the putative phosphorylation sites. The phospho-deficient *pot1-A-V5* mutants appeared to adopt a recombination-based telomere maintenance mechanism without going through the crisis period *wt* cells undergo after telomerase inactivation and prior to the adoption of recombination-based telomere maintenance mechanisms. In contrast, the 'phospho-mimic' mutant *pot1-2D-V5* retained most of the functions of a *wt* allele, suggesting that the constitutively phosphorylated form of Pot1 was almost sufficient for functional telomeres.

The above observations suggested that a switch between telomerase-dependent and recombination-dependent maintenance mechanisms could be controlled by modification of a single protein, Pot1; forcing the switch to be on the telomerase-dependent side by 'constitutive phosphorylation' hardly conferred any abnormality. This molecular switch, if proven true in human cells, could provide an excellent target for therapeutics in cancers that utilize the ALT mechanism.

The initial focus of this study was to confirm Pot1 phosphorylation by DDK and understand the mechanism behind the telomerase independence of the *pot1-A-V5* mutants. However, several pieces of data promoted us to re-visit the previous observations (see section 4.2 and 4.3). Therefore, much of the later work was dedicated to exploring the results of the previous study. We noticed several results that were inconsistent between the two, and formulated hypotheses to explain some of the differences by experimental procedure and variable penetrance. The following list highlights some of the current observations that initially appear to contradict what was previously recorded.

1. We found that the phospho-deficient *pot1-A-V5* mutants still engage telomerase; removal of telomerase from heterozygous led to immediate senescence after germination. As was described in section 4.3, the senescence indeed correlated with critically telomere shortening, suggesting that *trt1*△ *pot1-A-V5* mutants lose telomeres before engaging the recombination-based mechanism. The patching passage carried out in the previous study could facilitate the rapid enrichment of linear survivors as their faster growth allows them to overtake circular survivors as well as dying cells. Single colony passage, which follows the progression of a phenotype through one progeny line without selection based on growth rate, was used in most analyses in this study.

2. The *pot1-D-V5* mutant, which was initially believed to be largely wild-type with respect to most telomere phenotypes, was in fact defective in many aspects of telomere protection and maintenance. Phenotypes observed include telomere elongation, cell elongation and checkpoint activation, and sub-telomeric hyper-recombination. These phenotypes were less severe in cells harbouring Pot1-D-V5 than in those with Pot1-A-V5 (see section 3.2 and 3.3). However, the large variation in phenotypic severity in *pot1-D-V5* cells suggests that penetrance was incomplete. Since most of the analyses on this allele in the previous study were carried out using a single clone, the variation will have been masked. In this study, we deliberately conducted most of the phenotypic analyses in multiple clones to rule out clone-specific effects.

In summary, while the results in the previous study were genuine under their respective conditions, they failed to capture the true outcome of the mutant alleles. New observations made in this study allowed further investigation into the mechanisms underlying the phenotypes of the phospho-mutants of *pot1-V5*.

6.2 Pot1-ssDNA interaction

We found that *pot1-A-V5* mutants are synthetically sick with deletions of *taz1*$^+$ and *rap1*$^+$, the telomeric dsDNA-binding complex, and of *poz1*$^+$, the bridge between ds

and ssDNA-binding complex (see section 4.6 and 4.7). Therefore, recruitment to the telomeric dsDNA region appears to be important for the Pot1-A-V5 mutants to function. Different hypotheses could explain this result. In a *pot1-A-V5* background, Pot1 might be required for the telomeric dsDNA-binding complex in suppressing chromosome end-fusions, although this is unlikely since NHEJ is active only in G1 phase, which is negligible in cycling cells in the genetic backgrounds we used. Alternatively, the Pot1-A-V5 mutants may be unable to efficiently bind the telomeric ssDNA overhang, resulting in a *pot1Δ* phenotype when their binding is abolished *via* disruption of the dsDNA-binding complex.

One way to shed light on the defects of these mutants is to investigate which mechanism of chromosomal fusion the *taz1*Δ *pot1-A-V5* mutants employs. In fission yeast, two major pathways promoting chromosome end fusions, the choice of which depends heavily on the cause of telomere dysfunction (Wang and Baumann, 2008). Taz1-disrupted telomeres are prone to NHEJ-mediated chromosome fusion, which depends on Lig4 and Ku70 (Ferreira and Cooper, 2001). However, in fission yeast NHEJ is prominent only in G1-arrested cultures, and the telomere-telomere fusions typically retain telomeric DNA that can be detected on Southern blots. The fact that no telomere signal was observed in the *taz1*Δ *pot1-A-V5* mutants argues against NHEJ-mediated fusion. Another mechanism, single-strand annealing (SSA), mediates chromosomal fusion following telomere erosion at *pot1Δ* telomeres (Wang and Baumann, 2008). Triple mutant strains containing additional deletion of *rad16* or *swi10*, which are key components of the SSA pathway, could be used to test the dependence on SSA. SSA-mediated chromosome fusion in *taz1*Δ *pot1-A-V5* mutant backgrounds would be consistent with the hypothesis that the defect lies in the ssDNA-loading of Pot1-A-V5 molecules.

Furthermore, a genetic interaction between Pot1 and the dsDNA-binding complex has been reported in which *pot1*$^{+}$ overexpression rescues the telomere loss phenotype of *taz1*Δ cells harbouring the *rad11-D223Y* mutation, an RPA allele that is hypothesized to confer tighter telomere binding than wt RPA (Ono et al., 2003, Kibe et al., 2007). It was proposed that telomere-enriched Rad11-D223Y inhibits

binding of Pot1 to the ssDNA, which implies that reduced ssDNA-bound Pot1 leads to telomere loss in a *taz1*Δ background. The resemblence between *pot1-A-V5 taz1*Δ and *rad11-D223Y taz1*Δ phenotypes supports the idea that Pot1-A-V5 is defective in telomeric ssDNA-binding, again consistent with our hypothesis that loading of Pot1-A-V5 mutant requires recruitment via the dsDNA-binding complex.

To provide direct evidence for the hypothesis, however, the level of Pot1-ssDNA interaction in the *pot1-A-V5* background should be determined. Our attempt to assay this interaction *in vivo* by ChIP in strains lacking the Taz1-Rap1 complex was confounded by the synthetic effect of immediate telomere loss. New strategies need to be developed to provide this information. One way to explore is to use DNA pull down, in which telomeric ssDNA immobilized to beads is incubated with cell lysate of *pot1-V5* mutant strains to analyse Pot1 *in vitro* binding. Alternatively, we can investigate telomeric binding of RPA, which competes with Pot1 to bind telomeric ssDNA; an increase in RPA binding in the mutant backgrounds could suggest that binding of Pot1 is impaired, although as checkpoint is activated, it will be difficult to establish whether RPA binding is the cause or the result. We are still working to address these questions.

6.3 Requirement of the DDR pathway for telomere maintenance

Our data showed that several components of the DDR pathway, including Rad51, Chk1 and Rad3, are required for telomere maintenance in *pot1-V5* phosphorylation mutants (see section 3.4). Although both mutants are dependent on the same pathway, differential degree of requirement by *pot1-A-V5* and *pot1-D-V5*, i.e. immediate loss of telomere by *pot1-A-V5 chk1*Δ*/rad3*Δ and *pot1-D-V5 rad51*Δ but not *vice versa*, supports the idea that these mutants confer different defects in telomere maintenance and checkpoint suppression, in line with the idea that they should resemble constitutively unphosphorylated and phosphorylated forms.

How the DDR pathway is involved, however, was not clear from the genetic analysis. Interestingly, genetic interaction has been reported between the DDR

components and *ccq1*$^+$, which encodes Ccq1, a component of the Pot1-complex and is recruited to the chromosomal ends by Pot1-Tpp1. Chk1 is activated by *ccq1*$^+$ deletion, and activated Chk1 is required for the recombination-based telomere maintenance in late generation *ccq1*Δ cells (Tomita and Cooper, 2008), recalling the genetic interaction between *pot1-A-V5* and *chk1*$^+$.

Based on these observations, we hypothesize that the Rad3/Chk1-dependency in the *pot1-A-V5* background is due to reduced Ccq1 recruitment to the telomeric ssDNA. This would be in line with the idea that Pot1-A-V5 fails to interact with telomeric ssDNA. In this case, *pot1-A-V5* telomeres would be partially Ccq1-deficient, leading to the Chk1-dependence. We have performed preliminary ChIP experiment against tagged Ccq1 in the *pot1-V5* phospho-mutant backgrounds and saw no significant difference between different mutants; however, it should be noted that this again does not distinguish between recruitment *via* the ds vs. the ssDNA. A different strategy needs to be developed to support our hypothesis.

On the other hand, it is conceivable that the recombinase Rad51 assumes a more direct role in telomere maintenance in the mutant background, due to its ability to bind ssDNA. A possible role of Rad51 at the telomeres of *pot1-A-V5* mutants is to facilitate fork restart by template exchange after replication fork blockage (Lambert et al., 2010). Given that *pot1-A-V5* telomeres contain excessive ssDNA throughout the cell cycle (section 4.6), the replication fork may be stalled before reaching the end, as one of the templates is missing. This fork stalling would presumably affect only one of the two daughter strands, and only at telomeres displaying the excessive ssDNA. Therefore, telomere loss in the absence of *rad51*$^+$ should be gradual rather than immediate in the *pot1-A-V5* background, consistent with our observation (section 3.4). As Srs2 is required for efficient fork restart and template exchange (Lambert et al., 2010), this hypothesis would predict that *srs2*Δ *pot1-A-V5* mutants display similar telomeric phenotypes to *rad51*Δ *pot1-A-V5* mutants.

Importantly, the *pot1-D-V5* mutant phenotype in *rad51*Δ background is more dramatic than *pot1-A-V5*, leading to telomere loss immediately after germination (see section 3.4), even though in most other cases its phenotypes are milder and/or less penetrant, e.g. in telomere elongation, hyper-recombination and *taz1*$^+$

dependence. This dramatic telomere loss phenotype cannot be explained by the requirement for Rad51 to restart replication fork. As our data suggested that unlike Pot1-A-V5, Pot1-D-V5 binds telomeric ssDNA, it could be that this binding channels the ssDNA to deleterious outcomes if it is not protected by Rad51. This hypothesis could be tested by performing DNA 2DGE on internal telomeric sequences (see section 5.4), which allows visualization of the replication defect *pot1-D-V5 rad51*Δ may bear.

6.4 Control of DDK activity at telomeres

The fact that both *pot1-A-V5* and *pot1-D-V5* are partially defective in telomere protection suggests that both unphosphorylated and phosphorylated forms are essential for Pot1 to function properly, and the cell cycle regulation of DDK activity provides temporal control of these two forms. Importantly, our results and discussions above favour a model, in which telomere-bound Pot1 needs to be unphosphorylated when telomeres are being replicated, but becomes phosphorylated upon completion of replication to allow Pot1 to replace RPA from the telomeric ssDNA and resume its protective functions.

However, since DDK becomes active at the beginning of S phase, while telomere replication is not until late S/G2 phase, this model begs the question of how this DDK-mediated phosphorylation is controlled at telomeres. One possibility is that DDK becomes active at telomeres only after replication fork passage. This could be achieved by direct or indirect inhibition of DDK activity by telomeric proteins including Taz1 and Rif1 as suggested by several recent reports (Tazumi et al., 2012, Hayano et al., 2012). Another possibility is that a subpopulation of Pot1 is phosphorylated by DDK at the beginning of S phase, but becomes telomere-bound only following replication fork passage, perhaps due to higher affinity for telomeric ssDNA.

6.5 Summary and future work

The purpose of the work presented in this thesis was to investigate the function of the telomeric ssDNA-binding protein Pot1. A set of partial loss-of-function mutants was characterized in detail to provide insights on the role of Pot1 in telomere maintenance and protection through the cell cycle. We showed that the phospho-deficient mutants of Pot1 conferred defects both in telomere maintenance and protection, leading to erratic phenotypes including telomere elongation, checkpoint activation, and excessive ssDNA.

Based on our analysis, we propose that phosphorylation of Pot1 in its N-terminal OB-fold is crucial for efficient Pot1-ssDNA interaction, which in turn is important for the function of Pot1, both in inhibition of 5' resection and in promotion of Ccq1 recruitment. In a *wt* cell, Pot1 phosphorylation by DDK is regulated through the cell cycle. In S phase, recruitment of Pot1 via the dsDNA-binding complex reduces due to a 'loosened' telomere chromatin, unphosphorylated Pot1 may be displaced by RPA from the telomeric ssDNA, allowing telomeric end processing by exonucleases; in G2 phase, Pot1 is phosphorylated by DDK kinase and re-associates with the ssDNA to fulfil its function in telomerase recruitment and end protection (Figure 6.1). In the absence of phosphorylation (the *pot1-A-V5* scenario), the dsDNA-binding complex Taz1-Rap1 recruits Pot1 to the telomere region and facilitates its loading, and the DDR kinases Chk1 and Rad3 become essential for telomere protection.

Our future work will focus on three major areas. First, we will continue to investigate Pot1 phosphorylation by mass spectrometry. This remains a key issue of this work, as validation of phosphorylation is essential for either confirming or denying phosphorylation as the root cause of the mutants' phenotypes. Second, we hope to develop an assay to detect Pot1-ssDNA interaction *in vivo*; such an assay is important for understanding the molecular mechanisms underlying the effects of the OB-fold mutations of *pot1-V5*. Third, we will try to determine the role of the C-terminal tagging in the *pot1-V5* phenotypes, and further investigate the effect of Pot1 phosphorylation in an untagged setting.

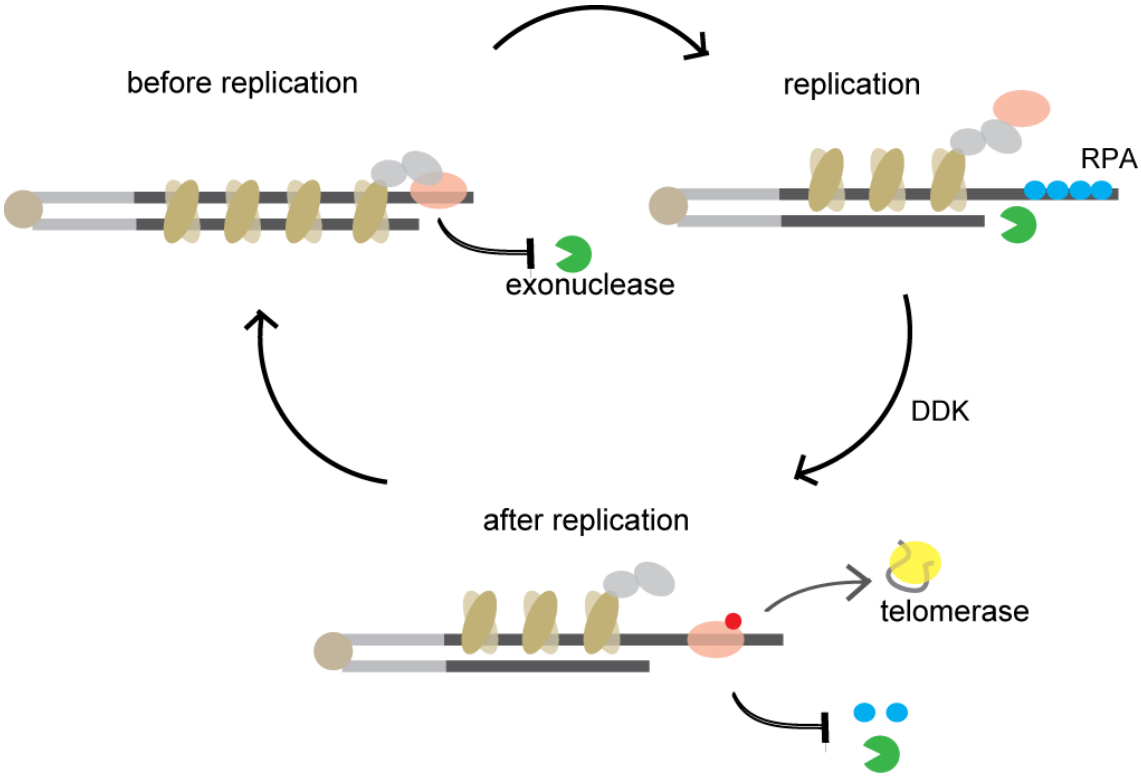

Figure 6.1 Model of Pot1 phosphorylation regulates telomere function

Model showing the molecular mechanisms of telomere regulation by Pot1 phosphorylation. Before telomere replication, Pot1 is recruited to the telomeric overhang via the dsDNA-binding complex. During replication, telomere chromatin loosen up, leading to reduced Pot1 recruitment via the dsDNA, allowing resection by exonucleases. After replication, phosphorylated Pot1 re-associate with telomeric overhang, which inhibits exonucleases activity and allow telomerase action.

Reference List

AKAMATSU, Y., DZIADKOWIEC, D., IKEGUCHI, M., SHINAGAWA, H. & IWASAKI, H. 2003. Two different Swi5-containing protein complexes are involved in mating-type switching and recombination repair in fission yeast. *Proc Natl Acad Sci U S A,* 100**,** 15770-5.

AKAMATSU, Y., TSUTSUI, Y., MORISHITA, T., SIDDIQUE, M. D. S. P., KUROKAWA, Y., IKEGUCHI, M., YAMAO, F., ARCANGIOLI, B. & IWASAKI, H. 2007. Fission yeast Swi5/Sfr1 and Rhp55/Rhp57 differentially regulate Rhp51-dependent recombination outcomes. *The EMBO Journal,* 26**,** 1352-1362.

AYLON, Y. & KUPIEC, M. 2004. DSB repair: the yeast paradigm. *DNA Repair (Amst),* 3**,** 797-815.

BAHLER, J., WU, J. Q., LONGTINE, M. S., SHAH, N. G., MCKENZIE, A., 3RD, STEEVER, A. B., WACH, A., PHILIPPSEN, P. & PRINGLE, J. R. 1998. Heterologous modules for efficient and versatile PCR-based gene targeting in Schizosaccharomyces pombe. *Yeast,* 14**,** 943-51.

BAUMANN, P. & CECH, T. R. 2000. Protection of telomeres by the Ku protein in fission yeast. *Mol Biol Cell,* 11**,** 3265-75.

BAUMANN, P. & CECH, T. R. 2001. Pot1, the Putative Telomere End-Binding Protein in Fission Yeast and Humans. *Science,* 292**,** 1171-1175.

BAUR, J. A., ZOU, Y., SHAY, J. W. & WRIGHT, W. E. 2001. Telomere position effect in human cells. *Science,* 292**,** 2075-7.

BIANCHI, A. & SHORE, D. 2007. Early Replication of Short Telomeres in Budding Yeast. *Cell,* 128**,** 1051-1062.

BIANCO, P. R., TRACY, R. B. & KOWALCZYKOWSKI, S. C. 1998. DNA strand exchange proteins: a biochemical and physical comparison. *Frontiers in Bioscience: A Journal and Virtual Library,* 3**,** D570-603-D570-603.

BIESSMANN, H., CARTER, S. B. & MASON, J. M. 1990. Chromosome ends in Drosophila without telomeric DNA sequences. *Proc Natl Acad Sci U S A,* 87**,** 1758-61.

BLACKBURN, E. H. & GALL, J. G. 1978. A tandemly repeated sequence at the termini of the extrachromosomal ribosomal RNA genes in Tetrahymena. *J Mol Biol,* 120**,** 33-53.

BONETTI, D., MARTINA, M., CLERICI, M., LUCCHINI, G. & LONGHESE, M. P. 2009. Multiple Pathways Regulate 3' Overhang Generation at S. cerevisiae Telomeres. *Molecular Cell,* 35**,** 70-81.

BOOTH, C., GRIFFITH, E., BRADY, G. & LYDALL, D. 2001. Quantitative amplification of single-stranded DNA (QAOS) demonstrates that cdc13-1 mutants generate ssDNA in a telomere to centromere direction. *Nucleic Acids Res,* 29**,** 4414-22.

BROCCOLI, D., SMOGORZEWSKA, A., CHONG, L. & DE LANGE, T. 1997. Human telomeres contain two distinct Myb-related proteins, TRF1 and TRF2. *Nat Genet,* 17**,** 231-5.

BRYAN, T. M., ENGLEZOU, A., DALLA-POZZA, L., DUNHAM, M. A. & REDDEL, R. R. 1997. Evidence for an alternative mechanism for maintaining telomere length in human tumors and tumor-derived cell lines. *Nat Med,* 3**,** 1271-4.

BUNCH, J. T., BAE, N. S., LEONARDI, J. & BAUMANN, P. 2005. Distinct Requirements for Pot1 in Limiting Telomere Length and Maintaining Chromosome Stability. *Mol. Cell. Biol.,* 25**,** 5567-5578.

CARNEIRO, T., KHAIR, L., REIS, C. C., BORGES, V., MOSER, B. A., NAKAMURA, T. M. & FERREIRA, M. G. 2010. Telomeres avoid end detection by severing the checkpoint signal transduction pathway. *Nature,* 467**,** 228-32.

CATLETT, M. G. & FORSBURG, S. L. 2003. Schizosaccharomyces pombe Rdh54 (TID1) Acts with Rhp54 (RAD54) to Repair Meiotic Double-Strand Breaks. *Molecular Biology of the Cell,* 14**,** 4707-4720.

CELLI, G. B. & DE LANGE, T. 2005. DNA processing is not required for ATM-mediated telomere damage response after TRF2 deletion. *Nat Cell Biol,* 7**,** 712-718.

CELLI, G. B., DENCHI, E. L. & DE LANGE, T. 2006. Ku70 stimulates fusion of dysfunctional telomeres yet protects chromosome ends from homologous recombination. *Nat Cell Biol,* 8**,** 885-90.

CESARE, A. J. & REDDEL, R. R. 2010. Alternative lengthening of telomeres: models, mechanisms and implications. *Nat Rev Genet,* 11**,** 319-330.

CHEN, L. Y., REDON, S. & LINGNER, J. 2012. The human CST complex is a terminator of telomerase activity. *Nature,* 488**,** 540-4.

CHEN, Q., IJPMA, A. & GREIDER, C. W. 2001. Two survivor pathways that allow growth in the absence of telomerase are generated by distinct telomere recombination events. *Mol Cell Biol,* 21**,** 1819-27.

CHIKASHIGE, Y., TSUTSUMI, C., YAMANE, M., OKAMASA, K., HARAGUCHI, T. & HIRAOKA, Y. 2006. Meiotic Proteins Bqt1 and Bqt2 Tether Telomeres to Form the Bouquet Arrangement of Chromosomes. *Cell,* 125**,** 59-69.

CHONG, L., VAN STEENSEL, B., BROCCOLI, D., ERDJUMENT-BROMAGE, H., HANISH, J., TEMPST, P. & DE LANGE, T. 1995. A human telomeric protein. *Science,* 270**,** 1663-7.

CHOW, T. T., ZHAO, Y., MAK, S. S., SHAY, J. W. & WRIGHT, W. E. 2012. Early and late steps in telomere overhang processing in normal human cells: the position of the final RNA primer drives telomere shortening. *Genes & Development,* 26**,** 1167-1178.

COHN, M. & BLACKBURN, E. H. 1995. Telomerase in yeast. *Science,* 269**,** 396-400.

COLGIN, L. M., BARAN, K., BAUMANN, P., CECH, T. R. & REDDEL, R. R. 2003. Human POT1 facilitates telomere elongation by telomerase. *Curr Biol,* 13**,** 942-6.

COOPER, J. P., NIMMO, E. R., ALLSHIRE, R. C. & CECH, T. R. 1997. Regulation of telomere length and function by a Myb-domain protein in fission yeast. *Nature,* 385**,** 744-747.

CORNFORTH, M. N. & EBERLE, R. L. 2001. Termini of human chromosomes display elevated rates of mitotic recombination. *Mutagenesis,* 16**,** 85-9.

CRISTOFARI, G. & LINGNER, J. 2006. Telomere length homeostasis requires that telomerase levels are limiting. *EMBO J,* 25**,** 565-74.

DAI, X., HUANG, C., BHUSARI, A., SAMPATHI, S., SCHUBERT, K. & CHAI, W. 2010. Molecular steps of G-overhang generation at human telomeres and its function in chromosome end protection. *EMBO J,* 29**,** 2788-801.

DE LANGE, T., SHIUE, L., MYERS, R. M., COX, D. R., NAYLOR, S. L., KILLERY, A. M. & VARMUS, H. E. 1990. Structure and variability of human chromosome ends. *Mol Cell Biol,* 10**,** 518-27.

DEHE, P. M., ROG, O., FERREIRA, M. G., GREENWOOD, J. & COOPER, J. P. 2012. Taz1 enforces cell-cycle regulation of telomere synthesis. *Mol Cell,* 46**,** 797-808.

DIONNE, I. & WELLINGER, R. J. 1996. Cell cycle-regulated generation of single-stranded G-rich DNA in the absence of telomerase. *Proceedings of the National Academy of Sciences of the United States of America,* 93**,** 13902-13907.

DOE, C. L., OSMAN, F., DIXON, J. & WHITBY, M. C. 2004. DNA repair by a Rad22–Mus81-dependent pathway that is independent of Rhp51. *Nucleic Acids Research,* 32**,** 5570-5581.

DU, L.-L., NAKAMURA, T. M. & RUSSELL, P. 2006. Histone modification-dependent and -independent pathways for recruitment of checkpoint protein Crb2 to double-strand breaks. *Genes & Development,* 20**,** 1583-1596.

DUBEY, D. D., ZHU, J., CARLSON, D. L., SHARMA, K. & HUBERMAN, J. A. 1994. Three ARS elements contribute to the ura4 replication origin region in the fission yeast, Schizosaccharomyces pombe. *EMBO J,* 13**,** 3638-47.

FAURE, V., COULON, S., HARDY, J. & GELI, V. 2010. Cdc13 and telomerase bind through different mechanisms at the lagging- and leading-strand telomeres. *Mol Cell,* 38**,** 842-52.

FERREIRA, M. G. & COOPER, J. P. 2001. The fission yeast Taz1 protein protects chromosomes from Ku-dependent end-to-end fusions. *Mol Cell,* 7**,** 55-63.

FERREIRA, M. G. & COOPER, J. P. 2004. Two modes of DNA double-strand break repair are reciprocally regulated through the fission yeast cell cycle. *Genes Dev,* 18**,** 2249-54.

FLORY, M. R., CARSON, A. R., MULLER, E. G. & AEBERSOLD, R. 2004. An SMC-domain protein in fission yeast links telomeres to the meiotic centrosome. *Mol Cell,* 16**,** 619-30.

FLYNN, R. L., CENTORE, R. C., O'SULLIVAN, R. J., RAI, R., TSE, A., SONGYANG, Z., CHANG, S., KARLSEDER, J. & ZOU, L. 2011. TERRA and hnRNPA1 orchestrate an RPA-to-POT1 switch on telomeric single-stranded DNA. *Nature,* 471**,** 532-6.

FOULADI, B., SABATIER, L., MILLER, D., POTTIER, G. & MURNANE, J. P. 2000. The relationship between spontaneous telomere loss and chromosome instability in a human tumor cell line. *Neoplasia,* 2**,** 540-54.

FRANK, C. J., HYDE, M. & GREIDER, C. W. 2006. Regulation of Telomere Elongation by the Cyclin-Dependent Kinase CDK1. *Molecular Cell,* 24**,** 423-432.

FRIEDMAN, K. L. & BREWER, B. J. 1995. Analysis of replication intermediates by two-dimensional agarose gel electrophoresis. *Methods Enzymol,* 262**,** 613-27.

GAO, H., CERVANTES, R. B., MANDELL, E. K., OTERO, J. H. & LUNDBLAD, V. 2007. RPA-like proteins mediate yeast telomere function. *Nat Struct Mol Biol,* 14**,** 208-214.

GARCIA-CAO, M., O'SULLIVAN, R., PETERS, A. H., JENUWEIN, T. & BLASCO, M. A. 2004. Epigenetic regulation of telomere length in mammalian cells by the Suv39h1 and Suv39h2 histone methyltransferases. *Nat Genet,* 36**,** 94-9.

GARVIK, B., CARSON, M. & HARTWELL, L. 1995. Single-stranded DNA arising at telomeres in cdc13 mutants may constitute a specific signal for the RAD9 checkpoint. *Mol Cell Biol,* 15**,** 6128-38.

GONG, Y. & DE LANGE, T. 2010. A Shld1-controlled POT1a provides support for repression of ATR signaling at telomeres through RPA exclusion. *Molecular Cell,* 40**,** 377-387.

GRANDIN, N. & CHARBONNEAU, M. 2003. The Rad51 Pathway of Telomerase-Independent Maintenance of Telomeres Can Amplify TG(1-3) Sequences in yku and cdc13 Mutants of Saccharomyces cerevisiae. *Mol Cell Biol,* 23**,** 3721-34.

GRANDIN, N., DAMON, C. & CHARBONNEAU, M. 2001. Cdc13 prevents telomere uncapping and Rad50-dependent homologous recombination. *Embo J,* 20**,** 6127-39.

HARLEY, C. B., FUTCHER, A. B. & GREIDER, C. W. 1990. Telomeres shorten during ageing of human fibroblasts. *Nature,* 345**,** 458-60.

HASHIDA-OKADO, T., YASUMOTO, R., ENDO, M., TAKESAKO, K. & KATO, I. 1998. Isolation and characterization of the aureobasidin A-resistant gene, aur1R, on Schizosaccharomyces pombe: roles of Aur1p+ in cell morphogenesis. *Curr Genet,* 33**,** 38-45.

HAYANO, M., KANOH, Y., MATSUMOTO, S., RENARD-GUILLET, C., SHIRAHIGE, K. & MASAI, H. 2012. Rif1 is a global regulator of timing of replication origin firing in fission yeast. *Genes Dev,* 26**,** 137-50.

HAYFLICK, L. & MOORHEAD, P. S. 1961. The serial cultivation of human diploid cell strains. *Experimental Cell Research,* 25**,** 585-621.

HECTOR, R. E., SHTOFMAN, R. L., RAY, A., CHEN, B.-R., NYUN, T., BERKNER, K. L. & RUNGE, K. W. 2007. Tel1p Preferentially Associates with Short Telomeres to Stimulate Their Elongation. *Molecular Cell,* 27**,** 851-858.

HENSON, J. D., NEUMANN, A. A., YEAGER, T. R. & REDDEL, R. R. 2002. Alternative lengthening of telomeres in mammalian cells. *Oncogene,* 21**,** 598-610.

HIRANO, Y., FUKUNAGA, K. & SUGIMOTO, K. 2009. Rif1 and rif2 inhibit localization of tel1 to DNA ends. *Mol Cell,* 33**,** 312-22.

HIRANO, Y. & SUGIMOTO, K. 2007. Cdc13 Telomere Capping Decreases Mec1 Association but Does Not Affect Tel1 Association with DNA Ends. *Mol. Biol. Cell,* 18**,** 2026-2036.

HOCKEMEYER, D., DANIELS, J. P., TAKAI, H. & DE LANGE, T. 2006. Recent expansion of the telomeric complex in rodents: Two distinct POT1 proteins protect mouse telomeres. *Cell,* 126**,** 63-77.

HORVATH, M. P. 2011. Structural anatomy of telomere OB proteins. *Critical Reviews in Biochemistry and Molecular Biology,* 46**,** 409-435.

HUANG, P., PRYDE, F. E., LESTER, D., MADDISON, R. L., BORTS, R. H., HICKSON, I. D. & LOUIS, E. J. 2001. SGS1 is required for telomere elongation in the absence of telomerase. *Curr Biol,* 11**,** 125-9.

HUERTAS, P., CORTES-LEDESMA, F., SARTORI, A. A., AGUILERA, A. & JACKSON, S. P. 2008. CDK targets Sae2 to control DNA-end resection and homologous recombination. *Nature,* 455**,** 689-92.

JAIN, D., HEBDEN, A. K., NAKAMURA, T. M., MILLER, K. M. & COOPER, J. P. 2010. HAATI survivors replace canonical telomeres with blocks of generic heterochromatin. *Nature,* 467**,** 223-7.

JEGGO, P. A., GEUTING, V. & LOBRICH, M. 2011. The role of homologous recombination in radiation-induced double-strand break repair. *Radiother Oncol,* 101**,** 7-12.

KANOH, J., FRANCESCONI, S., COLLURA, A., SCHRAMKE, V., ISHIKAWA, F., BALDACCI, G. & GELI, V. 2003. The fission yeast spSet1p is a histone H3-K4 methyltransferase that functions in telomere maintenance and DNA repair in an ATM kinase Rad3-dependent pathway. *J Mol Biol,* 326**,** 1081-94.

KANOH, J. & ISHIKAWA, F. 2001. spRap1 and spRif1, recruited to telomeres by Taz1, are essential for telomere function in fission yeast. *Curr Biol,* 11**,** 1624-30.

KARLSEDER, J., BROCCOLI, D., DAI, Y., HARDY, S. & DE LANGE, T. 1999. p53- and ATM-dependent apoptosis induced by telomeres lacking TRF2. *Science,* 283**,** 1321-5.

KARLSEDER, J., HOKE, K., MIRZOEVA, O. K., BAKKENIST, C., KASTAN, M. B., PETRINI, J. H. & DE LANGE, T. 2004. The telomeric protein TRF2 binds the ATM kinase and can inhibit the ATM-dependent DNA damage response. *PLoS Biol,* 2**,** E240.

KAZDA, A., ZELLINGER, B., ROSSLER, M., DERBOVEN, E., KUSENDA, B. & RIHA, K. 2012. Chromosome end protection by blunt-ended telomeres. *Genes Dev,* 26**,** 1703-13.

KHANNA, K. K., LAVIN, M. F., JACKSON, S. P. & MULHERN, T. D. 2001. ATM, a central controller of cellular responses to DNA damage. *Cell Death Differ,* 8**,** 1052-65.

KIBE, T., ONO, Y., SATO, K. & UENO, M. 2007. Fission Yeast Taz1 and RPA Are Synergistically Required to Prevent Rapid Telomere Loss. *Mol. Biol. Cell,* 18**,** 2378-2387.

KIBE, T., TOMITA, K., MATSUURA, A., IZAWA, D., KODAIRA, T., USHIMARU, T., URITANI, M. & UENO, M. 2003. Fission yeast Rhp51 is required for the maintenance of telomere structure in the absence of the Ku heterodimer. *Nucleic Acids Res,* 31**,** 5054-63.

KUZNETSOV, V. 2008. Cell cycle-dependent modification of Pot1 and its effects on telomere function. *PhD Thesis University College London*.

LAMBERT, S., MIZUNO, K., BLAISONNEAU, J., MARTINEAU, S., CHANET, R., FREON, K., MURRAY, J. M., CARR, A. M. & BALDACCI, G. 2010. Homologous recombination restarts blocked replication forks at the expense of genome rearrangements by template exchange. *Mol Cell,* 39**,** 346-59.

LARRIVEE, M., LEBEL, C. & WELLINGER, R. J. 2004. The generation of proper constitutive G-tails on yeast telomeres is dependent on the MRX complex. *Genes Dev,* 18**,** 1391-6.

LATRICK, C. M. & CECH, T. R. 2010. POT1-TPP1 enhances telomerase processivity by slowing primer dissociation and aiding translocation. *EMBO J,* 29**,** 924-33.

LAZZERINI DENCHI, E. & DE LANGE, T. 2007. Protection of telomeres through independent control of ATM and ATR by TRF2 and POT1. *Nature,* 448**,** 1068-1071.

LE, S., MOORE, J. K., HABER, J. E. & GREIDER, C. W. 1999. RAD50 and RAD51 define two pathways that collaborate to maintain telomeres in the absence of telomerase. *Genetics,* 152**,** 143-52.

LEI, M., PODELL, E. R., BAUMANN, P. & CECH, T. R. 2003. DNA self-recognition in the structure of Pot1 bound to telomeric single-stranded DNA. *Nature,* 426**,** 198-203.

LEI, M., PODELL, E. R. & CECH, T. R. 2004. Structure of human POT1 bound to telomeric single-stranded DNA provides a model for chromosome end-protection. *Nat Struct Mol Biol,* 11**,** 1223-1229.

LEVY, D. L. & BLACKBURN, E. H. 2004. Counting of Rif1p and Rif2p on Saccharomyces cerevisiae Telomeres Regulates Telomere Length. *Mol. Cell. Biol.,* 24**,** 10857-10867.

LI, S., MAKOVETS, S., MATSUGUCHI, T., BLETHROW, J. D., SHOKAT, K. M. & BLACKBURN, E. H. 2009. Cdk1-Dependent Phosphorylation of Cdc13 Coordinates Telomere Elongation during Cell-Cycle Progression. *Cell,* 136**,** 50-61.

LINGNER, J. & CECH, T. R. 1998. Telomerase and chromosome end maintenance. *Curr Opin Genet Dev,* 8**,** 226-32.

LINGNER, J., COOPER, J. P. & CECH, T. R. 1995. Telomerase and DNA end replication: no longer a lagging strand problem? *Science,* 269**,** 1533-4.

LOAYZA, D. & DE LANGE, T. 2003. POT1 as a terminal transducer of TRF1 telomere length control. *Nature,* 424**,** 1013-8.

LONGHESE, M. P. 2008. DNA damage response at functional and dysfunctional telomeres. *Genes Dev,* 22**,** 125-40.

LUNDBLAD, V. & BLACKBURN, E. H. 1993. An alternative pathway for yeast telomere maintenance rescues est1- senescence. *Cell,* 73**,** 347-60.

LUSTIG, A. J., KURTZ, S. & SHORE, D. 1990. Involvement of the silencer and UAS binding protein RAP1 in regulation of telomere length. *Science,* 250**,** 549-53.

MAKAROV, V. L., HIROSE, Y. & LANGMORE, J. P. 1997. Long G tails at both ends of human chromosomes suggest a C strand degradation mechanism for telomere shortening. *Cell,* 88**,** 657-66.

MANDELL, J. G., BAHLER, J., VOLPE, T. A., MARTIENSSEN, R. A. & CECH, T. R. 2005. Global expression changes resulting from loss of telomeric DNA in fission yeast. *Genome Biol,* 6**,** R1.

MARTÍN, V., DU, L.-L., ROZENZHAK, S. & RUSSELL, P. 2007. Protection of telomeres by a conserved Stn1–Ten1 complex. *Proceedings of the National Academy of Sciences,* 104**,** 14038-14043.

MCCLINTOCK, B. 1939. The Behavior in Successive Nuclear Divisions of a Chromosome Broken at Meiosis. *Proc Natl Acad Sci U S A,* 25**,** 405-16.

MCEACHERN, M. J. & HABER, J. E. 2006. Break-induced replication and recombinational telomere elongation in yeast. *Annu Rev Biochem,* 75**,** 111-35.

MILLER, K. M., ROG, O. & COOPER, J. P. 2006. Semi-conservative DNA replication through telomeres requires Taz1. *Nature,* 440**,** 824-8.

MIMITOU, E. P. & SYMINGTON, L. S. 2009. DNA end resection: Many nucleases make light work. *DNA Repair,* 8**,** 983-995.

MIYAKE, Y., NAKAMURA, M., NABETANI, A., SHIMAMURA, S., TAMURA, M., YONEHARA, S., SAITO, M. & ISHIKAWA, F. 2009. RPA-like mammalian Ctc1-Stn1-Ten1 complex binds to single-stranded DNA and protects telomeres independently of the Pot1 pathway. *Molecular Cell,* 36**,** 193-206.

MIYOSHI, T., KANOH, J., SAITO, M. & ISHIKAWA, F. 2008. Fission yeast Pot1-Tpp1 protects telomeres and regulates telomere length. *Science,* 320**,** 1341-4.

MOSER, B. A., CHANG, Y. T., KOSTI, J. & NAKAMURA, T. M. 2011. Tel1ATM and Rad3ATR kinases promote Ccq1-Est1 interaction to maintain telomeres in fission yeast. *Nat Struct Mol Biol,* 18**,** 1408-13.

MOSER, B. A., SUBRAMANIAN, L., CHANG, Y.-T., NOGUCHI, C., NOGUCHI, E. & NAKAMURA, T. M. 2009a. Differential arrival of leading and lagging strand DNA polymerases at fission yeast telomeres. *EMBO J,* 28**,** 810-820.

MOSER, B. A., SUBRAMANIAN, L., KHAIR, L., CHANG, Y.-T. & NAKAMURA, T. M. 2009b. Fission Yeast Tel1ATM and Rad3ATR Promote Telomere Protection and Telomerase Recruitment. *PLoS Genet,* 5**,** e1000622-e1000622.

MULLER, H. J. 1938. The remaking of chromosomes. *The Collecting Net, 1*3**,** 181–195.

MUNTONI, A., NEUMANN, A. A., HILLS, M. & REDDEL, R. R. 2009. Telomere elongation involves intra-molecular DNA replication in cells utilizing alternative lengthening of telomeres. *Human Molecular Genetics,* 18**,** 1017-1027.

MURZIN, A. G. 1993. OB(oligonucleotide/oligosaccharide binding)-fold: common structural and functional solution for non-homologous sequences. *EMBO J,* 12**,** 861-7.

NABETANI, A. & ISHIKAWA, F. 2009. Unusual telomeric DNAs in human telomerase-negative immortalized cells. *Molecular and Cellular Biology,* 29**,** 703-713.

NAITO, T., MATSUURA, A. & ISHIKAWA, F. 1998. Circular chromosome formation in a fission yeast mutant defective in two ATM homologues. *Nat Genet,* 20**,** 203-6.

NAKAMURA, A. J., REDON, C. E., BONNER, W. M. & SEDELNIKOVA, O. A. 2009. Telomere-dependent and telomere-independent origins of endogenous DNA damage in tumor cells. *Aging (Albany NY),* 1**,** 212-8.

NAKAMURA, T. M., COOPER, J. P. & CECH, T. R. 1998. Two modes of survival of fission yeast without telomerase. *Science,* 282**,** 493-6.

NANDAKUMAR, J., BELL, C. F., WEIDENFELD, I., ZAUG, A. J., LEINWAND, L. A. & CECH, T. R. 2012. The TEL patch of telomere protein TPP1 mediates telomerase recruitment and processivity. *Nature*.

NANDAKUMAR, J. & CECH, T. R. 2012. DNA-induced dimerization of the single-stranded DNA binding telomeric protein Pot1 from Schizosaccharomyces pombe. *Nucleic Acids Res,* 40**,** 235-244.

NUGENT, C. I., HUGHES, T. R., LUE, N. F. & LUNDBLAD, V. 1996. Cdc13p: a single-strand telomeric DNA-binding protein with a dual role in yeast telomere maintenance. *Science,* 274**,** 249-52.

ONO, Y., TOMITA, K., MATSUURA, A., NAKAGAWA, T., MASUKATA, H., URITANI, M., USHIMARU, T. & UENO, M. 2003. A novel allele of fission yeast rad11 that causes defects in DNA repair and telomere length regulation. *Nucleic Acids Res,* 31**,** 7141-9.

OSMAN, F., DIXON, J., BARR, A. R. & WHITBY, M. C. 2005. The F-Box DNA helicase Fbh1 prevents Rhp51-dependent recombination without mediator proteins. *Molecular and Cellular Biology,* 25**,** 8084-8096.

PALM, W. & DE LANGE, T. 2008. How shelterin protects mammalian telomeres. *Annu Rev Genet,* 42**,** 301-34.

PALM, W., HOCKEMEYER, D., KIBE, T. & DE LANGE, T. 2009. Functional Dissection of Human and Mouse POT1 Proteins. *Mol. Cell. Biol.,* 29**,** 471-482.

PENNOCK, E., BUCKLEY, K. & LUNDBLAD, V. 2001. Cdc13 delivers separate complexes to the telomere for end protection and replication. *Cell,* 104**,** 387-96.

PFEIFFER, V. & LINGNER, J. 2012. TERRA promotes telomere shortening through exonuclease 1-mediated resection of chromosome ends. *PLoS Genet,* 8**,** e1002747.

PITT, C. W. & COOPER, J. P. 2010. Pot1 inactivation leads to rampant telomere resection and loss in one cell cycle. *Nucleic Acids Res*.

QI, H. & ZAKIAN, V. A. 2000. The Saccharomyces telomere-binding protein Cdc13p interacts with both the catalytic subunit of DNA polymerase alpha and the telomerase-associated est1 protein. *Genes Dev,* 14**,** 1777-88.

REDON, S., REICHENBACH, P. & LINGNER, J. 2010. The non-coding RNA TERRA is a natural ligand and direct inhibitor of human telomerase. *Nucleic Acids Res,* 38**,** 5797-806.

ROG, O. & COOPER, J. P. 2008. Telomeres in drag: Dressing as DNA damage to engage telomerase. *Curr Opin Genet Dev,* 18**,** 212-20.

ROTHKAMM, K., KRUGER, I., THOMPSON, L. H. & LOBRICH, M. 2003. Pathways of DNA double-strand break repair during the mammalian cell cycle. *Mol Cell Biol,* 23**,** 5706-15.

SANDELL, L. L. & ZAKIAN, V. A. 1993. Loss of a yeast telomere: arrest, recovery, and chromosome loss. *Cell,* 75**,** 729-39.

SATO, M., DHUT, S. & TODA, T. 2005. New drug-resistant cassettes for gene disruption and epitope tagging in Schizosaccharomyces pombe. *Yeast,* 22**,** 583-91.

SCHLACHER, K., WU, H. & JASIN, M. 2012. A distinct replication fork protection pathway connects Fanconi anemia tumor suppressors to RAD51-BRCA1/2. *Cancer Cell,* 22**,** 106-16.

SEXTON, A. N., YOUMANS, D. T. & COLLINS, K. 2012. Specificity Requirements for Human Telomere Protein Interaction with Telomerase Holoenzyme. *J Biol Chem*.

SFEIR, A. & DE LANGE, T. 2012. Removal of shelterin reveals the telomere end-protection problem. *Science (New York, N.Y.),* 336**,** 593-597.

SFEIR, A., KABIR, S., VAN OVERBEEK, M., CELLI, G. B. & DE LANGE, T. 2010. Loss of Rap1 induces telomere recombination in the absence of NHEJ or a DNA damage signal. *Science,* 327**,** 1657-61.

SFEIR, A., KOSIYATRAKUL, S. T., HOCKEMEYER, D., MACRAE, S. L., KARLSEDER, J., SCHILDKRAUT, C. L. & DE LANGE, T. 2009. Mammalian Telomeres Resemble Fragile Sites and Require TRF1 for Efficient Replication. *Cell,* 138**,** 90-103.

SHAMPAY, J., SZOSTAK, J. W. & BLACKBURN, E. H. 1984. DNA sequences of telomeres maintained in yeast. *Nature,* 310**,** 154-7.

SHAY, J. W. & WRIGHT, W. E. 1989. Quantitation of the frequency of immortalization of normal human diploid fibroblasts by SV40 large T-antigen. *Exp Cell Res,* 184**,** 109-18.

SMOGORZEWSKA, A., KARLSEDER, J., HOLTGREVE-GREZ, H., JAUCH, A. & DE LANGE, T. 2002. DNA ligase IV-dependent NHEJ of deprotected mammalian telomeres in G1 and G2. *Curr Biol,* 12**,** 1635-44.

SORENSEN, C. S., HANSEN, L. T., DZIEGIELEWSKI, J., SYLJUASEN, R. G., LUNDIN, C., BARTEK, J. & HELLEDAY, T. 2005. The cell-cycle checkpoint kinase Chk1 is required for mammalian homologous recombination repair. *Nat Cell Biol,* 7**,** 195-201.

STEWART, J. A., CHAIKEN, M. F., WANG, F. & PRICE, C. M. 2012. Maintaining the end: roles of telomere proteins in end-protection, telomere replication and length regulation. *Mutation Research,* 730**,** 12-19.

SUBRAMANIAN, L., MOSER, B. A. & NAKAMURA, T. M. 2008. Recombination-based telomere maintenance is dependent on Tel1-MRN and Rap1 and inhibited by telomerase, Taz1, and Ku in fission yeast. *Mol Cell Biol,* 28**,** 1443-55.

SUBRAMANIAN, L. & NAKAMURA, T. M. 2010. To fuse or not to fuse: how do checkpoint and DNA repair proteins maintain telomeres? *Front Biosci,* 15**,** 1105-18.

SUN, J., YU, E. Y., YANG, Y., CONFER, L. A., SUN, S. H., WAN, K., LUE, N. F. & LEI, M. 2009. Stn1-Ten1 is an Rpa2-Rpa3-like complex at telomeres. *Genes & Development,* 23**,** 2900-2914.

SYMINGTON, L. S. & GAUTIER, J. 2011. Double-strand break end resection and repair pathway choice. *Annual Review of Genetics,* 45**,** 247-271.

TAKAI, H., SMOGORZEWSKA, A. & DE LANGE, T. 2003. DNA damage foci at dysfunctional telomeres. *Curr Biol,* 13**,** 1549-56.

TARSOUNAS, M., MUNOZ, P., CLAAS, A., SMIRALDO, P. G., PITTMAN, D. L., BLASCO, M. A. & WEST, S. C. 2004. Telomere maintenance requires the RAD51D recombination/repair protein. *Cell,* 117**,** 337-47.

TAZUMI, A., FUKUURA, M., NAKATO, R., KISHIMOTO, A., TAKENAKA, T., OGAWA, S., SONG, J. H., TAKAHASHI, T. S., NAKAGAWA, T., SHIRAHIGE, K. & MASUKATA, H. 2012. Telomere-binding protein Taz1 controls global replication timing through its localization near late replication origins in fission yeast. *Genes Dev,* 26**,** 2050-62.

TEIXEIRA, M. T., ARNERIC, M., SPERISEN, P. & LINGNER, J. 2004. Telomere length homeostasis is achieved via a switch between telomerase- extendible and -nonextendible states. *Cell,* 117**,** 323-35.

TENG, S. C., CHANG, J., MCCOWAN, B. & ZAKIAN, V. A. 2000. Telomerase-independent lengthening of yeast telomeres occurs by an abrupt Rad50p-dependent, Rif-inhibited recombinational process. *Mol Cell,* 6**,** 947-52.

TOMITA, K. & COOPER, J. P. 2008. Fission yeast Ccq1 is telomerase recruiter and local checkpoint controller. *Genes Dev,* 22**,** 3461-74.

TOMITA, K., KIBE, T., KANG, H.-Y., SEO, Y.-S., URITANI, M., USHIMARU, T. & UENO, M. 2004. Fission Yeast Dna2 Is Required for Generation of the Telomeric Single-Strand Overhang. *Molecular and Cellular Biology,* 24**,** 9557-9567.

TOMITA, K., MATSUURA, A., CASPARI, T., CARR, A. M., AKAMATSU, Y., IWASAKI, H., MIZUNO, K., OHTA, K., URITANI, M., USHIMARU, T., YOSHINAGA, K. & UENO, M. 2003. Competition between the Rad50 complex and the Ku heterodimer reveals a role for Exo1 in processing double-strand breaks but not telomeres. *Mol Cell Biol,* 23**,** 5186-97.

TOMMERUP, H., DOUSMANIS, A. & DE LANGE, T. 1994. Unusual chromatin in human telomeres. *Mol Cell Biol,* 14**,** 5777-85.

TORIGOE, H. & FURUKAWA, A. 2007. Tetraplex Structure of Fission Yeast Telomeric DNA and Unfolding of the Tetraplex on the Interaction with Telomeric DNA Binding Protein Pot1. *J Biochem,* 141**,** 57-68.

VAN DEN BOSCH, M., ZONNEVELD, J. B., VREEKEN, K., DE VRIES, F. A., LOHMAN, P. H. & PASTINK, A. 2002. Differential expression and requirements for Schizosaccharomyces pombe RAD52 homologs in DNA repair and recombination. *Nucleic Acids Res,* 30**,** 1316-24.

VISCARDI, V., BONETTI, D., CARTAGENA-LIROLA, H., LUCCHINI, G. & LONGHESE, M. P. 2007. MRX-dependent DNA damage response to short telomeres. *Mol Biol Cell,* 18**,** 3047-58.

VODENICHAROV, M. D. & WELLINGER, R. J. 2006. DNA Degradation at Unprotected Telomeres in Yeast Is Regulated by the CDK1 (Cdc28/Clb) Cell-Cycle Kinase. *Molecular Cell,* 24**,** 127-137.

WANG, F., PODELL, E. R., ZAUG, A. J., YANG, Y., BACIU, P., CECH, T. R. & LEI, M. 2007. The POT1-TPP1 telomere complex is a telomerase processivity factor. *Nature,* 445**,** 506-510.

WANG, R. C., SMOGORZEWSKA, A. & DE LANGE, T. 2004. Homologous recombination generates T-loop-sized deletions at human telomeres. *Cell,* 119**,** 355-68.

WANG, X. & BAUMANN, P. 2008. Chromosome fusions following telomere loss are mediated by single-strand annealing. *Mol Cell,* 31**,** 463-73.

WATSON, J. D. 1972. Origin of concatemeric T7 DNA. *Nat New Biol,* 239**,** 197-201.

WEINRICH, S. L., PRUZAN, R., MA, L., OUELLETTE, M., TESMER, V. M., HOLT, S. E., BODNAR, A. G., LICHTSTEINER, S., KIM, N. W., TRAGER, J. B., TAYLOR, R. D., CARLOS, R., ANDREWS, W. H., WRIGHT, W. E., SHAY, J. W., HARLEY, C. B. & MORIN, G. B. 1997. Reconstitution of human telomerase with the template RNA component hTR and the catalytic protein subunit hTRT. *Nat Genet,* 17**,** 498-502.

WELLINGER, R. J., ETHIER, K., LABRECQUE, P. & ZAKIAN, V. A. 1996. Evidence for a new step in telomere maintenance. *Cell,* 85**,** 423-33.

WELLINGER, R. J., WOLF, A. J. & ZAKIAN, V. A. 1993a. Origin activation and formation of single-strand TG1-3 tails occur sequentially in late S phase on a yeast linear plasmid. *Mol Cell Biol,* 13**,** 4057-65.

WELLINGER, R. J., WOLF, A. J. & ZAKIAN, V. A. 1993b. Saccharomyces telomeres acquire single-strand TG1-3 tails late in S phase. *Cell,* 72**,** 51-60.

WOTTON, D. & SHORE, D. 1997. A novel Rap1p-interacting factor, Rif2p, cooperates with Rif1p to regulate telomere length in Saccharomyces cerevisiae. *Genes Dev,* 11**,** 748-60.

WU, D., TOPPER, L. M. & WILSON, T. E. 2008. Recruitment and dissociation of nonhomologous end joining proteins at a DNA double-strand break in Saccharomyces cerevisiae. *Genetics,* 178**,** 1237-1249.

WU, G., LEE, W. H. & CHEN, P. L. 2000. NBS1 and TRF1 colocalize at promyelocytic leukemia bodies during late S/G2 phases in immortalized telomerase-negative cells. Implication of NBS1 in alternative lengthening of telomeres. *J Biol Chem,* 275**,** 30618-22.

WU, L., MULTANI, A. S., HE, H., COSME-BLANCO, W., DENG, Y., DENG, J. M., BACHILO, O., PATHAK, S., TAHARA, H., BAILEY, S. M., DENG, Y., BEHRINGER, R. R., S & CHANG, Y. 2006. Pot1 Deficiency Initiates DNA Damage Checkpoint Activation and Aberrant Homologous Recombination at Telomeres. *Cell,* 126**,** 49-62.

WU, Y. & ZAKIAN, V. A. 2011. The telomeric Cdc13 protein interacts directly with the telomerase subunit Est1 to bring it to telomeric DNA ends in vitro. *Proc Natl Acad Sci U S A,* 108**,** 20362-9.

XIN, H., LIU, D., WAN, M., SAFARI, A., KIM, H., SUN, W., O'CONNOR, M. S. & SONGYANG, Z. 2007. TPP1 is a homologue of ciliate TEBP-beta and interacts with POT1 to recruit telomerase. *Nature,* 445**,** 559-62.

YAMAZAKI, H., TARUMOTO, Y. & ISHIKAWA, F. 2012. Tel1ATM and Rad3ATR phosphorylate the telomere protein Ccq1 to recruit telomerase and elongate telomeres in fission yeast. *Genes & Development,* 26**,** 241-246.

YE, J. Z. S., HOCKEMEYER, D., KRUTCHINSKY, A. N., LOAYZA, D., HOOPER, S. M., CHAIT, B. T. & DE LANGE, T. 2004. POT1-interacting protein PIP1: a telomere length regulator that recruits POT1 to the TIN2/TRF1 complex. *Genes Dev,* 18**,** 1649-1654.

YEAGER, T. R., NEUMANN, A. A., ENGLEZOU, A., HUSCHTSCHA, L. I., NOBLE, J. R. & REDDEL, R. R. 1999. Telomerase-negative immortalized human cells contain a novel type of promyelocytic leukemia (PML) body. *Cancer Res,* 59**,** 4175-9.

ZAUG, A. J., PODELL, E. R., NANDAKUMAR, J. & CECH, T. R. 2010. Functional interaction between telomere protein TPP1 and telomerase. *Genes & Development,* 24**,** 613-622.

ZHAO, Y., HOSHIYAMA, H., SHAY, J. W. & WRIGHT, W. E. 2008. Quantitative telomeric overhang determination using a double-strand specific nuclease. *Nucleic Acids Res,* 36**,** e14.

ZHONG, F. L., BATISTA, L. F., FREUND, A., PECH, M. F., VENTEICHER, A. S. & ARTANDI, S. E. 2012. TPP1 OB-Fold Domain Controls Telomere Maintenance by Recruiting Telomerase to Chromosome Ends. *Cell,* 150**,** 481-94.

ZSCHENKER, O., KULKARNI, A., MILLER, D., REYNOLDS, G. E., GRANGER-LOCATELLI, M., POTTIER, G., SABATIER, L. & MURNANE, J. P. 2009. Increased sensitivity of subtelomeric regions to DNA double-strand breaks in a human cancer cell line. *DNA Repair (Amst),* 8**,** 886-900.